Superconductivity from repulsive interaction

Cite as: AIP Conference Proceedings **1550**, 3 (2013); https://doi.org/10.1063/1.4818400
Published Online: 14 August 2013

Saurabh Maiti, and Andrey V. Chubukov

Superconductivity from repulsive interaction

Saurabh Maiti and Andrey V. Chubukov

Department of Physics, University of Wisconsin, Madison, Wisconsin 53706, USA

Abstract. The BCS theory of superconductivity named electron-phonon interaction as a glue that overcomes Coulomb repulsion and binds fermions into pairs which then condense and super-conduct. We review recent and not so recent works aiming to understand whether a nominally repulsive Coulomb interaction can by itself give rise to a superconductivity. We first discuss a generic scenario of the pairing by electron-electron interaction, put forward by Kohn and Luttinger back in 1965, and then turn to modern studies of the electronic mechanism of superconductivity in the lattice models for the cuprates, the Fe-pnictides, and the doped graphene. We show that the pairing in all three classes of materials can be viewed as lattice version of Kohn-Luttinger physics, despite that the pairing symmetries are different. We discuss under what conditions the pairing occurs and rationalize the need to do parquet renormalization-group analysis. We also discuss the interplay between superconductivity and density-wave instabilities.

Keywords: Superconductivity, mechanism of high T_c,Kohn-Luttinger Mechanism, Renormalization group
PACS: 74.20.Mn,

INTRODUCTION

Superconductivity (SC) is one of most remarkable aspects of quantum physics of interacting electrons. Discovered in 1911 by Kamerlingh Onnes and his team of technicians [1] it preoccupied the minds of the most prominent physicists of the 20th century and remains at the forefront of condensed-matter physics in the 21st century. Many ideas developed first in the studies of superconductivity like the mass generation of the gauge field (the Meissner effect) [2, 3], and the mass generation of superconducting phase fluctuations [4], were later extended to other fields of physics and served as paradigms for the works by Higgs [5] and others to explain mass generation of the electro-weak gauge W and Z bosons in particle physics [6].

In simple words, superconductivity is the ability of fermions to carry electric current without dissipation. In quantum physics such phenomenon is generally associated with the appearance of a macroscopic condensate, i.e., a quantum state in which 10^{23} particles “hold together" at the lowest quantum level and do not allow individual particles to get swiped away by impurities, interactions with boundaries, etc. Bosons are capable to do this because any number of them can occupy a single quantum level, and the appearance of a macroscopic condensate of bosons is a well-known phenomenon of Bose-Einstein condensation [3]. Fermions, however, are "lone wolves"– by Pauli principle, only two of them (with opposite spins) can occupy a single quantum level, others are expelled. As a result, 10^{23} fermions occupy a comparable number of energy levels. In this situation, any coherent motion of fermions (e.g., a current) will only survive for a limited time, before fermions will

Lectures on the Physics of Strongly Correlated Systems XVII
AIP Conf. Proc. 1550, 3-73 (2013); doi: 10.1063/1.4818400

be individually affected by impurities, walls, etc.

There is a way to change this unwanted situation. If, somehow, fermions form bound pairs, quantum mechanics tells us that each pair has spin $S = 0$ or 1, i.e., it becomes a boson. Bosons can condense and behave as one monolithic object, i.e., if they are forced to move in one direction by an applied electric field, they will continue moving even after the field is turned off because 10^{23} bound fermionic pairs will not allow an individual fermion to change its direction due to, e.g., impurity scattering.

This simple reasoning tells us that the phenomenon of superconductivity can be straightforwardly explained if there will be an explanation why fermions form bound states. This is where the real difficulty is. An electron-electron interaction is repulsive and generally should not allow fermions to pair. That remained the mystery for almost 50 years after the discovery of superconductivity.

The breakthrough came in 1957 in a paper by Bardeen, Cooper, and Schrieffer (BCS) [7]. They found that the interaction between fermions and lattice vibrations effectively creates an attraction between fermions. An electron creates a disturbance of a lattice structure around it, another electron "feels" this disturbance and through it "feels" the other electron. BCS have demonstrated that the effective electron-electron interaction, mediated by quanta of lattice vibrations – phonons, is attractive at energies smaller than characteristic phonon frequency ω_D. On a first glance this may not be enough as electrons still repel each other by Coulomb interaction. However, Coulomb repulsion is known to become progressively smaller at smaller energies due to screening in the particle-particle channel [8, 9, 10], and it drops between fermionic bandwidth, which is typically of order few electron-volts, and Debye frequency, which is typically a few tens of millivolts. If the drop down to ω_D is strong enough, electron-phonon interaction overshoots electron-electron repulsion and the total interaction becomes attractive. The BCS theory was preceded by the observation by Cooper[11] that there is no threshold for the pairing, i.e., an arbitrary weak attractive interaction already gives rise to fermionic pairing. As a result, all what is required for pairing is that at energies of order ω_D electron-phonon interaction must exceed screened Coulomb interaction.

Electron-phonon mechanism of SC has been successfully applied to explain the pairing in a large variety of materials, from Hg and Al to recently discovered and extensively studied MgB_2 with T_c as high as $39K$ [12]. The phonon density of states, obtained by inelastic neutron scattering experiments, and the spectrum of the bosons which mediate pairing, as deduced from tunneling experiments, agree very well in systems like, e.g., Pb [13, 14]. This comparison of two independent experiments, together with the isotope effect[15, 16], are generally considered to be a very reliable proof of a phonon–mediated pairing state.

BCS theory also stimulated efforts to develop theoretical frameworks to describe the phenomenon of SC, and the outcomes were the fundamental Gorkov's theory of the SC state involving normal and anomalous Green's functions[17], and the controlled Eliashberg theory[18, 14, 19] of superconductivity, which goes beyond the BCS theory and includes fermionic self-energy and the dynamical part of the pairing interaction.

Non-phononic mechanisms of the pairing has been also discussed, most notably in

connection with the superfluidity of ^3He [20, 21], but didn't become the mainstream before the breakthrough discovery of SC in LaBaCuO in 1986 [22]. That discovery, and subsequent discoveries of superconductivity at higher T_c in other cuprates, signaled the beginning of the new era of "high-temperature superconductivity" [23]. The discovery, in 2008, of superconductivity in Fe-based pnictides[24] (binary compounds of the elements from the 5th group: N, P, As, Sb, Bi) with maximum T_c near $60K$ quickly established another direction of research in this field.

The high superconducting transition temperature is important but not the central feature of the phenomenon of "high-temperature superconductivity". After all, T_c in MgB_2 is higher than in many Fe-pnictides. What truly created an enormous interest to new superconductors is the observation, shared by most scientists(although not all of them) that electron-phonon interaction is too weak to account for observed T_c in these materials. The same belief holds for organic and heavy-fermion superconductors, for which T_c is smaller, but electron-phonon interaction is not the "glue" for superconductivity, by one reason or another.

If electron-phonon interaction is not the pairing glue, then what binds electrons together? The only other option is Coulomb interaction. But it is repulsive, how can it give rise to the pairing? It turns out, it can. This set of lecture notes is an attempt to present a comprehensive story of electron-electron pairing by the nominally repulsive Coulomb interaction.

The study of the pairing due to electron-electron interaction (often termed as electronic mechanism of superconductivity) has a long history. It has been known from early 1950th that screened Coulomb potential has a long-range oscillatory tail $\cos(2k_F r+\phi_0)/r^3$ at large distances r (k_F is Fermi momentum). These oscillations are often called Friedel oscillations [25]. Due to these oscillations, the screened Coulomb interaction gets over-screened at some distances and becomes attractive. Landau and Pitaevskii analyzed the pairing at non-zero orbital momentum l of the pair and found that the pairing problem decouples between different l (see Ref. [3]). Because of this decoupling, even if only one partial component of the interaction is attractive and all other repulsive, the system still undergoes a pairing instability into a state with l for which the interaction is attractive. Because the components of the interaction with large l come from large distances, it is conceivable that occasional over-screening of the Coulomb interaction at large distances may make some of partial interaction components with large l attractive.

A bold next step in this direction has been made by Kohn and Luttinger (KL) in 1965 [26, 27]. They analyzed the form of the fully screened irreducible pairing interaction at large l in three-dimensional, rotationally isotropic systems with $k^2/(2m)$ dispersion and separated the non-analytic $2k_F$ screening and the regular screening from other momenta. They incorporated the latter into the effective interaction $U(\mathbf{q})=U(q)$ ($q=|\mathbf{q}|$) and made no assumptions about the form $U(q)$ except that it is an analytic function of q^2. The full irreducible pairing interaction is $U(q)$ plus extra terms of $O\left(U^2(q)\right)$ coming from $2k_F$ screening. KL argued that contributions to partial components of the irreducible interaction from $2k_F$ scattering scale as $1/l^4$ due to the non-analyticity of the $2k_F$ screening, while the partial components of analytic $U(q)$ behave at large l as e^{-l}, i.e., are much smaller.

This smallness overshoots the fact that KL interaction is of second order in U and makes KL contribution larger than the direct first-order interaction term.

KL found that, for large l, partial components of the full irreducible interaction with even l are attractive when $U(0)/U(q=2k_F) > \sqrt{3}-1$, and components with odd l are attractive no matter what is the form of $U(q)$. As a result, any rotationally-invariant system with repulsive Coulomb interaction is unstable against pairing, at least at large enough odd l. When $U(0) = U(2k_F) = U$, both odd and even components are attractive.

The situation at smaller l is less definite as one no longer can separate the non-analytic $2k_F$ contribution to the irreducible pairing vertex and regular contributions from other momenta. In this situation, one can only do perturbation theory to second order in some bare $U(q)$. For momentum-independent $U(q) = U$, KL attraction survives down to $l = 1$ which is, by far, the largest of attractive components [28, 29]. For momentum-dependent interaction, a bare $U(q)$ has components for all l and whether second-order KL contribution can overshoot bare interaction is not obvious and depends on the details. One case when KL term definitely wins and again leads to $l = 1$ pairing instability, is when the Born parameter is of order one, i.e., the radius of the interaction in real space is about the same as $s-$wave scattering length a, and $ak_F/\hbar$ is small. In this situation, partial components of $U(q)$ scale as $(ak_F/\hbar)^{2l+1}$, while KL terms are of order $(ak_F/\hbar)^2$ for all l, i.e., the KL components are parametrically larger for all $l > 0$.

KL applied their results to ^3He. Back in 1965, it was widely believed that the pairing in ^3He should be with $l = 2$, so they approximated $U(q)$ by a constant U, expressed U in terms of s-wave scattering length a, used $ak_F/\hbar \approx 2$, known for ^3He, and obtained a ridiculously small $T_c \sim 10^{-17}K$. A few years later, in 1968, Fay and Layzer [28] extended KL calculations to $l = 1$, which a few years later (in 1972) was found experimentally [30] to be the actual pairing state in $3He$. For p-wave, the KL result for T_c is $\sim 10^{-3}K$, which by order of magnitude is the same as experimental $T_c \sim 2.5 \times 10^{-3}K$ (Ref. [30]).

The KL analysis in 2D is more involved. If the regular interaction $U(q)$ is momentum-independent, the $2k_F$ part is also momentum independent for all $q \leq 2k_F$, which are relevant for pairing (the pairing interaction connects momenta on the Fermi surface). However, a picture similar to that in 3D gets restored once we apply perturbation theory and go to third order in U [31]. Now the $2k_F$ part becomes momentum dependent and non-analytic at $q \to 2k_F$ from below. Its partial components at large l scale as $1/l^2$ and are attractive. Like in 3D, the largest KL attraction is for $l = 1$, but now it scales as U^3 rather than U^2. As an additional complication, the relation between $U(q)$ and the scattering amplitude in 2D is also logarithmically singular, but this does not affect the statement about KL attraction down to $l = 1$, only U^3 is replaced by $(1/\log ak_F)^3$.

We are now in a position to list the number of topics covered in these lecture notes. In the presence of a lattice, rotational symmetry is broken and one cannot simply expand in angular harmonics, but has to consider discrete irreducible representations for a particular lattice. We discuss how to analyze pairing in lattice systems and show that modified KL mechanism works here as well, particularly

when the bare interaction is momentum-independent. We consider three examples of lattice physics in two dimensions: the 2D model with two Fermi pockets in different parts of the Brillouin zone, and two different models with a single Fermi surface (FS), but with highly anisotropic density of states, which is peaked at particular points on the FS – the "patch models". We consider models with two and three non-equivalent patches. The model with Fermi pockets is applicable to Fe-pnictides [32], the two-patch model is applicable to overdoped cuprates [33], and three-patch model is applicable to doped graphene near 3/8 and 5/8 filling, and to fermions on triangular lattice near 3/4 filling [34].

We first discuss what is the condition on superconductivity in lattice systems, assuming that we deal with short-range repulsive interaction. We show that, in many aspects, the situation is similar to isotropic systems. Namely, for Hubbard U model, the bare pairing interaction is repulsive in a conventional $s-$-wave channel, and zero in other channels, which in the cases we consider are either d-wave like (in terms of how many times the pair wave function changes sign along the FS), or, for the case of Fe-pnictides, another $s-$wave, often called s^{+-}, in which the pair wave function changes sign between different FS pockets (the conventional $s-$wave is called s^{++}). We show that second-order KL contributions to the pairing interaction are attractive in these "other" channels, much like they are attractive in all channels with $l > 0$ in isotropic systems.

We then consider a more realistic case of a bare $U(q)$, which is still short-range, but does have momentum dependence and is larger at small q than at large q, as it is expected for a screened Coulomb interaction. We show that, in this situation, the bare interaction is repulsive in all non-s^{++} channels, and KL contributions alone cannot cure the situation. We discuss three approaches which give rise to pairing even in this case. All three explore the idea that there is another order which the system wants to develop in either spin or charge density-wave channel, and fluctuations of this order increase the strength of the attractive KL contribution and make it larger than the repulsive contribution from the bare interaction.

The first one a phenomenological "collective mode" approach [35]. It abandons the controllable weak coupling limit (i.e. expansion in U) and assumes that the pairing interaction between fermions can be thought of as being mediated by soft collective fluctuations of some density-wave order whose fluctuations develop at energies much larger than those at which superconductivity sets in. It is assumed that collective excitations are soft enough such that this effective interaction is large and exceeds the bare repulsive interaction. The form of the static pairing interaction mediated by soft bosons is obtained phenomenologically, based on physics intuition and experimental results.

The second approach assumes that superconductivity and density-wave instabilities are competing orders, which grow together and develop at about the same energies/temperatures. There is no pairing "mediated by collective bosons" in this case because collective bosons by themselves develop at the same scale as superconductivity. Still, the idea is that, as these fluctuations develop, they give progressively larger contribution to the pairing channel via KL mechanism, and below some energy, which is internally set by the system, the attractive KL interaction gets larger than the bare repulsion. This progressive increase of the KL interaction

with decreasing energy can be analyzed within the parquet renormalization-group (RG) approach (either conventional [32, 34, 36] or functional [37, 38]), which is still a weak-coupling approach, but it goes beyond second order in $U(q)$ ana allows one to sum up series of logarithmically singular KL contributions to the pairing interaction. One thing one should analyze in the RG approach is whether superconductivity is the leading instability, or density-wave order develops first.

And the third approach is to obtain the effective pairing interaction in an approximate computation scheme, called a random phase approximation (RPA), which amounts to a summation of a particular class of ladder diagrams [39]. In this effective interaction the bare repulsion and the KL contributions are the first and the second terms in the expansion in $U(q)$, however higher-order terms are not assumed to be small and in many cases the RPA pairing interaction is attractive in one of non-s^{++} channels. This approach is non-controlled, but its advantage is that it can be equally applied to the case when density-wave fluctuations develop before SC fluctuations and to the case when density-wave and SC fluctuations develop at the same energies.

Crudely speaking, in all these models, the KL effect is enhanced by enhanced density-wave fluctuations in either spin or charge channel. For repulsive interaction, the enhancement in the spin channel is a natural choice.

BACKGROUND INFORMATION: FERMI LIQUID THEORY

To understand and describe superconductivity, one needs to know the concept and the mathematical apparatus on how to treat interacting fermions at low temperatures. We first remind our readers the basic facts about a non-interacting (free) Fermi gas and then present a brief summary of properties of a weakly/moderately interacting system of fermions, which is often called a Fermi-liquid. We will not attempt to derive the well known Fermi-Liquid theory here (we direct the reader to Ref.[3]) and only state some of the important properties that will help us advance towards our goal of understanding the phenomenon of superconductivity from electron-electron interaction.

A Free Fermi gas

A classical gas is well described by the Boltzmann statistics [40], according to which an average number of particles at an energy E_k (the distribution function) is given by

$$n(k) = e^{(\mu - E_k)/T}, \tag{1}$$

where μ is the chemical potential, and T is the temperature. Throughout the text we set the Boltzmann constant $k_B = 1$ and measure temperature in units of energy.

The classical statistics is valid when thermal de Broglie wavelength of particles $\lambda_T \sim \hbar/(mT)^{1/2}$ is much smaller than their separation. At lower temperatures, λ_T becomes comparable to a separation between particles and quantum effects become

important. Depending on whether particles have half-integer spin or integer spin, they obey either Fermi statistics

$$n_F(k) = \frac{1}{e^{(E_k - \mu(T))/T} + 1} \tag{2}$$

or Bose statistics

$$n_B(k) = \frac{1}{e^{(E_k - \mu(T))/T} - 1} \tag{3}$$

We will focus on electrons, whose spin is $S = 1/2$, and only consider Fermi statistics.

The total number N of electrons in a volume V is, at any temperature is given by

$$\frac{N}{V} = 2 \int \frac{d^d k}{(2\pi\hbar)^d} n_F(k), \tag{4}$$

where the factor 2 is due to a summation over the two spin projections. If the ratio N/V is fixed, this relation determines μ as a function of T. At low T, μ is positive and is of order

$$T_F = \frac{\hbar^2}{m} \left(\frac{N}{V} \right)^{2/3} \tag{5}$$

At temperatures $T \geq T_F$, μ changes sign and becomes negative. At somewhat higher T, $e^{-\mu(T)/T}$ gets large and Fermi distribution function transforms into Boltzmann distribution function. We are interested in fermionic properties at low temperatures, so we will deal with Fermi statistics, Eq. (2).

Eq. (2) has the important property that at $T = 0$, $n_F(k) = 0$ when $E_k > \mu$ and $n_F(k) = 1$ for $E_k < \mu$. Because $E_k = k^2/2m$ for a free gas, and k is a good quantum number, the condition $E_k = \mu$ determines a sharp boundary in $k-$space (a FS) beyond which all states are empty and inside all states are filled. Its radius is called k_F, and the corresponding energy $E_F = k_F^2/(2m)$ is called the Fermi energy. By order of magnitude, $E_F \sim T_F$. The Fermi energy at $T = 0$ obviously coincides with the chemical potential μ.

In 3D, the FS is a sphere. The value of k_F is obtained from (4) and is given by $k_F = \left(\frac{3\pi^2 \hbar^3 N}{V} \right)^{1/3}$. In 2D, the FS is a circle, and $k_F = \left(\frac{2\pi^2 \hbar^2 N}{V} \right)^{1/2}$.

The region near k_F is the most relevant one for the low-energy physics. The fermionic dispersion at $k \approx k_F$ can be approximated by

$$E_k - \mu \approx \frac{k_F}{m}(k - k_F) = v_F(k - k_F) \tag{6}$$

where v_F is called Fermi velocity.

The total ground state energy E_0 is the sum of $k^2/2m$ over all occupied states. In 3D

$$E_0 = \frac{3}{5} N \varepsilon_F \tag{7}$$

At a finite T, a Fermi-Dirac distribution function deviates from the step function, and this gives rise to temperature dependencies of observables. In particular,

specific heat in linear in T. In 3D

$$C(T) = NT\frac{m\pi^2\hbar^2}{k_F^2} \tag{8}$$

Systems of interacting fermions

Fermi liquid theory

For interacting fermions, quantum states of the full system, ϵ_k do not reduce to a sum of quantum states of individual particles. Each ϵ_k should be understood as a collective excitation of the whole system of 10^{23} particles. In principle, there is no guarantee that an interacting system still has well defined excitations with a given momentum k. Nevertheless, the presence of such excitations is the key postulate of a Fermi-liquid theory developed by Landau in mid-1950s [3]. In Landau Fermi liquid (LFL) theory, excitations behave much like free fermions, despite the fact that each excitation is collectively produced by all fermions in the system. These new excitations, called quasiparticles, obey Fermi-Dirac statistics, and their number is the same as the number of the actual particles, which implies that k_F does not change with the interaction. The dispersion of quasiparticles ϵ_k is not known for a generic k but near k_F is assumed to have the same form as E_k for free particles, but with renormalized Fermi velocity:

$$\epsilon_k - \mu = v_F^*(k - k_F) \tag{9}$$

Because k_F is not renormalized, $v_F^* = k_F/m^*$, where m^* is the quasiparticle mass. The ratio m^*/m can be extracted from the measurements of the specific heat $C(T)$ and is one of the indicators of the strength of the interaction between fermions.

The change of the dispersion from E_k to ϵ_k can be viewed as if other fermions combine and create an effective field which acts on a given quasiparticle. But this is not the only effect. Interaction between fermions additionally forces them to jump from one level to the other, i.e., they only spend a finite amount of time at a given (renormalized) level ϵ_k. This implies that a lifetime of a quasiparticle with a given momentum is finite. A finite lifetime means that the quasiparticle energy has both real and imaginary parts. The imaginary part of ϵ_k can be obtained only perturbatively for k far away from k_F, but near k_F the result is

$$Im\epsilon_k \propto (k - k_F)^\alpha \tag{10}$$

The condition that quasiparticles are well defined near the FS implies that $Re\epsilon_k$ must be larger that $Im\epsilon_k$, i.e., that α must be larger than one. In the original Landau treatment of a 3D FL, $\alpha = 2$, and the extension of his arguments to arbitrary dimension, D, shows that it is the case for all $D > 2$. FLs with $\alpha = 2$ are sometimes called canonical FLs. In dimensions D between 1 and 2, $\alpha = D$, except for special cases, and in $D = 2$, $Im\epsilon_k \propto (k - k_F)^2 \log|k - k_F|$. Such systems are

called non-canonical FLs. Still, by Landau criterion, all these systems are Fermi liquids. In $D = 1$ real and imaginary parts of ϵ_k are of the same order, and the assumption of well-defined quasiparticles near the FS becomes invalid.

Microscopic treatment

Microscopic treatment of interacting fermions is under control when there is small parameter to justify perturbative expansion. There are two situations when perturbative expansion is possible. First is the case of Coulomb interaction $V(q)$ at small r_s, where in 3D $r_s = (3/4\pi)^{1/3}(V/N)^{1/3}(e^2m/\hbar^2)$ (r_s is small when the density N/V is large enough. A perturbative expansion in powers of r_s is a bit tricky as interaction between fermions accounts for the renormalization of fermionic dispersion from $E_k = k^2/(2m)$ to a quasiparticle ϵ_k and, at the same time, screens static long-range Coulomb interaction and transforms $V_q = \frac{4\pi e^2}{q^2}$ into

$$V_{\text{screened}} = \frac{V_q}{\epsilon(q)} = \frac{4\pi e^2}{q^2 + \kappa^2}, \tag{11}$$

where $\kappa^2 \propto k_F^2 r_s$. In real space, $V_{\text{screened}}(r)$ becomes a Yukawa potential $V_{\text{screened}}(r) = \frac{4\pi e^2}{r} e^{-\kappa r}$.

Another situation for which perturbative expansion is possible is the case when $r_s \geq 1$, but the magnitude of the screened interaction is small. For $r_s \geq 1$, screened interaction does not actually extend beyond a few nearest neighbors (a limiting case when only on-site interaction is essential is known as the Hubbard model). Once $U(r)$ is short-ranged and $U(q) = \int U(r) e^{i\mathbf{qr}} d^3r$ remains finite for all q, including $q = 0$, one can assume semi-phenomenologically that the overall magnitude of the screened $U(q)$ is smaller than the Fermi energy, and use $(N/V)U(0)/E_F$ as a small dimensionless parameter. In Born approximation, this small parameter can be written as $ak_F/\hbar$, where, as before, a is s-wave scattering length ($a = mU(0)/4\pi\hbar^2$). Because k_F^3 is proportional to fermionic density, one can also view the smallness of $ak_F/\hbar$ as the consequence of small density rather than small interaction. Beyond Born approximation, a is not linearly proportional to $U(0)$ and $ak_F/\hbar$ can still be a small parameter at small enough density even when U is not small.

Fermi liquid postulates have been verified and confirmed in both high-density and low-density expansions. In particular, in small ak_F the effective mass m^* is, in 3D

$$\frac{m^*}{m} = 1 + \frac{8}{15\pi^2}(7ln2 - 1)\left(\frac{ak_F}{\hbar}\right)^2, \tag{12}$$

and expansion of the total energy in powers of ak_F is

$$E_0 = \frac{3}{5} N\varepsilon_F \left[1 + \frac{10}{9\pi}\left(\frac{ak_F}{\hbar}\right) + \frac{4(11 - 2ln2)}{21\pi^2}\left(\frac{ak_F}{\hbar}\right)^2\right] \tag{13}$$

Green's Function Approach

The mathematical apparatus to treat interacting fermions was developed at about the same time as FL theory [3]. The two key elements in the theory are single-particle and two-particle fermionic Green's functions. A single-particle Green's function is defined in terms of the time-ordered product of the two coordinate- and time-dependent operators $\Psi = \Psi(x,t)$ in Heisenberg representation:

$$\begin{aligned} G_{\alpha\beta}(X_1, X_2) &= -i\langle T\Psi_\alpha(X_1)\Psi^\dagger_\beta(X_2)\rangle \\ &= \begin{array}{cc} -i\langle\Psi_\alpha(X_1)\Psi^\dagger_\beta(X_2)\rangle & \text{for} \quad t_1 > t_2 \\ i\langle\Psi^\dagger_\beta(X_2)\Psi_\alpha(X_1)\rangle & \text{for} \quad t_1 < t_2 \end{array} \end{aligned} \tag{14}$$

where $X = (\vec{x}, t)$, T stands for time-ordering, the brackets imply averaging over the ground state of an interacting system, and α, β are the spin indices. Translational invariance makes G a function of only one variable $X \equiv X_1 - X_2$ and one can conveniently introduce its Fourier transform $G(\vec{k}, \omega)$.

The few things we need to know about single-particle Green's function are

- Green's function of free fermions $G(\vec{k}, \omega)$ near the FS is

$$G_0(\vec{k}, \omega) = \frac{1}{\omega - v_F(k - k_F)/\hbar + i\delta sgn(\omega)} \tag{15}$$

- The Green's function of interacting fermions has poles and branch cuts. Poles describe quasiparticle excitations, and the quasiparticle energy spectrum $\omega = \epsilon_k$ is the solution of

$$G^{-1}(\omega, \vec{k}) = 0 \tag{16}$$

  The branch cuts describe fully incoherent excitations which cannot be attributed to a single quasi-particle with a given momentum.

- In a generic FL, Green's function near the FS has the form

$$G(\vec{k}, \omega) = \frac{Z}{\omega - v^*_F(k - k_F)/\hbar + i\delta sgn(\omega)} + G_{\text{inc}} \tag{17}$$

  where Z is the residue of the pole, v^*_F is the renormalized Fermi velocity, and G_{inc} describes the incoherent part. The damping term $(k - k_F)^\alpha$ is incorporated into the incoherent part. Alternatively, near the mass shell ($\omega = v^*_F(k - k_F)/\hbar$) it can be converted into $|\omega|^\alpha sgn(\omega)$ term and added to the pole part as a replacement to $i\delta sgn(\omega)$ term. In general, FL description is valid as long as $0 < Z < 1$. For free fermions, incoherent part is absent and $Z = 1$. At small $ak_F/\hbar$ in 3D,

$$Z = 1 - \frac{8\log 2}{\pi^2}(\frac{ak_F}{\hbar})^2 \tag{18}$$

- The momentum distribution function is obtained from the Green's function by integrating over frequencies

$$n_k = -i \lim_{t\to -0} \int_{-\infty}^{\infty} \frac{d\omega}{2\pi} G(\omega, \vec{k}) e^{-i\omega t} \tag{19}$$

The particular limit in this expression implies that the integral can be extended only to the upper frequency half-plane. For free fermions, frequency integration gives $n_k = \theta(k_F - k)$, as it should be ($\theta(x) = 0$ for $x < 0$ and $\theta(x) = 1$ for $x > 0$).

- The full Green's function G is related to the Green's function of free fermions G_0 by

$$G^{-1}(k,\omega) = G_0^{-1}(k,\omega) + \Sigma(k,\omega) \tag{20}$$

where Σ is called self-energy (see Fig. 1). The quasiparticle residue and the effective mass are expressed via partial derivatives of Σ as

$$\frac{1}{Z} = 1 + \frac{\partial \Sigma}{\partial \omega} \tag{21}$$

$$v_F^* = Z\left(v_F^* - \hbar \frac{\partial \Sigma}{\partial k}\right) \tag{22}$$

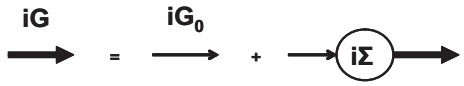

FIGURE 1. Diagrammatic representation of the full Green's Function in terms of the self energy Σ. The thin line is the bare Green's function G_0 and the thick lines are the fully renormalized Green's functions G.

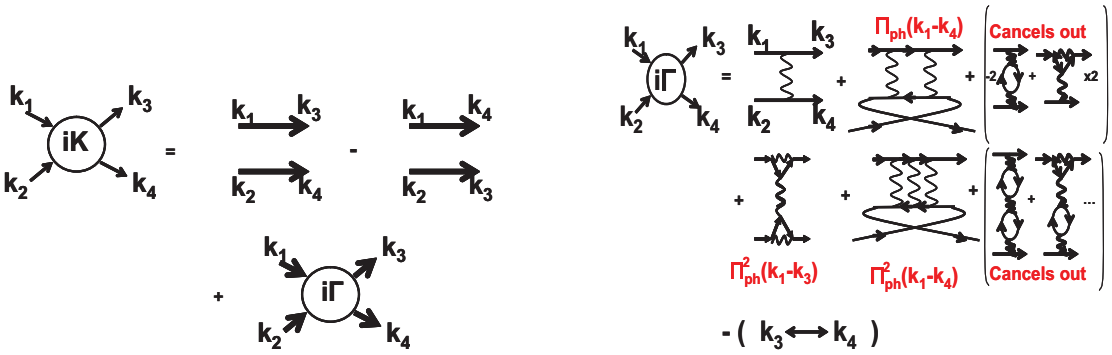

FIGURE 2. (Left) Diagrammatic representation of the full two particle Green's function as the anti-symmetrized product of two Green's functions plus the vertex function Γ. (Right) Diagrams that are included in the vertex function Γ. (All labels correspond to a case of a constant interaction.)

The other element of the mathematical apparatus is a two-particle Green's function

$$K_{\gamma\delta,\alpha\beta} = \langle T \Psi_\gamma \Psi_\delta \Psi_\alpha^\dagger \Psi_\beta^\dagger \rangle \tag{23}$$

The properties of the two-particle Green's functions are the following:

- For free fermions, $K_{\gamma\delta,\alpha\beta}$ reduces to an anti-symmetrized product of two Green's functions and does not provide additional information compared to a single-particle Green's function.
- For interacting fermions, K contains an additional term ΓG^4 (with a proper summation over spin indices), which cannot be factorized into the product of two Green's functions (see Fig.2). The quantity Γ is called the vertex function. It contains information about interactions and generally depends on frequencies and momenta of two incoming and two outgoing fermions subject to momentum and frequency conservation.
- To leading order in the interaction $U(q)$, the vertex Γ coincides with the antisymmetrized interaction

$$\begin{aligned}&\Gamma^0_{\alpha\beta,\gamma\delta}(k_1,k_2;k_3,k_4)\\&=-U(\vec{k}_1-\vec{k}_3)\delta_{\alpha\gamma}\delta_{\beta\delta}+U(\vec{k}_1-\vec{k}_4)\delta_{\alpha\delta}\delta_{\beta\gamma}\end{aligned} \tag{24}$$

  Using the identity

$$\vec{\sigma}_{\alpha,\gamma}\cdot\vec{\sigma}_{\beta\delta}=-\delta_{\alpha,\gamma}\delta_{\beta\delta}+2\delta_{\alpha,\delta}\delta_{\beta\gamma}, \tag{25}$$

  we can decompose Γ^0 into spin and charge components:

$$\Gamma^0_{\alpha\beta,\gamma\delta}(k_1,k_2;k_3,k_4)=\Gamma^0_c\delta_{\alpha\gamma}\delta_{\beta\delta}+\Gamma^0_s\vec{\sigma}_{\alpha,\gamma}\cdot\vec{\sigma}_{\beta\delta} \tag{26}$$

  where

$$\begin{aligned}\Gamma^0_c&=\frac{-2U(\vec{k}_1-\vec{k}_3)+U(\vec{k}_1-\vec{k}_4)}{2}\\\Gamma^0_s&=\frac{U(\vec{k}_1-\vec{k}_4)}{2}\end{aligned} \tag{27}$$

  The decomposition into spin and charge parts is the consequence of $SU(2)$ spin invariance and survives beyond the leading order, i.e., the full $\Gamma_{\alpha\beta,\gamma\delta}(k_1,k_2;k_3,k_4)$ has the same form as Eq. (26), but Γ^0_c and Γ^0_s are replaced by fully renormalized Γ_c and Γ_s, which generally depend on momenta and frequency, i.e., $\mathbf{k}_i\to(\mathbf{k}_i,\omega_i)$.
- In a generic FL, Γ, viewed as a function of either a total frequency of two incoming fermions or a transferred frequency, may have poles and branch cuts. The poles in Γ_c (or Γ_s) viewed as functions of a transferred frequency describe weakly damped collective excitations in the charge (or the spin) channel. Examples of such excitations at $T=0$ are zero sound waves in the charge channel and spin waves in the spin channel. To illustrate this, we present the expressions for spin and charge components of $\Gamma_{\alpha\beta,\gamma\delta}(k,p;k+q,p-q)$ for small transferred momentum q and frequency Ω. For a constant interaction U, one obtains, keeping the terms which depend only on q, (see Fig3)

$$\Gamma_c=-\frac{U}{2}\frac{1}{1+U\Pi_{ph}(q,\Omega)}\quad\Gamma_s=\frac{U}{2}\frac{1}{1-U\Pi_{ph}(q,\Omega)} \tag{28}$$

where $\Pi_{ph}(q,\Omega)$ is a particle-hole polarization operator (the product of two Green's functions with relative momentum q and relative frequency Ω). At zero frequency and in the limit of zero momentum, $\Pi_{ph}(0,0)$ coincides with the density of states at a Fermi level $N_0 = mk_F/2\pi^2\hbar^3$. At zero momentum and any finite frequency, $\Pi_{ph}(0,\Omega) = 0$. This last condition is the consequence of the conservation of the total number of particles. When both q and Ω are small, but the ratio $x \equiv \Omega/v_F q$ is arbitrary,

$$\Pi_{ph}(q,\Omega) = \Pi(x) = \frac{mk_F}{2\pi^2\hbar^3}\left(1 - \frac{x}{2}\log\left|\frac{1+x}{1-x}\right|\right). \tag{29}$$

In particular, $\Pi_{ph}(q,\Omega)$ can be made arbitrary large (and negative) when Ω approaches $v_F q$ from above. This property of $\Pi_{ph}(q,\Omega)$ ensures the existence of the pole in Γ_c at $\Omega \approx v_F q$ (a zero sound mode).

- The poles in Γ viewed as a function of a total frequency of two fermions describe two-particle (or two-hole) collective excitations of $S = 1/2$ fermions with the total spin of a pair either $S = 0$ or $S = 1$. These poles are most relevant for superconductivity.
- A fermionic system is stable as long as the poles of collective bosonic excitations are located in the lower half-plane of a complex frequency (either total or transferred). Under this condition, bosonic excitations decay with time. If the poles are located in the upper frequency half-plane, excitations increase with time and fermionic system becomes unstable.

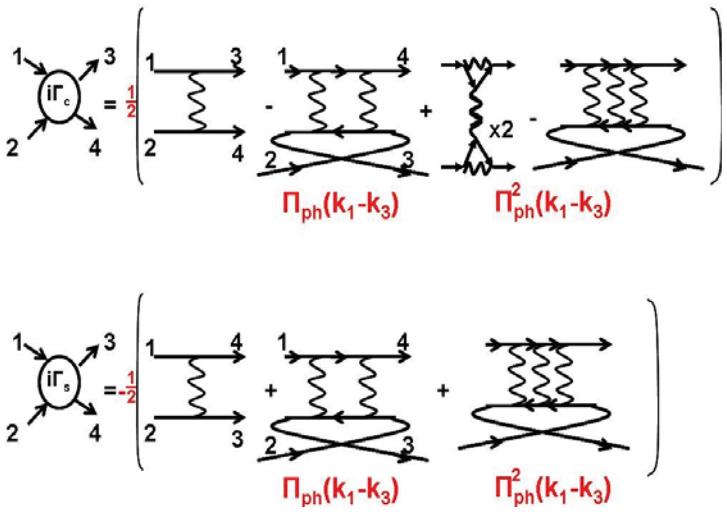

FIGURE 3. Diagrams up to third order in the interaction $U(q) = U$, that contribute to the charge and spin components of the full vertex function, Γ_c and Γ_s, respectively. Only diagrams with small $q = \mathbf{k}_1 - \mathbf{k}_3$ are shown.

SUPERCONDUCTIVITY

Like we said in the Introduction, superconductivity is the ability of fermions to carry a persistent non-dissipative current in thermodynamic equilibrium, without an applied field. This does not hold in conventional metals in which the current $\vec{j}$ appears as a response of a system to an external electric field $\vec{E}$, and is related to $\vec{E}$ by the Ohm formula

$$\vec{j} = \sigma \vec{E} \tag{30}$$

where σ is a conductivity. Resistivity, ρ, is inverse of conductivity. In the Drude theory, $\sigma = \frac{ne^2\tau}{m}$, where τ is the scattering time – the time between collisions imposed by either impurities or electron-electron interaction in non-isotropic systems. The current is dissipative in the sense that to carry a current j one needs to grab the energy from the field at the rate proportional to σE^2.

How can one get a non-dissipative current? Quantum mechanics teaches us that such a possibility exists, at least in principle. Namely, if a quantum-mechanical system is described by a macroscopic complex wave function $\Psi = |\Psi|e^{i\phi}$, it contains a density current associated with the phase of the complex wave function:

$$\vec{j} = \frac{\hbar}{2mi}\left(\Psi^*\vec{\nabla}\Psi - \Psi\vec{\nabla}\Psi^*\right) = \frac{|\Psi|^2}{m}\hbar\vec{\nabla}\phi \tag{31}$$

In a conventional metal, a macroscopic wave function is, to first approximation, an antisymmetrized product of single-fermion wave functions (the Slater determinant). The phases of individual wave functions are not correlated, and $\vec{\nabla}\phi$ vanishes after averaging over particles. The situation changes, however, if there a macroscopic number of particles in the same quantum-mechanical state. In this case, a wave function of the *whole* system has the form $\Psi = |\Psi|e^{i\phi}$, and $\vec{\nabla}\phi$ determines a macroscopic, non-dissipative current in the thermodynamic equilibrium. If particles are charged, a density current is proportional to a charge current, hence a persistent electric current also exists in an equilibrium.

The existence of a macroscopic condensate is a well-known property of bosonic systems, where a condensate emerges as a result of Bose-Einstein condensation. But electrons are fermions, and Pauli exclusion principle prevents fermions to accumulate on a single quantum level. But what if fermions are bound into pairs? A pair of fermions has spin $S = 0$ or $S = 1$ and therefore behaves as a boson. Bosons do condense, as we just said, and the condensation of bosons generates a persistent current (which is often called a supercurrent).

So, once fermions form bound pairs, they will eventually generate a supercurrent. The issue then is to identify the mechanism by which fermions are bound into pairs. This is a challenging task as electron-electron interaction is repulsive, and repulsive interaction is not expected to produce a bound state.

The solution[7], proposed by Bardeen, Cooper, and Schrieffer in 1957, is to use electron-phonon interaction as a pairing glue. A passing electron creates a perturbation of the lattice, another electron passing through the same area "feels" the perturbation, and through it "feels" another electron. In a more scientific

language, lattice vibrations (phonons) mediate the retarded interaction between fermions. One can show quite generally that such effective interaction is attractive at energies smaller or comparable to a Debye frequency ω_D. Still, to give rise to bound pairs, electron-phonon attraction has to overcome a supposedly much larger Coulomb repulsion. What helps is that Coulomb repulsion progressively gets smaller at smaller frequencies. If ω_D is small enough compared to the fermionic bandwidth, W, Coulomb interaction already gets reduced a lot between W and ω_D, and detailed calculations have found that electron-phonon attraction, which emerges below ω_D, well may overshoot this reduced Coulomb repulsion.

The weak coupling theory of superconductivity based on electron-phonon interaction has been developed by Bardeen, Cooper, and Schrieffer and is known as BCS theory. Gorkov and Melik-Barkhudarov [41] extended weak coupling theory one step ahead and found exact expression for T_c. The BCS theory has been further extended by Eliashberg[18], who demonstrated that the dynamical part of electron-phonon interaction can be incorporated into the theory in a controllable way. Both BCS and Eliashberg theories are actually not specific to electron-phonon interaction and, with some modifications, can be applied to any pairing mechanism.

Electron-phonon mechanism of superconductivity works well for some superconductors, but, as most of researchers believe, it does not account for the pairing symmetry and high T_c obtained in Cu and Fe-based superconducting materials and in several other families of superconductors. The only other alternative is superconductivity originating directly from repulsive electron-electron interaction.

To set the stage for the analysis of the pairing by electron-electron interaction, in the remainder of this section we will briefly review two generic issues about the pairing in isotropic (rotationally-invariant) systems: (i) that it emerges already for arbitrary weak attraction and (ii) that the pairing problem decouples between different angular momenta l and it is sufficient to have an attraction for just one angular component of the interaction (i.e., for just one value of l).

Pairing instability at arbitrary weak interaction

A constant interaction

In the mathematical apparatus developed to study interacting fermions, the information about the potential bound pairs is encoded in the 2-particle vertex function Γ which is a fully renormalized and antisymmetric interaction between quasi-particles. Consider first a system of fermions with a small constant attractive interaction U and compute Γ in perturbation theory. To first order in U, Γ is given by Eq. (24). Earlier, we had decoupled Γ into spin and charge parts. To study pairing, i.e., possible pair states with $S = 0$ or $S = 1$, it is more convenient to decompose Γ into singlet and triplet components. A singlet component has spin structure

$$\delta_{\alpha\gamma}\delta_{\beta\delta} - \delta_{\alpha\delta}\delta_{\beta\gamma} \tag{32}$$

and a triplet component is

$$\delta_{\alpha\gamma}\delta_{\beta\delta} + \delta_{\alpha\delta}\delta_{\beta\gamma} \tag{33}$$

For a constant U, only singlet component is present at the leading order, i.e.,

$$\Gamma^0_{\alpha\beta,\gamma\delta} = -U\left(\delta_{\alpha\gamma}\delta_{\beta\delta} - \delta_{\alpha\delta}\delta_{\beta\gamma}\right) \tag{34}$$

Let's go to next order. The four diagrams which give rise to the renormalization of Γ to order U^2 are shown in Fig. 4.

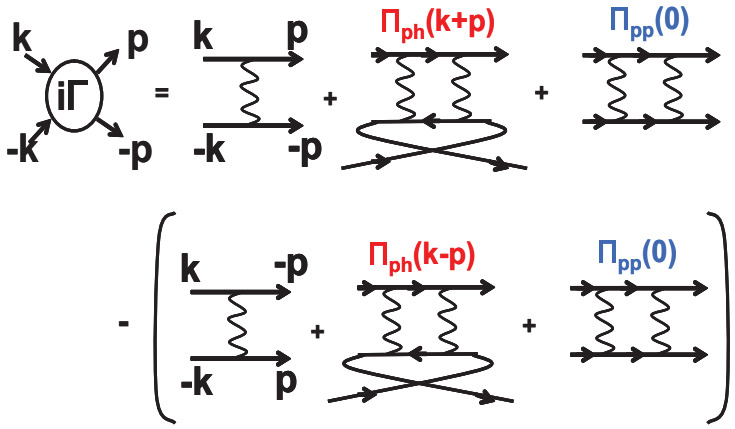

FIGURE 4. Diagrams to second order in the interaction $U(q) = U$, which contribute to the vertex function with zero total incoming momentum. There are contributions from both particle-hole and particle-particle channels. Other diagrams to order U^2 cancel each other and we do not show them.

Two of these diagrams contain a pair of fermionic Green's functions with opposite directions of the arrows. This pair is called a particle-hole bubble because one can immediately check that the momentum and frequency integral over the two Green's functions of intermediate fermions is non-zero at $T = 0$ only when one fermion is above FS, i.e., is a particle, and the other one is below FS, i.e., is a hole. The other two diagrams contain the product of two fermionic G's with the same direction of arrows. This combination is called particle-particle bubble because the momentum and frequency integral over these two Green's functions is non-zero at $T = 0$ when both fermions are above or below FS, i.e. both are particles, or both are holes.

The two diagrams with particle-hole bubbles contain particle-hole bubbles with different momentum combination ($\Pi_{ph}(k-p)$ and $\Pi_{ph}(k+p)$ in Fig4) and does affect the spin structure of the interaction, generating the triple component. These diagrams are singular when transferred frequency and transferred $v_F q$ are nearly equal, and this singularity gives rise to zero-sound waves. But we are interested in potential poles as a function of the total frequency of two fermions, while transverse frequencies and transferred momenta can be arbitrary. It is easy to verify that the particle-hole bubble is not singular for a generic transferred momentum and frequency and therefore is incapable to substantially modify Γ at small U.

The particle-particle bubble is a different story. Suppose we set the total momentum q of two fermions to be zero (by momentum conservation total incoming

and outgoing momenta are both zero). A straightforward computation shows that in this situation the renormalization in the particle-particle channel does not affect the spin structure of the interaction, and that at $T = 0$, each particle-particle bubble is logarithmically singular in the limit of small total frequency and behaves as

$$\begin{aligned} \Pi_{pp}(\Omega, q = 0) &= -i \int \frac{d^3 k d\omega}{(2\pi\hbar)^4} G_{k,\omega} G_{-k,-\omega+\Omega} \\ &= \frac{m k_F}{2\pi^2 \hbar^3} \left[ln\left(\frac{\omega_c}{\Omega}\right) + i\frac{\pi}{2} \right] \end{aligned} \tag{35}$$

where ω_c is the upper limit of the integration over $v_F(k - k_F)$, which, physically, is the upper end of the energy range in which U can be approximated by a constant.

The logarithmical divergence of $\Pi_{pp}(q = 0, \Omega)$ at $\Omega \to 0$ implies that the product $U\Pi_{pp}$ cannot be neglected even when the interaction is weak. Keeping this renormalization, we find that, to order U^2,

$$\Gamma^0_{\alpha\beta,\gamma\delta} = -U\left(1 - U\Pi_{pp}(0, \Omega)\right)\left(\delta_{\alpha\gamma}\delta_{\beta\delta} - \delta_{\alpha\delta}\delta_{\beta\gamma}\right) \tag{36}$$

We assume and then verify that the most relevant Ω are the ones for which $U\Pi_{pp}(q = 0, \Omega)$ are of order one. Let's go now to next order of U. The number of diagrams increase, but for $U\Pi_{pp} = O(1)$ all of them are small in U, except for the two diagrams with two particle-particle bubbles which give $(U\Pi_{pp})^2$ with prefactor equal to one The same holds for fourth and higher orders in U. One can easily make sure that perturbative series form geometric progression, hence the full Γ in this approximation is

$$\Gamma^{full}_{\alpha\beta,\gamma\delta} = -U\frac{1}{1 + U\Pi_{pp}(0, \Omega)}\left(\delta_{\alpha\gamma}\delta_{\beta\delta} - \delta_{\alpha\delta}\delta_{\beta\gamma}\right) \tag{37}$$

For positive (repulsive) U, Γ has no poles, but for negative (attractive) U, Γ has a pole at $\Omega = i\Omega_p$ where

$$\Omega_p = \omega_c e^{-2\pi^2\hbar^3/|U|mk_F} = \omega_c e^{-\frac{\pi\hbar}{2|a|k_F}}. \tag{38}$$

where, $a = mU/(4\pi\hbar^2)$ is s-wave scattering length in Born approximation. The pole exists at arbitrary small U and, as we see, is located in the *upper* half-plane of complex frequency Ω. A pole in the upper half-plane implies that, if we create an excitation with Ω_p, its amplitude will exponentially grow with time and destroy a Fermi liquid state that we departed from. What does it mean physically? The excitations, which grow with time, describe fluctuations in which a pair of fermions behaves as a single boson with total spin $S = 0$ and zero momentum. A natural suggestion would be that the new state, which replaces a Fermi liquid, contains a macroscopic number of such bosons in the same $q = 0$ state, i.e., the ground state has a macroscopic condensate. This is precisely what is needed for super-current.

The analysis of the pole in Γ can be extended to a to a non-zero total momentum q and to a finite temperature. Calculations show [17] that at a finite q the pole is located at $\Omega = i\Omega_p \left(1 - \frac{v_F^2 q^2}{6\hbar^2 \Omega_p^2}\right)$. Once q exceeds the critical value $\sqrt{6}\hbar\Omega_p/v_F$, the pole moves to the lower half-plane in which case a collective excitation decays with time and does not destroy a Fermi liquid. The consequence is that, for moving fermions, the pairing instability exists only when their velocity is below the critical value. A finite T leads to the same effect: the pole is located in the upper frequency half-plane only at $T < T_c$, where T_c is comparable to Ω_p. At larger T, the pole is in the lower frequency half-plane, and a Fermi-liquid state is stable. Note by passing that in weak coupling theory bound pairs appear and condense at the same T. Beyond weak coupling, pairs condense at a lower T than the one at which they appear. This difference between the two temperatures may be large at strong coupling in lattice systems. This phenomenon is often termed as BCS-BEC crossover (BEC stands for Bose-Einstein condensation) [42] The meaning is that at strong coupling pairs of fermions appear at high $T = T_{pair}$, and condense at low $T = T_{BE}$, and between T_{BE} and T_{pair} the system can be described as a weakly/moderately interacting gas of uncondensed bosons.

The two main messages here are (i) the pairing instability can be detected from Fermi-liquid analysis as the appearance of the pole in Γ in the upper half-plane of the total frequency of two fermions, and (ii) there is no threshold for such phenomenon – Fermi liquid state gets destroyed already at infinitesimally small attraction between fermions.

Momentum-dependent interaction

How this helps our consideration of a possible pairing due to repulsive electron-electron interaction? If fully screened electron-electron interaction was a positive constant, we surely would not get any superconductivity as attraction is still a must condition for the pairing. But the screened electron-electron interaction $U(q)$ is generally a function of q. Let's see what we obtain for the pairing when the interaction $U(q)$ is still weak, but momentum-dependent.

The input for the analysis is the observation that the logarithmical singularity in Π_{pp} comes from fermions in the immediate vicinity of the Fermi surface. To logarithmic accuracy, the interaction between fermions with incoming momenta $\mathbf{k}, -\mathbf{k}$ and outgoing momenta $\mathbf{p}$ and $-\mathbf{p}$ can then be constrained to particles on the FS, such that $U(q = |\mathbf{k} - \mathbf{p}|)$ depends only the angle θ between incoming $\mathbf{k}_F$ and outgoing $\mathbf{p}_F$. The decomposition of the vertex function Γ into spin-singlet and spin-triplet channels now gives

$$\begin{aligned}
&\Gamma^0_{\alpha\beta,\gamma\delta} = -U(\theta)\delta_{\alpha\gamma}\delta_{\beta\delta} + U(\pi-\theta)\delta_{\alpha\delta}\delta_{\beta\gamma} \\
&= -\frac{U(\theta)+U(\pi-\theta)}{2}\left(\delta_{\alpha\gamma}\delta_{\beta\delta} - \delta_{\alpha\delta}\delta_{\beta\gamma}\right) \\
&-\frac{U(\theta)-U(\pi-\theta)}{2}\left(\delta_{\alpha\gamma}\delta_{\beta\delta} + \delta_{\alpha\delta}\delta_{\beta\gamma}\right) \qquad (39)
\end{aligned}$$

The way to proceed is to expand the interaction $U(\theta)$ into angular momentum harmonics. In 3D, we have

$$U(\theta) = \sum_l (2l+1) P_l(\theta) U_l, \tag{40}$$

where $P_l(\theta)$ are the Legendre polynomials: $P_0(\theta) = 1$, $P_1(\theta) = \cos\theta$, $P_2(\theta) = (3\cos^2\theta - 1)/2$, etc. Even components $\Pi_{l=2m}(\theta)$ satisfy $\Pi_{2m}(\theta) = \Pi_{2m}(\pi - \theta)$, odd components satisfy $\Pi_{2m+1}(\theta) = -\Pi_{2m+1}(\pi - \theta)$. Substituting into (39), we obtain that spin-singlet contribution is the sum of even components, and spin-triplet contribution is the sum of odd components.

$$\begin{aligned}
&\Gamma^0_{\alpha\beta,\gamma\delta}(\theta) = \\
&-\sum_{m=0}^{\infty} \Big[(4m+1) P_{2m}(\theta) U_{2m} \left(\delta_{\alpha\gamma}\delta_{\beta\delta} - \delta_{\alpha\delta}\delta_{\beta\gamma} \right) \\
&+(4m+3) P_{2m+1}(\theta) U_{2m+1} \left(\delta_{\alpha\gamma}\delta_{\beta\delta} + \delta_{\alpha\delta}\delta_{\beta\gamma} \right) \Big]
\end{aligned} \tag{41}$$

One can easily make sure that the spin structure of Γ is reproduced at every order, if we restrict with renormalizations in the particle-particle channel, i.e., even and odd angular momentum components do not mix. As a result, the full Γ in this approximation is given by

$$\begin{aligned}
&\Gamma^{full}_{\alpha\beta,\gamma\delta}(\theta) = \\
&-\sum_{m=0}^{\infty} \Big[(4m+1) P_{2m}(\theta) U^{full}_{2m} \left(\delta_{\alpha\gamma}\delta_{\beta\delta} - \delta_{\alpha\delta}\delta_{\beta\gamma} \right) \\
&+(4m+3) P_{2m+1}(\theta) U^{full}_{2m+1} \left(\delta_{\alpha\gamma}\delta_{\beta\delta} + \delta_{\alpha\delta}\delta_{\beta\gamma} \right) \Big]
\end{aligned} \tag{42}$$

Even more, using the property of the Legendre polynomials

$$\int \frac{d\Omega_q}{4\pi} P_m(\cos\theta_{k,q}) P_n(\cos\theta_{q,p}) = \frac{1}{2m+1} \delta_{m,n} P_m(\cos\theta_{k,p}) \tag{43}$$

where $\theta_{k,q}$ is the angle between fermions with momenta $\mathbf{k}_F$ and $\mathbf{q}_F$ and $d\Omega_q$ is the element of the solid angle for $\mathbf{q}_F$, one can show that components with different m also do not mix up, i.e., each partial component U^{full}_l of the full interaction is expressed only via U_l. The relations are the same as at $l = 0$, i.e.,

$$U^{full}_l(q = 0, \Omega) = \frac{U_l}{1 + U_l \Pi_{pp}(q = 0, \Omega)} \tag{44}$$

This result is very important for our story. It states that, even if the angular-independent component $U_{l=0}$ is repulsive, the pairing instability may still occur at some finite angular momentum l. All what is needed is that just one partial channel is attractive, either for even or for odd l. This may, in principle, occur even if overall the interaction is repulsive. A good hint comes from the analysis of screened

Coulomb interaction. As a reader surely knows, a screened potential far away from a charge contains Friedel oscillations – ripples of positive and negative regions of charge density (see Fig.5) Overall, screened interaction is indeed repulsive, but the negative regions can provide attraction at some angular momenta, particularly at large l, because dominant contributions to components U_l with $l >> 1$ come from $U(r)$ at large distances. The magnitude U_l is not an issue because, as we know, Π_{pp} is logarithmically singular at small frequencies. Furthermore, an attraction in just one channel is a sufficient condition for a superconducting instability, because if one of U_l^{full} has a pole in the upper half-plane of Ω, the full vertex $\Gamma^{full}_{\alpha\beta,\gamma\delta}(\theta)$ also has such pole. The only difference with the case of a constant attractive U is that when the instability occurs at some $l > 0$ a two-fermion bound pair has a non-zero angular momentum l.

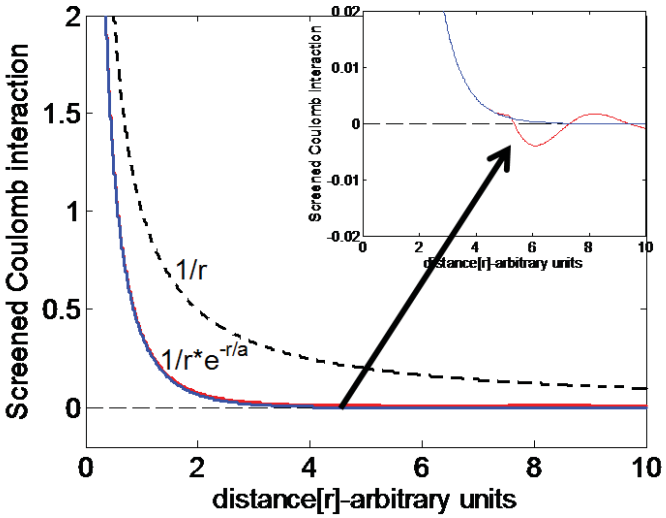

FIGURE 5. The screened coulomb potential as a function of r. $\frac{1}{r}$ (dashed line) is the bare coulomb potential. $\frac{1}{r}e^{-r/a}$ (blue line) is the Yukawa potential which includes regular screening and dies of exponentially (a is some characteristic screening length). The fully screened potential (red line) includes the contribution from the $2k_F$ scattering which gives rise to Friedel oscillations at large r. These oscillations are responsible for the attraction in large angular momentum channels. The inset is a zoomed in version, which shows the oscillations.

KOHN-LUTTINGER MECHANISM

Friedel oscillations at large distances occur by the special reason – the static particle-hole polarization bubble $\Pi_{ph}(q)$ is non-analytic at $q = 2k_F$. For free

fermions with spherical FS,

$$\begin{aligned}\Pi_{ph}(q,\Omega=0) &= i\int\frac{d^3kd\omega}{(2\pi\hbar)^4}G(k,\omega)G(k+q,\omega)\\ &= \frac{mk_F}{2\pi^2\hbar^3}\left(\frac{1}{2}+\frac{1-x^2}{4x}ln\left|\frac{1+x}{1-x}\right|\right)\end{aligned} \tag{45}$$

where $x\equiv\frac{q}{2k_F}$. Near $q=2k_F$ (or $x=1$), $\Pi(x)\propto(1-x)\log|1-x|$, and its derivatives over x are singular at $x=1$. This $2k_F$ non-analyticity is a universal property of a FL and it survives even if one adds self-energy and vertex corrections to the bubble. One can also show quite generally that the screening due to $2k_F$ scattering acts on top of "conventional" screening which transforms Coulomb potential into Yukawa-type short-range potential. In this respect, Friedel oscillations can be considered starting from either bare Coulomb, or Yukawa, or even Hubbard interaction potential.

Note in passing that the $2k_F$ non-analyticity is an example of the special role played by "hidden" 1D processes in a multi-dimensional FL [43]. Indeed, when $q=|\mathbf{k}_F-\mathbf{p}_F|$ is near $2k_F$, $\mathbf{p}_F$ is antiparallel to $\mathbf{k}_F$. One can make sure that the two internal fermions, which contribute to $(1-x)\log|1-x|$ term in $\Pi_{ph}(x)$, are also located near $\mathbf{k}_F$ and $-\mathbf{k}_F$, i.e., everything comes from fermions moving in direction along or opposite to $\mathbf{k}_F$

The effect of $2k_F$ oscillations on superconductivity was first considered by Kohn and Luttinger [26, 27], and the result is known as Kohn-Luttinger (KL) mechanism of superconductivity. The idea of KL was the following: let's incorporate all non-singular corrections to the interaction into new $U(\theta)$ and treat it as unknown, but regular function of θ. A simple exercise with Legendre polynomials shows that for any regular function of θ, partial components with angular momentum l (U_l in our case) scale as e^{-l}, i.e., are exponentially small at large l. It is natural to assume that this bare interaction is entirely repulsive, i.e., all $U_l>0$. If we substituted these U_l into (44), we would obviously not obtain any pairing instability. However, the input for the pairing problem is the full irreducible anti-symmetrized vertex function $\bar{\Gamma}^0$ in which incoming fermions have momenta $(\mathbf{k}_F,-\mathbf{k}_F)$ and outgoing fermions have momenta $(\mathbf{p}_F,-\mathbf{p}_F)$ (the word "irreducible" means that this vertex function does not contain contributions with the particle-particle bubble at zero total momentum). Such irreducible $\bar{\Gamma}^0$ contains additional contributions from non-analytic $2k_F$ scattering. KL computed $2k_F$ contribution to irreducible $\bar{\Gamma}^0(\theta)$ to second order in the renormalized $U(\theta)$. The corresponding diagrams are shown in Fig 6 The result is

$$\begin{aligned}&\bar{\Gamma}^0_{\alpha\beta,\gamma\delta}(\theta)=\\ &-A(\theta)\left(\delta_{\alpha\gamma}\delta_{\beta\delta}-\delta_{\alpha\delta}\delta_{\beta\gamma}\right)-B(\theta)\left(\delta_{\alpha\gamma}\delta_{\beta\delta}+\delta_{\alpha\delta}\delta_{\beta\gamma}\right)\end{aligned} \tag{46}$$

where

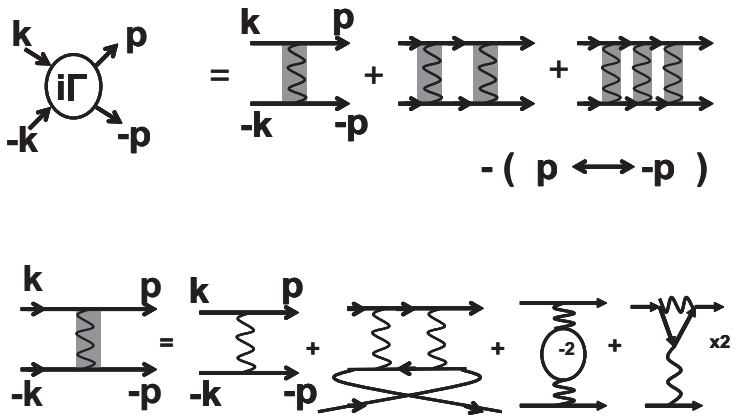

FIGURE 6. (Top) The fully renormalized vertex function in the Cooper channel is the sum of the particle-particle diagrams. The boxed wavy line is the irreducible pairing vertex which is the sum of all diagrams with the structure different from the Cooper channel. (Bottom) The expansion of the irreducible vertex to second order in the interactions. The second order terms are particle-hole channel contributions (Kohn-Luttinger diagrams)

$$A(\theta) = \frac{U(\theta)+U(\pi-\theta)}{2} - \Big(2U^2(\pi) - 2U(0)U(\pi) - U^2(0)\Big)\,\frac{\Pi_{ph}(\theta)+\Pi_{ph}(\pi-\theta)}{2}$$
$$B(\theta) = \frac{U(\theta)-U(\pi-\theta)}{2} - \Big(2U^2(\pi) - 2U(0)U(\pi) + U^2(0)\Big)\,\frac{\Pi_{ph}(\theta)-\Pi_{ph}(\pi-\theta)}{2} \tag{47}$$

$$\Pi_{ph}(\theta) \approx -(mk_F/16\pi^2\hbar^3)(1+\cos\theta)\log(1+\cos\theta), \tag{48}$$

and in the factors $(\Pi_{ph}(\theta) \pm \Pi_{ph}(\pi-\theta)$ in Eq. (47) one should keep only the term $\Pi_{ph}(\theta)$ for θ close to π and only the term $\Pi_{ph}(\pi-\theta)$ for θ close to 0.

Note that $U(0)$ terms in the prefactors for $\Pi_{ph}(\theta)$ in $A(\theta)$ and $B(\theta)$ have different signs. This is the consequence of the fact that these terms are of exchange type (two crossed interaction lines), and in the internal parts of the corresponding diagrams θ and $\pi-\theta$ are interchanged compared to other terms. Note also that for a constant U the exchange terms are the only ones which do not cancel out.

Now expand $A(\theta)$ and $B(\theta)$ into harmonics and consider large l. Like we said, regular terms coming from $U(\theta)$ are exponentially small. However, the terms of order U^2 are non-analytic, and integrating them with Legendre polynomials one finds that partial harmonics decay as $1/l^4$ rather than exponentially. Specifically, at large l,

$$S_l = -\int \frac{d\Omega_q}{4\pi}\Pi_{ph}(\theta)P_l(\cos\theta) \approx \frac{mk_F}{8\pi^2\hbar^3}\frac{(-1)^l}{l^4} \tag{49}$$

One can easily verify that A_l are again non-zero when $l=2m$ and B_l are non-zero when $l=2m+1$. In explicit form we obtain

$$\begin{aligned} &A_{l=2m} = U_{2m} + \\ &\Big(2U^2(\pi) - 2U(0)U(\pi) - U^2(0)\Big)\, S_{2m} \\ &B_{l=2m+1} = U_{2m+1} + \\ &\Big(2U^2(\pi) - 2U(0)U(\pi) + U^2(0)\Big)\, S_{2m+1} \end{aligned} \tag{50}$$

Al large l, U_l is exponentially small and can be neglected compared to $S_l \propto 1/l^4$. Because S_{2m+1} is negative and $2U^2(\pi) - 2U(0)U(\pi) + U^2(0) = (U(2k_F) - U(0))^2 + U^2(\pi)$ is positive for any form of $U(q)$, B_{2m+1} are definitely negative at large m. As a result, an isotropic system with initially repulsive interaction is still unstable towards pairing, at least with large odd angular momentum of a Cooper pair. The harmonics with even l are attractive when $U(0)/U(\pi) > \sqrt{3}-1$.

The KL scenario for the pairing can be extended in several directions. First, one can consider the case of strong regular screening, when the bare $U(q)$ can be approximated by a constant (the Hubbard model). In this situation, without $2k_F$ renormalization, the bare interaction is repulsive in $l=0$ ($s-$wave) channel, but zero in all other channels. Once $2k_F$ renormalization is included, $\bar{\Gamma}^0$ acquires angular dependence, and both odd and even partial components become attractive because for $U(0) = U(\pi) = U$, $A_{2m} = -U^2 S_{2m}$, $B_{2m+1} = U^2 S_{2m+1}$, and $S_{2m} > 0, S_{2m+1} < 0$. The issue is: at which l the coupling is most attractive? The analysis of this last issue requires some caution because at $l = O(1)$, all transferred momenta q, not only those near $2k_F$, contribute to partial components of $\bar{\Gamma}^0(\theta)$. One has to be careful here because some of regular contributions from q away from $2k_F$ may be already included into the renormalization of the Coulomb interaction into short-range, Hubbard U. If we just neglect this potential double counting, i.e., assume that the screening from Coulomb interaction into a Hubbard U is produced by the processes different from the KL ones, we can extend the KL analysis for a constant U to arbitrary l. It then turns out that attraction survives down to $l=1$, and the $l=1$ component is the strongest [28, 29]. In explicit form,

$$B_1 = -\frac{mk_F U^2}{2\pi^2\hbar^3}\,\frac{(2\log 2 - 1)}{5}. \tag{51}$$

Substituting this B_1 into the pairing channel, we obtain the pole in the triple component of the full $\Gamma^{full}(\theta)$ at $\Omega = i\Omega_p^{l=1}$, where

$$\Omega_p^{l=1} \propto e^{-B\left(\frac{\hbar}{ak_F}\right)^2}, \tag{52}$$

$B = 5\pi^2/(4(2\log 2 - 1))$, and, as before, $a = mU/4\pi\hbar^2$ is $s-$wave scattering length in Born approximation. The calculation of the prefactor requires quite serious efforts as one needs to include terms up to fourth order in the interaction (see Ref. [44]).

The $p-$wave pairing can be rationalized even when the bare interaction is angle-dependent. Because the momentum dependence is via $q^2 = 2k_F^2(1-\cos\theta)$, higher angular harmonics of $U(q)$ contain higher powers of k_F. In particular, $U_1 \sim U(r_0 k_F/\hbar)^2$, where r_0 is the radius of the interaction. Suppose it is repulsive. The p-wave component of the effective irreducible interaction, which we obtained, is of order $U(ak_F/\hbar)$ (see Eq. (51). The ratio a/r_0 is the Born parameter. When it is of order one, a and r_0 are of the same order, i.e., $ak_F \sim r_0 k_F$ are small. The induced attraction then wins because it contains a smaller power of the small parameter [28]. This reasoning, however, works only when $a \sim r_0$. If we treat interaction as small and k_F is arbitrary, bare repulsion is generally larger than induced attraction, unless a bare $U(q)$ is a constant.

Before we move forward, let us make a quick remark about KL effect in 2D systems. The eigenfunctions of the angular momenta in 2D are $P_l^{d=2} = \cos(l\theta)$ for $l \neq 0$ and $P_0^{d=2} = 1$. The expansion of the irreducible interaction in these eigenfunctions yields

$$U(\theta) = U_0 + 2\sum_{l>0} U_l \cos l\theta \tag{53}$$

The situation in 2D is more tricky than in 3D because in 2D Π_{ph} for free fermions remains flat all the way up to $q = 2k_F$, i.e., for a constant U, $U^2\Pi_{pp}(q)$ does not depend on the angle between incoming and outgoing fermions. Then harmonics with non-zero l do not appear, i.e., there is no KL effect. There is a non-analyticity in $\Pi_{ph}(q)$ at $2k_F$ also in 2D, but it is one-sided: at $q \geq 2k_F$, $\Pi_{ph}(q)$ behaves as $\Pi_{ph}(q) = \Pi_{ph}(2k_F) - a\sqrt{q^2 - 4k_F^2}$ $(a > 0)$, while at $q < 2k_F$, $\Pi_{ph}(q) = \Pi_{ph}(2k_F)$. However, the non-analyticity at $q > 2k_F$ is irrelevant for the pairing problem because we need the interaction between fermions right on the FS, and for them the largest momentum transfer is $2k_F$. The situation changes when we move to next order in U and include vertex corrections to particle-hole bubble. These corrections make $\Pi_{ph}(q)$ momentum-dependent also for $q < 2k_F$, and, most important, $2k_F$ non-analyticity becomes two-sided. At large l, partial harmonics of $\bar{\Gamma}^0(\theta)$ scale as $1/l^2$ and, like in 3D, are attractive for both even and odd l, if we set the bare pairing interaction, fully renormalized by vacuum corrections, to be a constant. The largest interaction is again in $l = 1$ ($p-$wave) channel, and the pole in the spin-triplet part of the full $\Gamma^{full}(\theta)$ is located at $\Omega = i\Omega_{2D}^{l=1}$, where $\Omega_{2D}^{l=1} \propto e^{-0.24/(ak_F/\hbar)^3}$.

Details and other discussion on the KL mechanism and its application to $p-$wave superconductivity in systems with strong ferromagnetic fluctuations can be found in Refs.[28, 29, 31, 44, 45, 46, 47, 48, 49, 50]. The rest of these lecture notes will be devoted to discussion of superconductivity in lattice models, where k_F is generally not small and rotational symmetry is broken.

SUPERCONDUCTIVITY IN LATTICE MATERIALS: APPLICATION TO PNICTIDES, CUPRATES AND DOPED GRAPHENE

In studying superconductivity in solid-state systems one has to deal with fermions moving on a lattice rather than in isotropic media. Lattice systems have only discrete symmetries, and in general FS does not have an isotropic form (spherical in 3D or circular in 2D) and may even be an open electron FS, meaning that its does not form a closed object centered at $k = 0$ and instead ends at the boundaries of the Brillouin zone. (The locus of points where energy is larger than E_F is a closed object in this situation, and such a FS is often called a closed hole FS). Also, in many cases electronic structure is such that there are several different FS's which can be either closed or open. We show examples in Fig. 7.

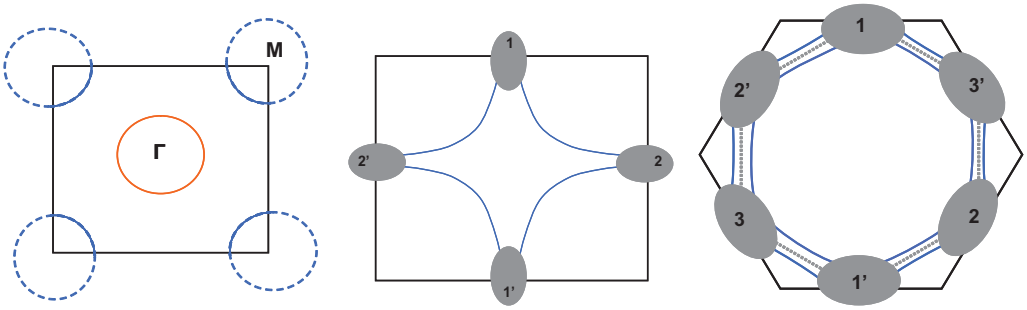

FIGURE 7. FS topologies for a "simplified" pnictide(left), for hole-overdoped cuprate(center) and doped graphene(right). In pnictides there are two kinds of FS's electrons and holes(blue and orange circles, respectively). For cuprates and graphene one can have disconnected pieces or a singly-connected FS, depending on the doping. The doping at which an open FS changes its character to a closed one is called the Van-Hove doping. At this doping the density of states is logarithmically singular near the saddle points. This points with enhanced density of states are marked by grey patches.

We will consider systems with inversion symmetry and $SU(2)$ spin symmetry. For such systems, the pairing instability is still towards a creation of a bound pair of two fermions with momenta $\mathbf{k}$ and $-\mathbf{k}$ in either spin-singlet or spin-triplet channel. However, if one attempts to expand the interaction into eigenfunctions of momenta for isotropic systems (Legendre polynomials $P_l(\theta)$ in 3D and $\cos(l\theta)$ in 2D), one finds that different angular components no longer decouple.

One can still do a partial decoupling, however, due to discrete symmetries of lattice systems. As an example, consider 2D fermions on a square lattice. Fermionic dispersion and interactions are invariant with respect to rotations by multiples of $\pi/2$ ($x \to y, y \to -x$ and $x \to -x, y \to -y$), with respect to reflections across x or y axis ($x \to -x$ or $y \to -y$), and with respect to reflections across diagonals ($x \to y$ or $x \to -y$). The corresponding symmetry group C_{4v} contains 8 elements and has four one-dimensional representations called A_1, A_2, B_1, B_2 and one two-dimensional representation E. Eigenfunctions from A_1 remain invariant under rotations and reflections, eigenfunctions from B_1 change sign under rotation by $\pi/2$ 2and under reflections across diagonals, but invariant under rotation by π and reflection across

TABLE 1. Basic functions in 1D representations of the square-lattice group D_{4h}

A_{1g}	$s-$wave	$\cos k_x + \cos k_y$, $\cos k_x \cos k_y$
A_{2g}	$g-$wave	$\sin k_x \sin k_y (\cos k_x - \cos k_y)$
B_{1g}	$d-$wave	$\cos k_x - \cos k_y$
B_{2g}	$d-$wave	$\sin k_x \sin k_y$

x or y, eigenfunctions from B_2 change sign under rotations by $\pi/2$, and under reflections across x, y, and one of diagonals, but remain invariant under rotation by π, and under reflection across another diagonal, and so on. In real 3D systems, interactions are also invariant with respect to $z \to -z$ inversion, and the symmetry group extends to D_{4h}, which includes 16 elements - 8 are even under to $z \to -z$ and 8 are odd (g and u subgroups). We will restrict our consideration to spin-singlet superconductivity with pair wave-functions symmetric with respect to $z \to -z$. Accordingly, we stick with four one-dimensional representations A_{1g}, A_{2g}, B_{1g} and B_{2g}. Each of these representations contains infinite number of eigenfunctions: 1, $\cos k_x + \cos k_y$, $\cos 2k_x + \cos 2k_y$, etc for A_{1g}, $\cos k_x - \cos k_y$, $\cos 2k_x - \cos 2k_y$, etc for B_{1g}, $\sin k_x \sin k_y$, $\sin 2k_x \sin 2k_y$, etc for B_{2g}, and so on. (For convenience, for Brillouin Zone variables we measure k in units of $\hbar/a$-where a is the lattice constant. This makes k dimensionless). The basic functions in each representation are summarized in Table 1.

If we try to group eigenfunctions of momenta from the isotropic case into these representations, we find that eigenfunctions with $l = 4n$ belong to A_{1g}, eigenfunctions with $l = 4n+1$ belong to E, eigenfunctions with $l = 4n+2$ belong to B_{1g} or B_{2g}, and eigenfunctions with $l = 4n+3$ belong to A_{2g}. Because of this decomposition, A_{1g} representation is often called $s-$wave, E is called p-wave, B_{1g} and B_{2g} are called d-wave ($d_{x^2-y^2}$ and d_{xy}, respectively), and A_{2g} is called g-wave. We will use these notations below.

Now, if we now expand the interactions in eigenfunctions of D_{4h} group and consider the pairing problem in the same way as we did before, we find that functions belonging to different representations decouple, but infinite set of functions within a given representation remain coupled. In this situation, the KL result for the isotropic case that the system will eventually be unstable against pairing with some angular momentum, is no longer valid because large l components from any given representation mix with smaller l components from the same representation, and the latter can be repulsive and larger in magnitude. Indeed, we will see below that for lattice systems, there is no guarantee that the pairing will occur, i.e., a non-superconducting state well may survive down to $T = 0$. We refer a reader to several papers in which superconductivity has either been ruled out at large U [51] or found to be present using the controllable approximation at any U (Ref. [52]).

At the same time, we will see that another part of KL-type analysis can be straightforwardly extended from isotropic to lattice systems. Namely, if we approximate the bare interaction $U(q)$ by a constant $U > 0$, we get a repulsive interaction in $s-$wave channel, but nothing in $p-$wave, $d-$wave, and g-wave channel. Once we include KL contribution to order U^2, we do get interaction in these channels. We

recall that in the isotropic case, the induced interaction in all non-s-wave channels is attractive. We show that the same happens in lattice systems, at least in the examples we consider below.

And there is more: even within $s-$wave channel, the full $\Gamma^{full}(\mathbf{k},-\mathbf{k};\mathbf{p},-\mathbf{p})$ is the solution of the coupled set of equations for infinite number of A_{1g} eigenfunctions. Diagonalizing the set one obtains infinite number of coupling constants (effective interactions). For a constant U, some eigenfunction are positive (repulsive), but some are zero. This can be easily understood by looking at the first two wavefunctions: 1 and $\cos k_x + \cos k_y$. The first is invariant under the shift $\mathbf{k} \to \mathbf{k} + (\pi, \pi)$, while the second changes sign under this transforation. A constant U cannot create a pairing wavefunction which changes sign under $\mathbf{k} \to \mathbf{k} + (\pi, \pi)$, hence the bare coupling for such a state is zero. KL terms produce momentum dependence of the irreducible interaction in the pairing channel and shift the eigenvalue for the sign-changing wavefunction. If this eigenvalue is attractive, then KL physics gives rise to an s-wave attractive interaction, which may be even stronger than KL-induced attraction in other channels.

We will discuss KL pairing in three representative families of materials: Fe-pnictides, cuprates, and doped graphene. Superconductivity in cuprates and Fe-pnictides (and Fe-chalcogenides) has been detected in numerous experiments. Superconductivity in doped graphene has been predicted theoretically but so far not detected experimentally. Although historically, cuprates were discovered first in 1986, for pedagogical reasons it is convenient to start with Fe-pnictides, where we show that superconductivity is due to KL-induced attraction in A_{1g} channel. We then discuss cuprates and show that KL renormalization of the pairing interaction gives rise to attraction in B_{1g} channel. Finally, we consider graphene doped to van-Hove density (or, equivalently, fermions on a triangular lattice at van-Hove doping) and show that KL mechanism gives rise to a doubly-degenerate pairing state, whose components can be viewed as $B1g$ and $B2g$ using square-lattice representations (or E_{2g} using representations for a hexagonal lattice).

There is extensive literature on all three classes of systems, and superconductivity is one of many interesting and still puzzling properties of these materials. Some researchers believe that in either all or some of these systems superconductivity is ultimately related to Mott physics[53], and some believe that superconductivity may be mediated by phonons[54, 55, 56, 57, 58]. We will not dwell into these issues and simply discuss the conditions and consequences of the electronic mechanism of superconductivity in these materials for the portions of the phase diagrams where electronic correlations are not strong enough to localize the electrons. The goal of these lectures is to discuss how much information about pairing one can extract from the analysis of the KL scenario. Our key conclusion is that the pairing in all three classes of materials can be traced to the same KL physics, which, however, predicts different pairing symmetries in each class of materials.

Superconductivity in Fe-Pnictides

Fe-pnictides are binary compounds of pnictogens, which are the elements from the 5th group: N, P, As, Sb, Bi. Superconductivity in these materials has been discovered in 2008 by Hosono and his collaborators [24]. Later, superconductivity has been found also in Fe-chalcogenides – Fe-based compounds with elements from the 16th group: S, Se, Te [59, 60, 61, 62].

The family of Fe-based superconductors (FeSCs) is already quite large and keeps growing. It includes 1111 systems RFeAsO (R=rare earth element) [24, 63, 64, 65], 122 systems XFe_2As_2(B=Ba,Na, K) [66, 67, 68, 69, 70] and AFe_2Se_2 (A = K, Rb, Cs) [71, 72], 111 systems like LiFeAs [73], and 11 systems, like $FeTe_{1-x}Se_x$ [74].

Parent compounds of most of FeSCs are metallic antiferromagnets [75]. Because electrons, which carry magnetic moments, can travel relatively freely from site to site, antiferromagnetic order is often termed as a "spin-density-wave" (SDW), by analogy with e.g., magnetism in Cr, rather than "Heisenberg antiferromagnetism" – the latter term is reserved for systems in which electrons are "nailed down" to particular lattice sites by very strong Coulomb repulsion.

Superconductivity in Fe-pnictides emerges upon either hole or electron doping (see Fig. 8), but can also be induced by pressure or by isovalent replacement of one pnictide element by another, e.g., As by P (Ref. [76]). In some systems, like LiFeAs [73] and LaFePO [77], superconductivity emerges already at zero doping, instead of a magnetic order.

magnetism, the electronic structure, the normal state properties of FeSCs, and the interplay between FeSCs and cuprate superconductors have been reviewed in several recent publications [78, 79, 80, 81, 82, 83, 84, 85, 86, 87, 88, 89, 90, 91]. Below we shall not dwell into the intricacies of the phase diagram but only focus on the superconductivity.

The electronic structure of FeSCs is fairly complex with multiple FS's surfaces extracted from ARPES and quantum oscillations measurements. In most systems, there are two or three near-cylindrical hole FS's centered at $k_x = k_y = 0$ and two electron FS's centered at (π, π). For electron pockets, states inside the pockets are occupied, for hole pockets, states inside the pockets are empty.

This electronic structure agrees with the one obtained theoretically from the ten-orbital model, which includes five Fe d-orbitals and takes into account the fact that an elementary unit cell contains two Fe-atoms because As atoms are located above and below an Fe plane. All d-orbitals hybridize, and to convert to band description one has to diagonalize the Hamiltonian in the orbital basis. The diagonalized quadratic Hamiltonian $H_2 = \sum_{i=1}^{10} \epsilon_{i,k} a^\dagger_{i,k} a_{i,k}$ describes ten fermionic bands, some of which cross chemical potential and give rise to hole and electron pockets. The interactions between these band fermions are the original interactions in the orbital basis, dressed up by the "coherence factors" associated with the transformation from orbital to band fermions (the coherence factors are the coefficients in the linear transformation from original fermions describing d-orbitals to new fermions which diagonalize the quadratic Hamiltonian). Interactions in the orbital basis are local, to a reasonably good accuracy, but the coherence factors know about

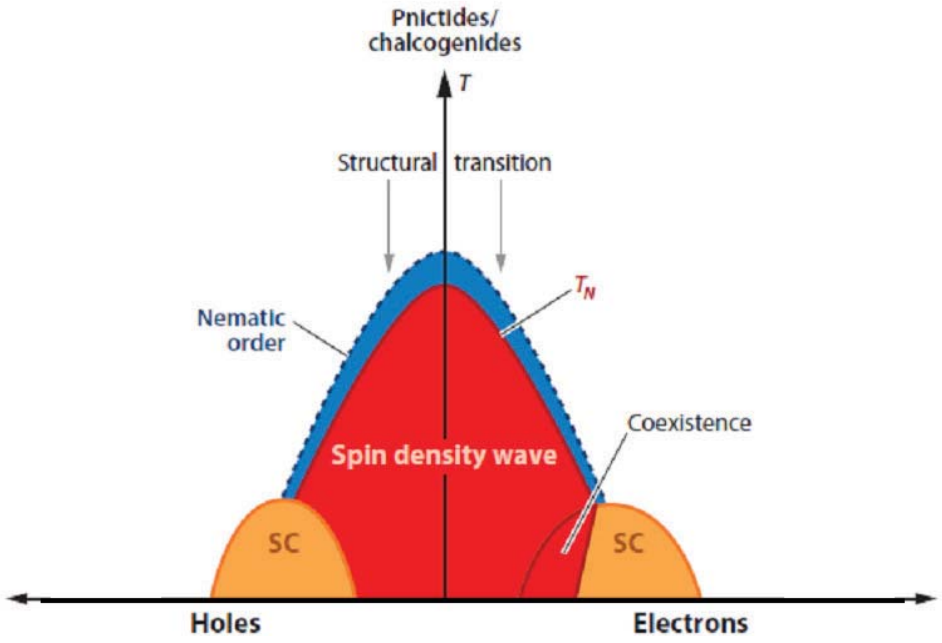

FIGURE 8. Schematic phase diagram of Fe-based pnictides upon hole or electron doping. In the shaded region, superconductivity and antiferromagnetism co-exist. Not all details/phases are shown. Superconductivity can be initiated not only by doping but also by pressure and/or isovalent replacement of one pnictide element by another [76]. Nematic phase at $T > T_N$ is another interesting subject but we don't discuss this in the text. Taken from Ref. [88].

fermion hopping from site to site and depend on momenta. As the consequence, the interactions between band fermions acquire momentum dependence, which leads to several new and interesting phenomena like the appearance of accidental zeros in the two-particle bound state wave function [92].

For proof-of-concept we consider a simpler problem: a 2D two-pocket model with one hole and one electron FS, both circular and of equal sizes (see Fig.7), and approximately momentum-independent.

The free-fermion Hamiltonian is the sum of kinetic energies of holes and electrons:

$$H_2 = \sum_{k,\sigma} \varepsilon_c c^\dagger_{k,\sigma} c_{k,\sigma} + \varepsilon_f f^\dagger_{k,\sigma} f_{k,\sigma} \tag{54}$$

where c stands for holes, f stands for electrons, and $\varepsilon_{c,f}$ stand for their respective dispersions with the property the $\varepsilon_c(k) = -\varepsilon_f(k+Q)$, where $\mathbf{Q}$ is the momentum vector which connects the centers of the two fermi surfaces. The density of states N_0 is the same on both pockets, and the electron pocket 'nests' perfectly within the hole pocket when shifted by $\mathbf{Q}$.

There are five different types of interactions between low-energy fermions: two intra-pocket density-density interactions, which we treat as equal, interaction between densities in different pockets, exchange interaction between pockets, and

pair hopping term, in which two fermions from one pocket transform into two fermions from the other pocket. We show these interactions graphically in Fig 9.

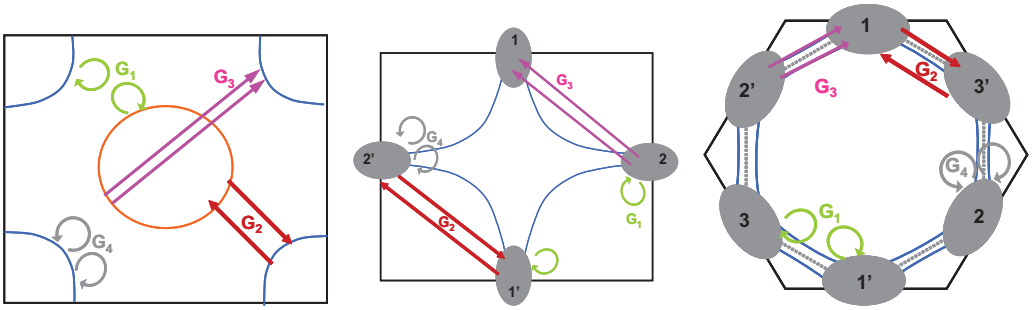

FIGURE 9. The interactions between patches/pockets in the pnictides(left), cuprates (center) and graphene (right). G_1 is a density-density interaction between fermions from different pockets/patches. G_2 is an exchange between the pockets/patches, G_3 is a pair hopping process between the pockets/patches, and G_4 is a density-density interaction within the same pocket/patch. All interactions are repulsive (positive).

In explicit form

$$\begin{aligned} H_{\rm int} &= G_1 \sum_{[k,\sigma]} c^\dagger_{k_1\sigma} f^\dagger_{k_2\sigma'} f_{k_3\sigma'} c_{k_4\sigma} \\ &+ G_2 \sum_{[k,\sigma]} f^\dagger_{k_1\sigma} c^\dagger_{k_2\sigma'} f_{k_3\sigma'} c_{k_4\sigma} \\ &+ \sum_{[k,\sigma]} \frac{G_3}{2} \left(c^\dagger_{k_1,\sigma_1} c^\dagger_{k_2,\sigma_2} f_{k_3,\sigma_2} f_{k_4,\sigma_1} + \text{h.c} \right) \\ &+ \sum_{[k,\sigma]} \left(\frac{G_4}{2} c^\dagger_{k_1,\sigma_1} c^\dagger_{k_2,\sigma_2} c_{k_3,\sigma_2} c_{k_4,\sigma_1} + c \leftrightarrow f \right) \end{aligned} \tag{55}$$

where $\sum_{[k,\sigma]}$ is short for the sum over the spins and the sum over all the momenta constrained to $k_1 + k_2 = k_3 + k_4$ modulo a reciprocal lattice vector.

As we did for isotropic systems, consider the vertex function for fermions on the FS, for zero total incoming momentum. Because there are two pockets, there are three relevant vertices: $\Gamma_{hh}(\mathbf{k}_F, -\mathbf{k}_F, \mathbf{p}_F, -\mathbf{p}_F); \Gamma_{ee}(\mathbf{k}_F, -\mathbf{k}_F, \mathbf{p}_F, -\mathbf{p}_F)$, where $\mathbf{k}_F$ and $\mathbf{p}_F$ belong to the same pocket, and $\Gamma_{he}(\mathbf{k}_F, -\mathbf{k}_F, \mathbf{p}_F, -\mathbf{p}_F)$, where $\mathbf{k}_F$ and $\mathbf{p}_F$ belong to different pockets (see Fig. 10). To first order in G_i, we have

$$\begin{aligned} \Gamma^0_{hh}(\mathbf{k}_F, -\mathbf{k}_F, \mathbf{p}_F, -\mathbf{p}_F) &= -G_4 \\ \Gamma^0_{ee}(\mathbf{k}_F, -\mathbf{k}_F, \mathbf{p}_F, -\mathbf{p}_F) &= -G_4 \\ \Gamma^0_{he}(\mathbf{k}_F, -\mathbf{k}_F, \mathbf{p}_F, -\mathbf{p}_F) &= -G_3 \end{aligned} \tag{56}$$

where the spin dependence for both terms is $\delta_{\alpha\gamma}\delta_{\beta\delta} - \delta_{\alpha\delta}\delta_{\beta\gamma}$. Let's now solve for the full G, restricting with the renormalizations in the pairing channel (i.e., with

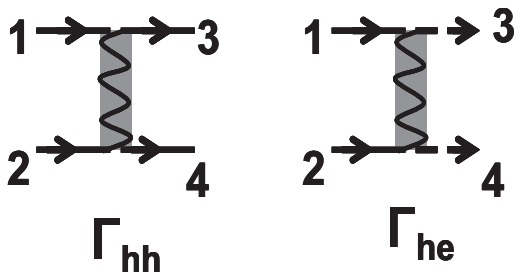

FIGURE 10. Vertices $\Gamma_{hh}=\Gamma_{ee}$ and Γ_{he} introduced in the 2 pocket model.

only Cooper logarithms). A simple analysis shows that the full Γ is given by

$$\begin{aligned}\Gamma_{hh}^{full} &= -\frac{1}{2}\left(\frac{G_4+G_3}{1+(G_4+G_3)\Pi_{pp}}+\frac{G_4-G_3}{1+(G_4-G_3)\Pi_{pp}}\right)\\ \Gamma_{ee}^{full} &= \Gamma_{hh}^{full}\\ \Gamma_{he}^{full} &= -\frac{1}{2}\left(\frac{G_4+G_3}{1+(G_4+G_3)\Pi_{pp}}-\frac{G_4-G_3}{1+(G_4-G_3)\Pi_{pp}}\right)\end{aligned} \tag{57}$$

and $\Pi_{pp}=\Pi_{pp}(q,\Omega)$ has the same logarithmical form as before. For $q=0$, $\Pi_{pp}(0,\Omega)=N_0(\log|\omega_c/\Omega|+i\pi/2)$, where N_0 is the density of states at the FS (and is the same on both electron and hole pockets)

We see that the presence or absence of a pole in Γ^{full}, depends on the signs of G_3+G_4 or G_4-G_3. If both are positive, there are no poles, i.e., non-superconducting state is stable. In this situation, at small Ω, $\Gamma_{hh}^{full}\approx -1/\Pi_{pp}$, $\Gamma_{he}^{full}\approx -(G_3/(G_4^2-G_3^2))\Pi_{pp}^2$, i.e., both vertex functions decrease (inter-pocket vertex decreases faster). If one (or both) combinations are negative, there are poles in the upper frequency half-plane and fermionic system is unstable against pairing. The condition for the instability is $|G_3|>G_4$. G_4 is inter-pocket interaction, and there are little doubts that it is repulsive, even if to get it one has to transform from orbital to band basis. G_3 is interaction at large momentum transfer, and, in principle, it can be either positive or negative depending on the interplay between intra- and inter-orbital interactions. In most microscopic multi-orbital calculations, G_3 turns out to be positive, and we set $G_3>0$ in our analysis (for the case $G_3<0$ see Ref. [54]).

For positive G_3, the condition for the pairing instability is $G_3>G_4$. What kind of a pairing state we get? First, both Γ_{hh}^{full} and Γ_{he}^{full} do not depend on the direction along each of the two pockets, hence the pairing state is necessary $s-$wave. On the other hand, the pole is in Γ_2, which appears with opposite sign in Γ_{hh}^{full} and Γ_{he}^{full}. The pole components of the two vertex functions then also differ in sign, which implies that the two-fermion pair wave function changes sign between pockets. Such an $s-$wave state is often call s^{+-} to emphasize that the pair wave function changes sign between FSs. This wave function much resembles the second wave

function from A_{1g} representation: $\cos k_x + \cos k_y$. It is still $s-$wave, but it changes sign under $\mathbf{k} \to \mathbf{k} + (\pi, \pi)$, which is precisely what is needed as hole and electron FSs are separated by (π, π). We caution, however, that the analogy should not be taken too far because the pairing wave function is defined *only* on the two FSs, and any function from A_{1g} representation which changes sign under $\mathbf{k} \to \mathbf{k} + (\pi, \pi)$ would work equally well.

Having established the pairing symmetry, we now turn to the central issue: how to get an attraction. Like we did in the isotropic case, let's start with the model with a momentum-independent (Hubbard) interaction in band basis. For such interaction, all G_i are equal, and, in particular, $G_3 = G_4$. Then Γ_2 just vanishes, i.e., at the first glance, there is no pole. However, from KL analysis for the isotropic case, we know that do decide whether or not there is an attraction in some channel, we need to analyze the full irreducible vertex function. To first order in G_i, the irreducible vertex function coincides with the (anti-symmetrized) interaction, but to order G_i^2, there appear additional terms. Let's see how they look like in the two pocket model.

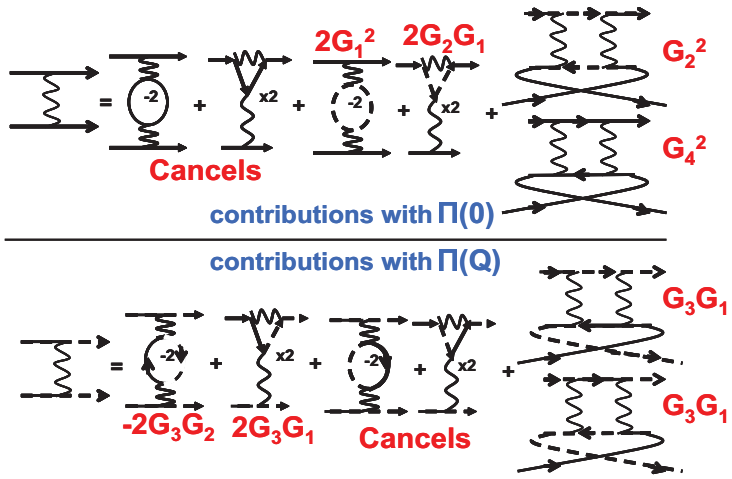

FIGURE 11. Contributions to the irreducible vertices $\bar{\Gamma}^0_{hh}$(top) and $\bar{\Gamma}_{he}$(bottom). $\bar{\Gamma}^0_{hh}$ only gets contributions form $\Pi(0)$ while $\bar{\Gamma}^0_{he}$ gets contribution from $\Pi(Q)$.

The contributions to irreducible $\bar{\Gamma}^0_{hh}$ and $\bar{\Gamma}^0_{he}$ are shown in Fig 11. In analytical form we have (keeping the notations G_i for better clarity)

$$\begin{aligned} \bar{\Gamma}^0_{hh} &= -G_4 - \left(G_4^2 + G_2^2 - 2G_1(G_1 - G_2)\right)\Pi_{ph}(0), \\ \bar{\Gamma}^0_{he} &= -G_3 - 2G_3(2G_1 - G_2)\Pi_{ph}(Q), \end{aligned} \tag{58}$$

where $\mathbf{Q} = (\pi, \pi)$. For a constant G, this reduces to

$$\begin{aligned} \bar{\Gamma}^0_{hh} &= -G\left(1 + 2G\Pi_{ph}(0)\right), \\ \bar{\Gamma}^0_{he} &= -G\left(1 + 2G\Pi_{ph}(Q)\right), \end{aligned} \tag{59}$$

The relation (57) still holds when we replace G_3 by $-\bar{\Gamma}^0_{he}$ and G_4 by $-\bar{\Gamma}^0_{hh}$. It can be very easily shown that $\Gamma^{full}_{ee} = \Gamma^{full}_{hh}$ and thus we will only deal with Γ^{full}_{hh} and Γ^{full}_{he} which are given by

$$\begin{aligned}
\Gamma^{full}_{hh} &= \frac{1}{2}\left(\frac{\bar{\Gamma}^0_{he}+\bar{\Gamma}^0_{hh}}{1-(\bar{\Gamma}^0_{he}+\bar{\Gamma}^0_{hh})\Pi_{pp}} + \frac{\bar{\Gamma}^0_{hh}-\bar{\Gamma}^0_{he}}{1-(\bar{\Gamma}^0_{hh}-\bar{\Gamma}^0_{he})\Pi_{pp}}\right), \\
\Gamma^{full}_{he} &= \frac{1}{2}\left(\frac{\bar{\Gamma}^0_{he}+\bar{\Gamma}^0_{hh}}{1-(\bar{\Gamma}^0_{he}+\bar{\Gamma}^0_{hh})\Pi_{pp}} - \frac{\bar{\Gamma}^0_{hh}-\bar{\Gamma}^0_{he}}{1-(\bar{\Gamma}^0_{hh}-\bar{\Gamma}^0_{he})\Pi_{pp}}\right),
\end{aligned} \tag{60}$$

and the condition for the pairing instability becomes $\bar{\Gamma}^0_{hh} > |\bar{\Gamma}^0_{he}|$. Comparing the two irreducible vertex functions, we find

$$\bar{\Gamma}^0_{hh} - \bar{\Gamma}^0_{he} = 2G^2\left(\Pi_{ph}(Q) - \Pi_{ph}(0)\right) \tag{61}$$

i.e., the condition for the pairing is satisfied when $\Pi_{ph}(Q) > \Pi_{ph}(0)$. For a gas of fermions with one circular FS, $\Pi_{ph}(q)$ either stays constant or decreases with q, and the condition $\Pi_{ph}(Q) > \Pi_{ph}(0)$ cannot be satisfied. However, in our case, there are two FS's separated by $\mathbf{Q}$, and, moreover, one FS is of hole type, while the other is of electron type. One can easily verify that, in this situation, $\Pi_{ph}(Q)$ is enhanced comparable to $\Pi_{ph}(0)$. We present the plot of $\Pi_{ph}(q)$ along $q_x = q_y$ in Fig 12. Indeed, $\Pi_{ph}(Q)$ is much larger than $\Pi_{ph}(0)$.

We see therefore that for the two-pocket model with circular hole and electron FSs and a constant repulsive electron-electron interaction

- the KL mechanism – the renormalization of the bare interaction into an irreducible pairing vertex, does give rise to a pairing,
- the pair wave function has A_{1g} (s-wave) symmetry, but changes sign between hole and electron pockets

Comparing isotropic and lattice cases, we see two differences. First, because of the lattice, particle-hole bubble $\Pi_{ph}(q)$ no longer has to be a decreasing function of q. In fact, as we just found, in the two-pocket model the KL mechanism leads to a pairing instability precisely because $\Pi_{ph}(Q)$ is larger than $\Pi_{ph}(0)$. Second, because we deal with fermions with circular FSs located near particular $k-$points, polarization operators at small momentum transfer and momentum transfer $\mathbf{Q} = (\pi, \pi)$ can be approximated by constants. Then the irreducible vertex function has only an $s-$wave (A_{1g}) harmonic, like the bare interaction, i.e. KL renormalization does not generate interactions in other channels. Treating pockets as circular is indeed an approximation, because for square lattice the only true requirement is that each FS is symmetric with respect to rotations by multiples of $\pi/2$ (C_4 symmetry). For small pocket sizes, deviations from circular forms are small, but nevertheless are generally finite. If we include this effect, we find that the KL effect does generate interactions in other channels (B_{1g}, B_{2g}, and A_{2g}), which may be attractive, and also leads to more complex structure of the pair

wave function in s^{+-} channel, which now acquires angular dependence along hole and electron pockets, consistent with C_4 symmetry[92, 93]

The situation changes when we consider the actual bare interactions G_i, extracted from the multi-orbital model. Then $G_4 - G_3$ is generally non-zero already before KL renormalization. It is natural to expect that the bare interaction is a decreasing function of momenta, in which case G_4, which is the interaction at small momentum transfer, is larger than the interaction G_3 at momentum transfer near Q. Then the KL term has to compete with the first-order repulsion. As long as $G\Pi_{ph}(Q)$ is small, KL renormalization cannot overshoot bare repulsion, and the bound state does not appear. The situation may change when we include momentum dependence of the interaction and non-circular nature of the pockets. In this last case, there appears infinite number of A_{1g} harmonics, which all couple to each other, and in some cases one or several eigenfunctions may end up as attractive [94]. Besides, angle dependence generates $d-$wave and $g-$wave harmonics, and some of eigenfunctions in these channels may also become attractive and compete[95]. Still, however, in distinction to the isotropic case, there is no guarantee that "some" eigenfunction from either A_{1g}, or B_{1g}, or B_{2g}, or A_{2g}, will be attractive. A lattice system may well remain in the normal state down to $T = 0$.

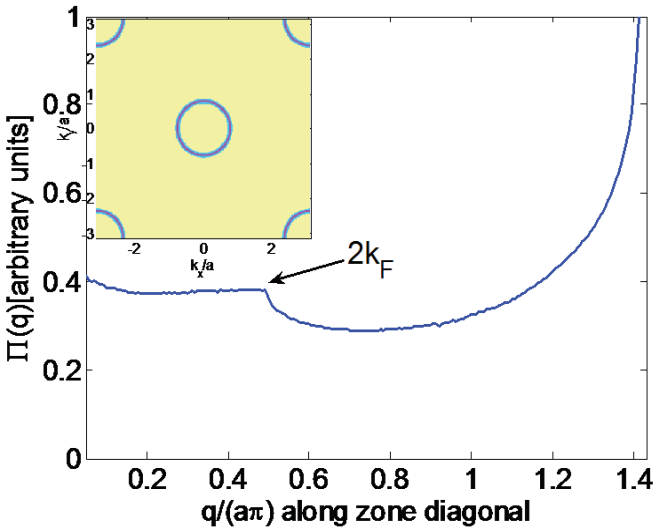

FIGURE 12. The plot of $\Pi(q)$ for a 2-pocket model with $\vec{q}$ along the zone diagonal. When $\vec{q} < 2k_F$, $\Pi(q)$ saturates, as it is expected for a 2D system with a circular Fermi surface. Note the $2k_F$ cusp-like feature, which is the one-sided $2k_F$ non-analiticity of $\Pi(q)$ in 2D. At larger q, $\Pi(q)$ gets larger and almost diverges at $\vec{q} \sim \vec{Q}$ due to near-nesting. The inset shows the FS topology for which $\Pi(q)$ has been calculated. The arcs at the corners are parts of the electron pocket and the one in the center is the hole pocket.

We will discuss how to go beyond second order in G in the next section. In the remainder of this section we discuss KL physics in the two other classes of systems – cuprates and doped graphene.

Superconductivity in cuprates

Cuprates are layered materials with one or more crystal planes consisting of Cu and O atoms (two O per Cu), and charge reservoirs between them. Superconductivity is widely believed to originate from electron-electron interactions in these CuO_2 planes. The undoped parent compounds are Mott insulators/Heisenberg antiferromagnets due to very strong Coulomb repulsion which prevents electron hopping from Cu to Cu and therefore localizes electrons near lattice sites. Doping these insulating CuO_2 layers with carriers (by adding/removing electrons from/to charge reservoir) leads to a (bad) metallic behavior and to the appearance of high-temperature superconductivity. A schematic phase diagram of doped cuprates is shown in Fig. 13. The richness of this phase diagram generated a lot of efforts, both in experiment and in theory to understand the key physics of the cuprates (see e.g. Refs.[35, 39, 53, 96, 97, 98, 99, 100, 101, 102, 103, 104, 105, 106, 107]. There are several features in the phase diagram, like the pseudogap in hole-doped cuprates, which are still not fully understood, although a substantial progress has been made over the last few years on the issue of the interplay between pseudogap and superconductivity [108, 109, 110]

By all accounts, the symmetry of the superconducting state does not change between small doping, where pseudogap physics is relevant, and doping above the optimal one. For these larger dopings, ARPES and quantum oscillation experiments show a large FS (see Fig. 14) consistent with Luttinger count for fermionic states. In this doping range, it is natural to expect that the pairing symmetry can be at least qualitatively understood by performing weak coupling analysis.

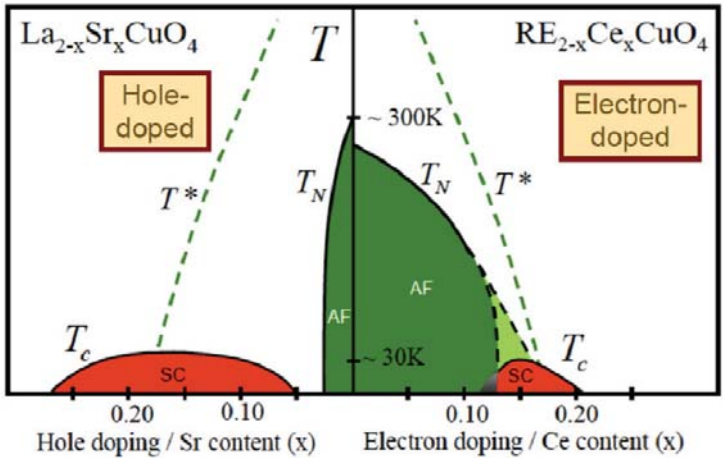

FIGURE 13. Typical phase diagram for the cuprates for electron and hole doping. The similarity of this phase diagram with pnictides is the proximity to the antiferromagnetic phase. Amongst differences, the most important one is the fact that the antiferromagnetic phase in cuprates stems out of a Mott insulator in the parent compounds. Others are a remarkable asymmetry between electron and hole doping and pseudogap phase indicated by the T^* line. T_N is the transition into the antiferromagnetic state and T_c is the transition into the superconducting state. We shall only focus on the superconducting aspect of this phase diagram. Taken from Ref. [99].

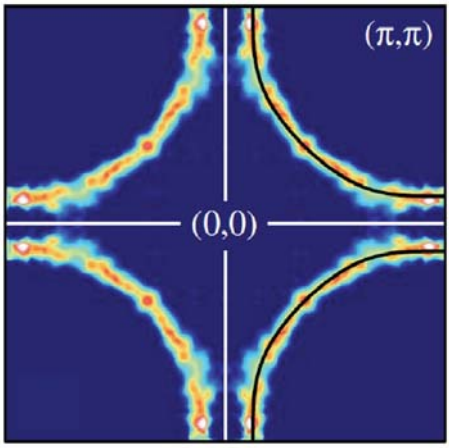

FIGURE 14. Angle resolved Photoemission data from Ref.[111], showing the presence of a large FS for doped $Tl_2Ba_2CuO_{6+\delta}$. The FS is extracted from the position of the peak of the spectral function in the $k-$space.

The FS for hole-doped cuprates is an is open electron FS shown in Fig. 7(center) and Fig. 14. Central to our consideration is the fact that the fermionic density of states is the largest near the points $(0, \pm\pi)$ and $(\pm\pi, 0)$, where two FS lines come close to each other (one can show that the density of states is logarithmically enhanced and actually diverges[112] when the two FS lines merge at $(0, \pm\pi)$ and $(\pm\pi, 0)$). The FS regions with the largest DOS mostly contribute to superconductivity, and, to first approximation, one can consider the FS in Fig. 7(center) as consisting of four patches. We focus on spin-singlet pairing, in which case a pair wave function is an even function of momentum, and it has the same form in the pairs of patches which transform into each other under inversion. This leaves two non-equivalent patches, which for definiteness we choose to be near $(0, \pi)$ and $(\pi, 0)$.

The resulting two-patch model is in many respects similar to the two-pocket model for Fe-pnictides, only instead of hole-hole, electron-electron, and hole-electron interaction we now have intra-patch and inter-patch interactions for two patches, which we label as 1 and 2. The interaction Hamiltonian contains four terms, like in Eq. 55, and the full pairing vertices $\Gamma_{11}^{full} = \Gamma_{22}^{full}$ and Γ_{12}^{full} are

$$\begin{aligned}
\Gamma_{11}^{full} &= \frac{1}{2}\left(\frac{\bar{\Gamma}_{12}^0 + \bar{\Gamma}_{11}^0}{1-(\bar{\Gamma}_{12}^0 + \bar{\Gamma}_{11}^0)\Pi_{pp}} + \frac{\bar{\Gamma}_{11}^0 - \bar{\Gamma}_{12}^0}{1-(\bar{\Gamma}_{11}^0 - \bar{\Gamma}_{12}^0)\Pi_{pp}}\right), \\
\Gamma_{12}^{full} &= \frac{1}{2}\left(\frac{\bar{\Gamma}_{12}^0 + \bar{\Gamma}_{11}^0}{1-(\bar{\Gamma}_{12}^0 + \bar{\Gamma}_{11}^0)\Pi_{pp}} - \frac{\bar{\Gamma}_{11}^0 - \bar{\Gamma}_{12}^0}{1-(\bar{\Gamma}_{11}^0 - \bar{\Gamma}_{12}^0)\Pi_{pp}}\right),
\end{aligned} \tag{62}$$

or

$$\begin{aligned}\Gamma^{full}_{11}+\Gamma^{full}_{12} &= \frac{\bar\Gamma^0_{12}+\bar\Gamma^0_{11}}{1-(\bar\Gamma^0_{12}+\bar\Gamma^0_{11})\Pi_{pp}}\\ \Gamma^{full}_{11}-\Gamma^{full}_{12} &= \frac{\bar\Gamma^0_{11}-\bar\Gamma^0_{12}}{1-(\bar\Gamma^0_{11}-\bar\Gamma^0_{12})\Pi_{pp}}\end{aligned} \tag{63}$$

where, as before, $\bar\Gamma^0$ are irreducible pairing vertices and $\Pi_{pp}=\Pi_{pp}(q,\Omega)$ contains the Cooper logarithm. To first order in the interaction $\bar\Gamma^0_{11}=\Gamma^0_{11}=-G_4$, and $\bar\Gamma^0_{12}=\Gamma^0_{12}=-G_3$, such that $\bar\Gamma^0_{12}+\bar\Gamma^0_{11}=-(G_4+G_3), \bar\Gamma^0_{11}-\bar\Gamma^0_{12}=-(G_4-G_3)$. Superconductivity requires $\bar\Gamma^0_{11}+\bar\Gamma^0_{12}$ or $\bar\Gamma^0_{11}-\bar\Gamma^0_{12}$ to be positive. For Hubbard interaction $G_i=G$, the bare $\Gamma^0_{11}+\Gamma^0_{12}=-(G_3+G_4)=-2G$ is negative, hence there is no pairing instability which would lead to a state with sign-preserving wave-function. At the same time, $\Gamma^0_{11}-\Gamma^0_{12}=G_3-G_4=0$, hence the coupling vanishes for a potential instability towards a pairing with a wave function which changes sign between patches. To obtain the information about the sign of the irreducible $\Gamma^0_{11}-\Gamma^0_{12}$ one then needs to include KL renormalization. The result is, predictably, the same as in two-pocket model, namely

$$\bar\Gamma^0_{11}-\bar\Gamma^0_{12}=2G^2\left(\Pi_{ph}(Q)-\Pi_{ph}(0)\right) \tag{64}$$

where $Q=(\pi,\pi)$ is now the distance between patches. The two particle-hole polarization bubbles can be straightforwardly calculated for $t-t'$ model of fermionic dispersion with hopping between nearest and next nearest neighbors. The result is that $\Pi_{ph}(Q)>\Pi_{ph}(0)$ (see Fig. 15). Then $\bar\Gamma^0_{11}-\bar\Gamma^0_{12}>0$, and the combination of full vertices $\Gamma^{full}_{11}-\Gamma^{full}_{12}$ has a pole in the upper frequency half-plane, at $\Omega=i\Omega_p$, which is the solution of $2G^2\left(\Pi_{ph}(Q)-\Pi_{ph}(0)\right)\Pi_{pp}(i\Omega_p)=1$.

So far, everything is the same as in the two-pocket model. But there is qualitative difference between the two cases. In the two-pocket model, the sign-changing pair wave-function changes sign between different FS pockets, but preserves the same sign along a given pocket. Such a wave function belongs to A_{1g} representation. In two-patch model, the sign-changing wave function changes sign between the two ends of the same "arc" of the FS. In other words, it changes sign under $\pi/2$ rotation from x to y axis. According to classification scheme, such a wave function belongs to B_{1g} representation, i.e., has a d-wave symmetry. Further, if we move along the FS arc away from patches and assume that the pairing wave function does not vanish on the FS, except may be special points, we immediately conclude that it should change sign right at the center of the arc, i.e., at the direction along zone diagonal. By symmetry, this should happen along each diagonal. The prototype wave function for such a state is $\cos k_x-\cos k_y$. We caution, however, that in the patch model we only know the wave function near $(0,\pi)$ and $(\pi,0)$ and its evolution between the patches is generally described by the whole subset of wave functions from B_{1g} representation with the form $\cos((2m+1)k_x)-\cos((2m+1)k_y)$.

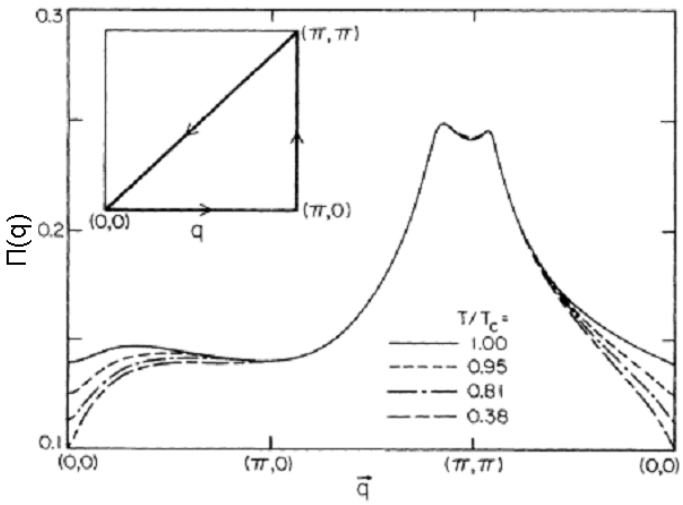

FIGURE 15. The plot of $\Pi(q)$ for a FS topology shown in Fig. 14 with $\vec{q}$ along the directions in the Brillouin Zone shown in the inset. Different lines are for different temperatures. Observe that $\Pi(Q)$ is always larger that $\Pi(0)$. Taken from Ref. [104]

We see therefore that for two-patch model with a constant repulsive electron-electron interaction

- the KL mechanism again gives rise to pairing,
- the pair wave function has B_{1g} (d-wave) symmetry, and changes sign twice along the open electron FS

The KL consideration can also be applied to electron-doped cuprates [113], but the analysis in this case is somewhat different as hot spots are located close to Brillouin zone diagonals [99].

Superconductivity in doped graphene

Graphene is a two-dimensional array of carbon atoms on a honeycomb lattice. The energy dispersion of graphene has two bands due two non-equivalent positions of atoms on a honeycomb lattice. The two bands touch each other at six points in the Brillouin zone, and the dispersion near these points is $\pm|\vec{k}|$ what brought them the name Dirac points. At zero doping, the Fermi level passes right through Dirac points, what gives rise to highly interesting low-energy physics[114]. Upon doping by either electron or holes, six separate pockets of carriers emerge. Upon further doping, these pockets grow, merge at some doping x_c, and at even larger dopings form a large hexagonal FS (see Fig. 7 right). Such a high doping of a single layer graphene has been achieved in Ref. [115] by placing Ca and K dopants above and below a graphene layer. At $x = x_c$ the system passes through a Van-Hove

singularity which results in an enhanced density of states at the six saddle points where nearest pockets merge. The fermionic dispersion at $x = x_c$ is very similar to that in the cuprates at the Van-Hove doping, but the tendency to the nesting (the existence of parallel pieces of the Fermi surface) is more pronounced here because in graphene the tight-binding band structure is not sensitive to the second neighbor hopping[114, 116].

The increase of the density of states near Van Hove doping increases the relative strength of the interaction effects, and brings in a possibility that already at a weak coupling the Fermi liquid state will become unstable towards some kind of order. A number of candidate ordered states has been considered, including superconductivity, SDW order, nematic order and so on. See [34, 114, 116, 117, 118, 119, 120, 121, 122]. Because the density of state diverges at the saddle points at Van Hove doping, each state can be can be self-consistently obtained at weak coupling. A phase diagram of doped graphene is shown in Fig. 16. Superconductivity has also been observed and analyzed in graphite intercalated compounds like C_6Ca and C_6Yb [123]. This superconductivity may be due to electron-electron interaction [124], but most likely the pairing interaction in these materials is mediated by intercalant phonons and/or acoustic phonons.

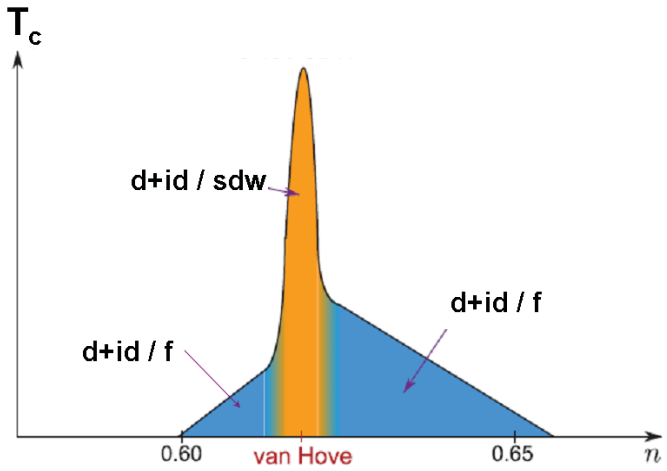

FIGURE 16. Schematic phase diagram of doped graphene. T_c is the instability temperature towards spin singlet $d+id$ or spin triplet $f-$wave SC states, or SDW state. T_c is plotted against doping (n). Doped Graphene is expected to be mostly superconducting with competition with the SDW phase near the Van-Hove region. Taken from Ref. [122]

The presence of saddle (Van-Hove) points along the FS is the feature that draws our attention and invites us to perform an analysis similar to that in the cuprates, but with three rather than two non-equivalent patches (overall there are six Van Hove points along the FS, but only three are unique, the three others are related by inversion symmetry (see Fig7 right). The treatment of doped graphene parallels the description in the above two subsections, but we will see that there are interesting details here, not present in the earlier models.

We treat the low-energy physics of doped graphene within the effective three

patch model, just like we did for the cuprates. We introduce intra-patch and inter-patch vertices Γ_{ij},$i,j \in (1,2,3)$ with $\Gamma_{ij} = \Gamma_{ji}$. Because the three patches are fully symmetric, the total number of independent vertices is just two:

$$\begin{aligned} \Gamma^0_{11} = \Gamma^0_{22} = \Gamma^0_{33} = -G_4 = \Gamma^0_u \\ \Gamma^0_{12} = \Gamma^0_{13} = \Gamma^0_{23} = -G_3 = \Gamma^0_v \end{aligned} \tag{65}$$

We follow the same line of reasoning as before. The full pairing vertices Γ^{full}_{11} and Γ^{full}_{12} are expressed in terms of irreducible vertices $\bar{\Gamma}^0_u$ and $\bar{\Gamma}^0_v$ as

$$\begin{aligned} \Gamma^{full}_{11} &= \bar{\Gamma}^0_u + \bar{\Gamma}^0_u \Gamma^{full}_{11} \Pi_{pp} + \bar{\Gamma}^0_v \left(\Gamma^{full}_{21} + \Gamma^{full}_{31} \right) \Pi_{pp} \\ \Gamma^{full}_{12} &= \bar{\Gamma}^0_v + \bar{\Gamma}^0_u \Gamma^{full}_{12} \Pi_{pp} + \bar{\Gamma}^0_v \left(\Gamma^{full}_{22} + \Gamma^{full}_{32} \right) \Pi_{pp} \end{aligned} \tag{66}$$

The solutions of this set are

$$\begin{aligned} \Gamma^{full}_{11} &= \frac{1}{3} \left(\frac{\bar{\Gamma}^0_u + 2\bar{\Gamma}^0_v}{1 - (\bar{\Gamma}^0_u + 2\bar{\Gamma}^0_v)\Pi_{pp}} + 2 \frac{\bar{\Gamma}^0_u - \bar{\Gamma}^0_v}{1 - (\bar{\Gamma}^0_u - \bar{\Gamma}^0_v)\Pi_{pp}} \right) \\ \Gamma^{full}_{12} &= \frac{1}{3} \left(\frac{\bar{\Gamma}^0_u + 2\bar{\Gamma}^0_v}{1 - (\bar{\Gamma}^0_u + 2\bar{\Gamma}^0_v)\Pi_{pp}} - \frac{\bar{\Gamma}^0_u - \bar{\Gamma}^0_v}{1 - (\bar{\Gamma}^0_u - \bar{\Gamma}^0_v)\Pi_{pp}} \right) \end{aligned} \tag{67}$$

or

$$\begin{aligned} \Gamma^{full}_{11} + 2\Gamma^{full}_{12} &= \frac{\bar{\Gamma}^0_u + 2\bar{\Gamma}^0_v}{1 - (\bar{\Gamma}^0_u + 2\bar{\Gamma}^0_v)\Pi_{pp}} \\ \Gamma^{full}_{11} - \Gamma^{full}_{12} &= \frac{\bar{\Gamma}^0_u - \bar{\Gamma}^0_v}{1 - (\bar{\Gamma}^0_u - \bar{\Gamma}^0_v)\Pi_{pp}} \end{aligned} \tag{68}$$

we see that to get the pairing we need either $\bar{\Gamma}^0_u + 2\bar{\Gamma}^0_v$ or $\bar{\Gamma}^0_u - \bar{\Gamma}^0_v$ to be positive. To first order in the interaction we have $\bar{\Gamma}^0_u = \Gamma^0_u = -G_4$ and $\bar{\Gamma}^0_v = \Gamma^0_v = -G_3$, hence the conditions for the pairing are $G_4 + 2G_3 < 0$ or $G_3 > G_4$. The first condition is analogous to $G_3 + G_4 < 0$ for the two-patch model and is never satisfied for a repulsive interaction, when G_4 and G_3 are both positive. The second condition is exactly the same as in two-patch model and requires inter-patch interaction to be larger than intra-patch interaction. If the bare interaction is momentum-independent, $G_3 = G_4 = G$, and one of the two pairing channels is neither repulsive nor attractive.

Continue with the Hubbard interaction. To second order in U, we have from KL renormalization

$$\begin{aligned} \bar{\Gamma}^0_u &= -G_4 - \Pi_{ph}(0) \left[G_4^2 + 2G_2^2 - 4G_1(G_1 - G_2) \right] \\ \bar{\Gamma}^0_v &= -G_3 - \Pi_{ph}(Q) \left[2G_3(2G_1 - G_2) \right] \end{aligned} \tag{69}$$

and $\bar{\Gamma}^0_u - \bar{\Gamma}^0_v$ becomes

$$\bar{\Gamma}^0_u - \bar{\Gamma}^0_v = G^2(2\Pi_{ph}(Q) - 3\Pi_{ph}(0)) \tag{70}$$

Like in the previous two examples, if $\Pi_{ph}(Q)$ is larger than $\Pi_{ph}(0)$ (specifically, if $\Pi_{ph}(Q) > (3/2)\Pi_{ph}(0)$) the irreducible pairing interaction is attractive. The particle-hole bubble can be straightforwardly computed and the result is, predictably, that near Van-Hove doping, $\Pi_{ph}(Q) > (3/2)\Pi_{ph}(0)$. This result was fist obtained by Gonzales[116] and reproduced in more recent work [34].

So far, the results are virtually undistinguishable from the previous two cases. The new physics in the three-patch model reveals itself when we note that the presence of the pole for the combination $\Gamma^{full}_{11} - \Gamma^{full}_{12}$ and its absence for $\Gamma^{full}_{11} + 2\Gamma^{full}_{12}$ in Eq. (68) implies that near the instability the fully renormalized intra-patch and inter-patch pairing vertices must satisfy

$$\Gamma^{full}_{11} = -2\Gamma^{full}_{12} \tag{71}$$

together with the symmetry-imposed conditions $\Gamma^{full}_{11} = \Gamma^{full}_{22} = \Gamma^{full}_{33}$ and $\Gamma^{full}_{12} = \Gamma^{full}_{13} = \Gamma^{full}_{23}$. In other words if intra-patch $\Gamma^{full}_{ii} = D$, then inter-patch $\Gamma^{full}_{ij} = -\frac{D}{2}$ for $i \neq j$. Now, if we view each Γ^{full}_{ii} as the modulus square of the superconducting order parameter $|\Delta_i|^2$ and Γ^{full}_{ij} as $Re[\Delta_i \Delta^*_j]$, we immediately find that Eq. (71) implies that the relative phase of the superconducting order parameter must change by $\pm\frac{2\pi}{3}$ between each pair of patches ($\cos\frac{2\pi}{3} = -\frac{1}{2}$). In other words, if the order parameter in patch 1 is Δ_1, then $\Delta_2 = \Delta_1 e^{\pm 2\pi i/3}$ and $\Delta_3 = \Delta_1 e^{\pm 4\pi i/3}$. The two resulting Δ structures are shown in Fig. 17. We used the fact that this is spin-singlet pairing, hence $\Delta(-k) = \Delta(k)$. This is a $d-$wave gap because if we extend the gap structure to all FS, we find that the gap changes sign twice along the FS. However, we also need to pick one sign of the phase change or the other, and this choice breaks the Z_2 symmetry, which in our case is time-reversal symmetry because it changes the order parameter to its complex conjugate. Putting it differently, Z_2 symmetry corresponds to the freedom of choice of counter clockwise or clockwise phase winding by 4π along the full FS. Such a state is called $d + id$ or $d - id$. It has a rich phenomenology and is highly desirable for applications[129, 130, 131, 132, 133, 134, 135, 136].

Although intuitively it seems obvious that Z_2 symmetry is broken in a $d + id$ state, one actually needs to do full Ginzburg-Landau (GL) analysis and make sure that the superconducting condensation energy is the largest when only $d + id$ or only $d - id$ solution develops, but not both of them. This, however, requires one to go beyond the instability point, while our goal is to get as much information as possible from the normal state analysis. We just refer to Ref [34] where GL functional has been derived and analyzed. The result of that study is that Z_2 symmetry is indeed broken below T_c.

Another way to see that the two d-wave states are degenerate by symmetry is to look at the representations of the symmetry group D_{6h}. The two d-wave wave-functions $\cos k_x - \cos k_y$ and $\sin k_x \sin k_y$ belong to a two-dimensional E_{2g} representation of D_{6h} and must indeed be degenerate by symmetry.

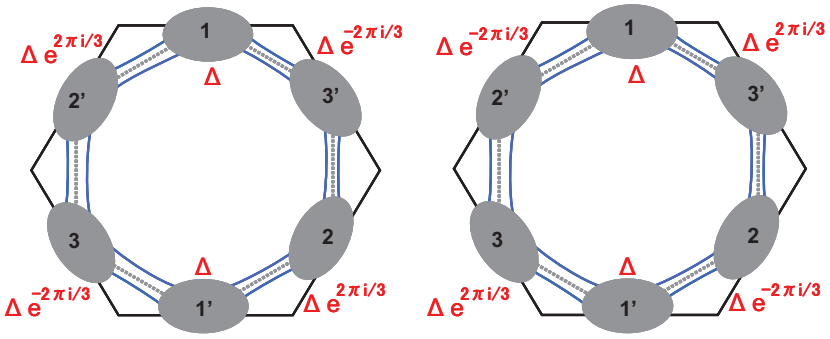

FIGURE 17. The phases of the pair-wave functions at the patches (regions with enhanced density of states). The left and right represent the two Z_2 breaking $d-$wave solutions $d+id$ or $d-id$.

We see therefore that for a three-patch model with a constant repulsive electron-electron interaction

- the KL mechanism again gives rise to pairing,
- the pair wave function has $d+id$ or $d-id$ symmetry. In each of the two states phase of the wave-function winds by 4π along the FS either clockwise or anticlockwise and time reversal symmetry is broken.

We have seen therefore that in all the three systems which we analyzed the condition for the pairing instability (the emergence of the pole in the vertex function in the upper frequency half plane) is that irreducible inter-pocket/inter-patch pairing vertex should be larger by absolute value than the absolute value of the irreducible intra-pocket/intra-patch vertex. For a momentum-independent bare interaction, this reduces to the condition of having $\Pi_{ph}(Q) > a\Pi_{ph}(0)$, where a is some numerical factor of $O(1)$ that depends on the model. Now we will discuss how one still get an attraction if the bare interaction is momentum-dependent.

A final remark about doped graphene. The KL mechanism has been also applied to somewhat smaller dopings, when the FS still contains six disconnected pieces. In this doping range, KL-based analysis yields a novel spin-triplet f-wave superconductivity [115, 116, 46, 122].

WHAT TO DO IF THE BARE IRREDUCIBLE VERTEX IS REPULSIVE

We recall that setting $G_3 = G_4$ is indeed a crude approximation. In reality, G_4 is the interaction at small momentum transfer, while G_3 is the interaction at momentum transfer comparable to inverse lattice spacing. By conventional wisdom, one should expect G_4 to be larger G_3, and microscopic calculations generally confirm this, although in multi-orbital systems the interplay between G_3 and G_4 is more involved as both appear (in the band basis) even if we only consider on-site interaction in the orbital basis. In this latter case, $G_4 > G_3$ if Hubbard interaction for fermions

belonging to the same orbital is larger than Hubbard interaction between fermions belonging to different orbitals.

If $G_4 > G_3$, the attractive KL contribution of order $G^2\Pi_{ph}$ has to compete with the repulsive first-order term. At weak coupling and for a non-nested FS, second-order term is expected to be smaller than first-order term, i.e., superconductivity does not occur. The situation may change when we include momentum dependence of the interaction and non-circular nature of the pockets. In this case, there appears an infinite number of harmonics in each of the channels A_{1g}, B_{1g}, B_{2g}, or A_{2g}, which all couple to each other, and in some cases one or several eigenfunctions may end up as attractive. Still, however, in distinction to the isotropic case, there is no guarantee that "some" eigenfunction from will be attractive. In other words, a lattice system well may remain in the normal state down to $T = 0$.

How can we still get superconductivity in this situation? A first step is to realize that there is a similarity between the renormalization of the irreducible particle-particle interaction to order G^2 and the renormalization to the same order in the particle-hole channel at small momentum transfer. Recall that for the latter case, the renormalization can be extended to higher orders because the momentum transfer q and frequency transfer Ω, $\Pi_{ph}(q,\Omega)$ can be large and one can sum up series in $G\Pi(q,\Omega)$ by restricting in perturbation series only with the particle-hole bubbles at small q and Ω. In this situation, charge and spin components of the full $\Gamma^{full}_{\alpha\beta,\gamma\delta}(k_1,k_2;k_3,k_4) = \Gamma_c\delta_{\alpha\gamma}\delta_{\beta\delta} + \Gamma_s\vec{\sigma}_{\alpha,\gamma}\cdot\vec{\sigma}_{\beta\delta}$ can be viewed as effective interactions mediated by collective excitations in charge and spin channel, respectively,

$$\Gamma_c = -\frac{G}{2}\frac{1}{1+G\Pi_{ph}(q,\Omega)} \quad \Gamma_s = \frac{G}{2}\frac{1}{1-G\Pi_{ph}(q,\Omega)} \tag{72}$$

We have $\bar{\Gamma}^0_{\alpha\beta,\gamma\delta}(k,-k;p,-p) = \Gamma_c(k-p)\delta_{\alpha\gamma}\delta_{\beta\delta} + \Gamma_s(k-p)\vec{\sigma}_{\alpha,\gamma}\cdot\vec{\sigma}_{\beta\delta}$. Restricting with the diagrams containing $\Pi_{ph}(k-p)$ and neglecting terms with $\Pi_{ph}(k+p)$ (this is often called the RPA), we obtain for k and p at the same pocket/patch, when $k-p$ is small

$$\Gamma_c(0) = -\frac{G_4}{2}\frac{1}{1+G_4\Pi_{ph}(0)} \quad \Gamma_s(0) = \frac{G_4}{2}\frac{1}{1-G_4\Pi_{ph}(0)} \tag{73}$$

and for k and p at different pockets/patches, when $k-p \approx Q$

$$\Gamma_c(Q) = -\frac{G_3}{2}\frac{1}{1+G_3\Pi_{ph}(Q)} \quad \Gamma_s(Q) = \frac{G_3}{2}\frac{1}{1-G_3\Pi_{ph}(Q)} \tag{74}$$

Re-expressing $\bar{\Gamma}^0_{\alpha\beta,\gamma\delta}(k,-k;p,-p)$ in terms of singlet and triplet components as

$$\begin{aligned}
&\bar{\Gamma}^0_{\alpha\beta,\gamma\delta}(k,-k;p,-p) = \\
&\Gamma_{\mathrm{s}=0}(k-p)\left(\delta_{\alpha\gamma}\delta_{\beta\delta} - \delta_{\alpha\delta}\delta_{\beta\gamma}\right) + \\
&\Gamma_{\mathrm{s}=1}(k-p)\left(\delta_{\alpha\gamma}\delta_{\beta\delta} + \delta_{\alpha\delta}\delta_{\beta\gamma}\right)
\end{aligned} \tag{75}$$

We obtain

$$\begin{aligned}\Gamma_{\mathrm{s}=0} &= \frac{1}{2}\left(\Gamma_c - 3\Gamma_s\right)\\ \Gamma_{\mathrm{s}=1} &= \frac{1}{2}\left(\Gamma_c + \Gamma_s\right)\end{aligned} \tag{76}$$

i.e.

$$\begin{aligned}\Gamma_{\mathrm{s}=0}(0) &= -\frac{G_4}{4}\left(\frac{1}{1+G_4\Pi_{ph}(0)} + \frac{3}{1-G_4\Pi_{ph}(0)}\right)\\ \Gamma_{\mathrm{s}=1}(0) &= \frac{G_4}{4}\left(\frac{1}{1-G_4\Pi_{ph}(0)} - \frac{1}{1+G_4\Pi_{ph}(0)}\right)\\ \Gamma_{\mathrm{s}=0}(Q) &= -\frac{G_3}{4}\left(\frac{1}{1+G_3\Pi_{ph}(Q)} + \frac{3}{1-G_3\Pi_{ph}(Q)}\right)\\ \Gamma_{\mathrm{s}=1}(Q) &= \frac{G_3}{4}\left(\frac{1}{1-G_3\Pi_{ph}(Q)} - \frac{1}{1+G_3\Pi_{ph}(Q)}\right)\end{aligned} \tag{77}$$

Let's compare this result with what we obtained in the KL formalism. Focus on the singlet channel and expand in (77) to second order in $G_{3,4}$. We have

$$\begin{aligned}&\Gamma_{\mathrm{s}=0}(0) \approx -\frac{G_4}{2}\left(1 + \frac{1}{1-G_4\Pi_{ph}(0)}\right)\\ &\approx -G_4\left(1 + 0.5G_4\Pi_{ph}(0)\right)\\ &\Gamma_{\mathrm{s}=0}(Q) \approx -\frac{G_3}{2}\left(1 + \frac{1}{1-G_3\Pi_{ph}(Q)}\right)\\ &\approx -G_3\left(1 + 0.5G_3\Pi_{ph}(Q)\right)\end{aligned} \tag{78}$$

Apart from the factor of 1/2 (which is the consequence of an approximate RPA scheme) $\Gamma_{\mathrm{s}=0}(0)$ is the same as irreducible vertex $\bar{\Gamma}^0_{11}$, which we obtained in KL calculation in the previous section, and $\Gamma_{\mathrm{s}=0}(Q)$ the same as $\bar{\Gamma}^0_{12}$ By itself, this is not surprising, as in $\Gamma_{\mathrm{s}=0}$ we included the same particle-hole renormalization of the bare pairing interaction as in the KL formalism.

The outcome of this formula is the observation that KL term is the first term in the series for the irreducible pairing vertex. In the RPA scheme, the full series gives,

$$\begin{aligned}\Gamma_{\mathrm{s}=0}(0) &= -\frac{1}{4}\left(\frac{G_4}{1+G_4\Pi_{ph}(0)} + \frac{3G_4}{1-G_4\Pi_{ph}(0)}\right)\\ \Gamma_{\mathrm{s}=0}(0) &= -\frac{1}{4}\left(\frac{G_3}{1+G_3\Pi_{ph}(Q)} + \frac{3G_3}{1-G_4\Pi_{ph}(Q)}\right),\end{aligned} \tag{79}$$

For repulsive interaction, the charge contribution only gets smaller when we add higher terms in G, but spin contribution gets larger. A conventional recipe is to neglect all renormalizations in the charge channel and approximate $\Gamma_{s=0}$ with the sum of a constant and the interaction in the spin channel. The irreducible interaction in the $s+-$ channel in the pnictides or in the $d-$wave channel in the cuprates and in doped graphene is then

$$\Gamma_{s=0}(0)-\Gamma_{s=0}(Q)= \\ -G_4+G_3-\frac{3}{4}\left(\frac{G_4}{1-G_4\Pi_{ph}(0)}-\frac{G_3}{1-G_3\Pi_{ph}(Q)}\right) \tag{80}$$

Like we said before if $G_4\Pi_{ph}(0)$ and $G_3\Pi_{ph}(Q)$ are both small, G_4-G_3 term is the largest, and the pairing interaction is repulsive for $G_4>G_3$. However, we see that there is a way to overcome the initial repulsion: if $G_3\Pi_{ph}(Q)>G_4\Pi_{ph}(0)$, one can imagine a situation when $G_3\Pi_{ph}(Q)\approx 1$, and the correction term in (80) becomes large and positive and can overcome the negative first-order term.

What does it mean from physics perspective? The condition $G_3\Pi_{ph}(Q)=1$ implies that the spin component of the vertex function, viewed as a function of transferred momentum, diverges. This obviously implies an instability of a metal towards SDW order with momentum Q. We don't need the order to develop, but we need SDW fluctuations to be strong and to mediate pairing interaction between fermions. Once spin-mediated interaction exceeds bare repulsion, the irreducible pairing interaction in the corresponding channel becomes attractive. Notice in this regard that we need magnetic fluctuations to be peaked at large momentum transfer Q. If they are peaked at small momenta, $\Pi_{ph}(0)$ exceeds $\Pi_{ph}(Q)$, and the interaction in the singlet channel remains repulsive.

The importance of spin fluctuations for spin-singlet pairing was pointed out by many authors, starting from mid-80s. With respect to the cuprates, d-wave pairing in the Hubbard model near half-filling was first analyzed by Scalapino, Loh, and Hirsch [96] for the Hubbard model near half-filling. They used RPA to obtain irreducible pairing vertices in spin-singlet and spin-triplet channels and found spin-singlet d-wave pairing to be the dominant instability in the situation when $\Pi_{ph}(\mathbf{q})$ is peaked at $\vec{q}$ near (π,π). This work and subsequent works [125, 126] also analyzed the role of FS nesting for d-wave superconductivity.

In general, spin-mediate pairing interaction can be obtained either within RPA[83, 84, 96] or, using one of several advanced numerical methods developed over the last decade, or just introduced semi-phenomenologically. The semi-phenomenological model is often called the spin-fermion model[35]. Quite often, interaction mediated by spin fluctuations also critically affects single-fermion propagator (the Green's function), and this renormalization has to be included into the pairing problem. As another complication, the interaction mediated by soft spin fluctuations has a strong dynamical part due to Landau damping – the decay of a spin fluctuation into a particle-hole pair. This dynamics also has to be included into consideration, which makes the solution of the pairing problem near a magnetic instability quite involved theoretical problem.

There are two crucial aspects of the spin-fluctuation approach. First, magnetic fluctuations have to develop at energies much larger than the ones relevant for the pairing, typically at energies comparable to the bandwidth W. It is crucial for spin-fluctuation approach that SDW magnetism is the *only* instability which develops at such high energies. There may be other instabilities (e.g., charge order), but the assumption is that they develop at small enough energies and can be captured within the low-energy model with spin fluctuations already present[127, 128]. Second, spin-fluctuation approach is fundamentally not a weak coupling approach. In the absence of nesting, $\Pi_{ph}(Q)$ and $\Pi_{pp}(0)$ are generally of order $1/W$, and $\Pi_{ph}(Q)$ is only larger numerically. Then the interaction G_3, required to get a strong magnetically-mediated component of the pairing interaction, must be of order W.

Generally one way to proceed in this situation is to introduce the spin-fermion model with static magnetic fluctuations built into it, and then assume that within this model the interaction between *low-energy* fermions $\bar{g}$ is smaller than W and do controlled low-energy analysis treating $\bar{g}/W$ as a small parameter[35, 127, 128]. There are several ways to make the assumptions $\bar{g} \ll W$ and $G \sim W$ consistent with each other, e.g., if microscopic interaction has length Γ_0 and $\Gamma_0 k_F/\hbar \gg 1$, then $\bar{g}$ is small in $1/(\frac{\Gamma_0 k_F}{\hbar})$ compared to G (Refs.[137, 138]). At the same time, the properties of the spin-fermion model do not seem to crucially depend on $\bar{g}/W$ ratio, so the hope is that, even if the actual $\bar{g}$ is of order $G \sim W$, the analysis based on expansion in $\bar{g}/W$ captures the essential physics of the pairing system behavior near a SDW instability in a metal.

We will not discuss in detail spin-fluctuation approach, which requires a separate review. Instead, we ask the question can we possibly get an attraction in at least one pairing channel already at *weak* coupling, despite that $G_4 > G_3$, i.e., the bare pairing interaction is repulsive in all channels. The answer is actually yes, it is possible, but under a special condition that $\Pi_{ph}(Q)$ is singular and diverges logarithmically at zero frequency or zero temperature, in the same way as the particle-particle bubble $\Pi_{pp}(0)$. This condition is satisfied exactly when there is a perfect nesting between fermionic excitations separated by Q. A situation with a perfect nesting can be found for all three examples for which we analyzed KL mechanism (another example is quasi-1D organic conductor [36]). For Fe-pnictides, it implies that hole and electron FSs perfectly match each other when one is shifted by Q, for cuprates and doped graphene nesting implies the existence of parallel pieces of the FS.

We show below that $\Pi_{ph}(Q)$ and $\Pi_{pp}(0)$ do have exactly the same logarithmic singularity at perfect nesting. At the moment, let's take it for granted and compare the relevant scales. First, no fluctuations develop at energies/temperatures of order W because at such high scales the logarithmical behavior of Π_{pp} and Π_{ph} is not yet developed and both bubbles scale as $1/W$. At weak coupling $G/W << 1$, hence corrections to bare vertices are small. Second, we know that the pairing vertex evolves at $(G_3 - G_4)\Pi_{pp}(0) \sim O(1)$, and that corrections to the bare irreducible pairing vertex become of order one when $G_3\Pi_{ph}(Q) \sim O(1)$. But we also know from, e.g., (74) that at the same scale the SDW vertex begins to evolve. Moreover other inter-pocket interactions, which we didn't include so far: density-density and exchange interactions (which here and below we label as G_1 and G_2, respectively)

also start evolving because their renormalization involves terms $G_1\Pi_{ph}(Q)$ and $G_2\Pi_{ph}(Q)$ which also become of $O(1)$ when all bare interactions are of the same order. Once $G_{1,2}\Pi_{ph}(Q)$ becomes of order one, the renormalization of G_3 by G_1 and G_2 interactions also becomes relevant. The bottom line here is that renormalization of all interactions become relevant at the same scale. At this scale we can expect superconductivity, if the corrections to $G_4 - G_3$ overcome the sign of the pairing interaction, and at the same time we can expect an instability towards SDW and, possibly, some other order. The issue then is whether it is possible to construct a rigorous description of the system behavior in the situation when all couplings are small compared to W, but $G_i\Pi_{ph}(Q)$ and $G_i\Pi_{pp}(0)$ are of order one. The answer is yes, and the corresponding procedure is called a parquet renormalization group (pRG).

To re-iterate: the pRG approach is a controlled weak coupling approach. It assumes that no correlations develop at energies comparable to the bandwidth, but that there are several competing orders whose fluctuations develop simultaneously at a smaller scale. Superconductivity is one of them, others include SDW and potential charge-density-wave (CDW), nematic and other orders. The pRG approach treats superconductivity, SDW, CDW and other potential instabilities on equal footings. Correlations in each channel grow up with similar speed, and fluctuations in one channel affect the fluctuations in the other channel and vise versa. For superconductivity, once the corrections to the pairing vertex become of order one, and there is a potential to convert initial repulsion into an attraction. We know that second-order contribution to the pairing vertex from SDW channel works in the right direction, and one may expect that higher-order corrections continue pushing the pairing interaction towards an attraction. However even if attraction develops, there is no guarantee that the system will actually undergo a SC transition because it is entire possible that SDW instability comes before SC instability.

The pRG approach addresses both of these issues. It can be also applied to a more realistic case of non-perfect nesting if deviations from nesting are small in the sense that there exist a wide range of energies where $\Pi_{ph}(Q)$ and $\Pi_{pp}(0)$ are approximately equal. Below some energy scale, ω_0, the logarithmical singularity in $\Pi_{ph}(Q)$ is cut. If this scale is smaller than the one at which the leading instability occurs, a deviation from a perfect nesting is an irrelevant perturbation. If it is larger, then pRG runs up to ω_0, and at smaller energies only SC channel continues to evolve in BCS fashion.

There also exists a well-developed numerical computational procedure called functional RG (fRG)[37, 38]. Its advantage is that it is not restricted to a small number of patches and captures the evolution of the interactions in various channels even if the interactions depend on the angles along the FS. The “price" one has to pay is the reduction in the control over calculations – fRG includes both leading and subleading logarithmical terms. If only logarithmical terms are left, the angle dependence of the interaction does not change in the RG flow, only the overall magnitude changes[139] So far, the results of fRG and pRG analysis for various systems fully agree. Below we focus on the pRG approach. For a thorough tutorial on the RG technique, we direct the reader to Ref. [140].

Parquet Renormalization Group

We follow the same order of presentation as before – first consider Fe-pnictides and then discuss patch models for cuprates and doped graphene. We recall that in Fe-pnictides a bubble with momentum transfer Q contains one hole (c) and one electron (f) propagator, and at perfect nesting the dispersions of holes and electrons are just opposite. $\varepsilon_c(k) = -\varepsilon_f(k+Q)$. The particle-hole and particle-particle bubbles are

$$\begin{aligned} \Pi_{pp}(0) &= -i\int \frac{d^2k\, d\omega}{(2\pi\hbar)^3} G^c(k,\omega)G^c(-k,-\omega) \\ \Pi_{ph}(Q) &= i\int \frac{d^2k\, d\omega}{(2\pi\hbar)^3} G^c(k,\omega)G^f(Q+k,\omega) \end{aligned} \tag{81}$$

where $G^{c,f} = \frac{1}{\omega - \varepsilon_k^{c,f}/\hbar + i\delta sgn(\omega)}$. Substituting into Eq. 81 and using $\varepsilon_c(k) = -\varepsilon_f(k+Q)$ one can easily make sure that the two expressions in Eq. 81 are identical. Evaluating the integrals we obtain

$$\Pi_{pp}(0) = \Pi_{ph}(Q) = N_0 L + ... \tag{82}$$

where $N_0 = m/2\pi\hbar^2$ is the 2D density of states,

$$L = \frac{1}{2}\log\left(\frac{W}{E}\right), \tag{83}$$

E is typical energy of external fermions, and the dots stand for non-logarithmic terms. The factor $1/2$ is specific to the pocket model and accounts for the fact that for small pocket sizes, the logarithm comes from integration over positive energies $W > E > E_F$. At non-perfect nesting, the particle-particle channel is still logarithmic, but the particle-hole channel gets cut by the energy difference (δE) associated with the nesting mismatch, such that

$$\Pi_{ph}(Q) = N_0 \log\frac{W}{\sqrt{E^2 + \delta E^2}} \tag{84}$$

The main idea of pRG (as of any RG procedure) is to consider E as a running variable, assume that initial E is comparable to W and $G_i \log\left(\frac{W}{E}\right) = G_i L$ is small, calculate the renormalizations of all couplings by fermions with energies larger than E, and find how the couplings evolve as E approaches the region where $G_i L = O(1)$.

This procedure can be carried out already in BCS theory, because Cooper renormalizations are logarithmical. For an isotropic system, the evolution of the interaction U_l in a channel with angular momentum l due to Cooper renormalization can be expressed in RG treatment as

$$\frac{dU_l^{full}}{dL} = -N_0\left(U_L^{full}\right)^2. \tag{85}$$

The solution of (85) is

$$U_l^{full}(L) = \frac{U_l}{1 + U_l N_0 L} \tag{86}$$

which is the same as Eq. (44). Similar formulas can be obtained in lattice systems when there are no competing instabilities, i.e., only renormalizations in the pairing channel are relevant. For example, in the two-pocket model for the pnictides, the equations for the full vertices $\Gamma_{hh}^{full} = -G_4^{full}$ and $\Gamma_{he}^{full} = -G_3^{full}$, Eqs. (57), can be reproduced by solving the two coupled RG equations

$$\begin{aligned} \frac{dG_3^{full}}{dL} &= -2N_0 G_3^{full} G_4^{full} \\ \frac{dG_4^{full}}{dL} &= -N_0 \left(\left(G_3^{full}\right)^2 + \left(G_4^{full}\right)^2 \right) \end{aligned} \tag{87}$$

with boundary conditions $G_4^{full}(L=0) = G_4$, $G_3^{full}(L=0) = G_3$. The set can be factorized by introducing $G_A^{full} = G_3^{full} + G_4^{full}$ and $G_B^{full} = G_4^{full} - G_3^{full}$ to

$$\frac{dG_A^{full}}{dL} = -N_0 \left(G_A^{full}\right)^2, \quad \frac{dG_B^{full}}{dL} = -N_0 \left(G_B^{full}\right)^2 \tag{88}$$

The solution of the set yields

$$\begin{aligned} G_A^{full} &= G_4^{full} + G_3^{full} = \frac{G_3 + G_4}{1 + N_0 L (G_3 + G_4)} \\ G_B^{full} &= G_4^{full} - G_3^{full} = \frac{G_4 - G_3}{1 + N_0 L (G_4 - G_3)} \end{aligned} \tag{89}$$

Solving this set and using $\Gamma_{hh}^{full} = -G_4^{full}$, $\Gamma_{he}^{full} = -G_3^{full}$, we reproduce (57). This returns us to the same issue as we had before, namely if $G_4 > G_3$, the fully renormalized pairing interaction does not diverge at any L and in fact decays as L increases: G_4^{full} decays as $1/L$ and G_3^{full} decays even faster, as $1/L^2$.

We now consider how things change when $\Pi_{ph}(Q)$ is also logarithmical and the renormalizations in the particle-hole channel have to be included on equal footings with renormalizations in the particle-particle channel.

pRG in a 2-pocket model

Because two types of renormalizations are relevant, we need to include into consideration all vertices with either small total momentum or with momentum transfer near Q i.e., use the full low-energy Hamiltonian of Eq. (55). There are couplings G_3 and G_4 which are directly relevant for superconductivity, and also the couplings G_1 and G_2 for density-density and exchange interaction between hole and electron pockets, respectively. These are shown in Fig 18.

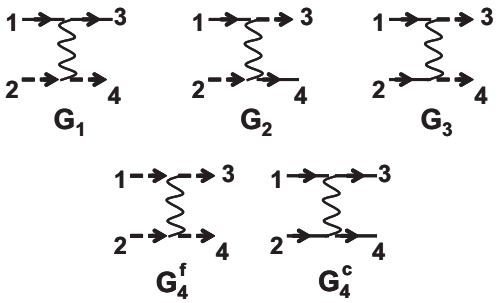

FIGURE 18. The couplings G_1 (inter-pocket density-density interaction), G_2 (fermion exchange), G_3 (pair hopping), G_4^c and G_4^f (intra-pocket density-density interaction). For equivalent hole pockets $G_4^c = G_4^f = G_4$. The solid lines correspond to hole Green's functions and the dashed lines to electron Green's functions.

The strategy to obtain one-loop pRG equations, suitable to our case, is the following: One has to start with perturbation theory and obtain the variation of each full vertex δG_i to order $G_i G_j L$. Then one has to replace $\delta G_i/L$ by dG_i^{full}/dL and also replace $G_i G_j$ in the r.h.s. by $G_i^{full} G_j^{full}$. The result is the set of coupled differential equations for dG_i^{full}/dL whose right sides are given by bilinear combinations of $G_i^{full} G_j^{full}$. The procedure may look a bit formal, but one can rigorously prove that it is equivalent to summing up series of corrections to G_i in powers of $G_i L$, neglecting corrections terms with higher powers of G_i than of L. One can go further and collecting correction terms of order $G_i G_j G_k L$. This is called 2-loop order, and 2-loop terms give contributions of order $(G^{full})^3$ to the right side of the equations for dG_i^{full}/dL. 2-loop calculations are, however, quite involved[141] and below we only consider 1-loop pRG equations.

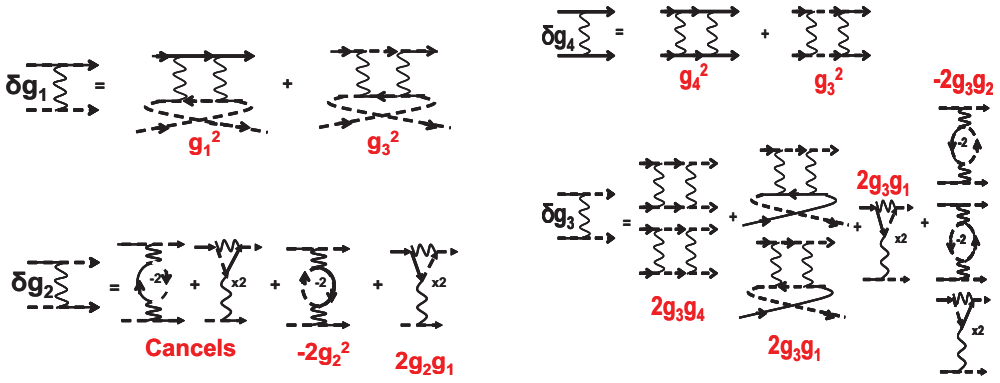

FIGURE 19. The diagrams to 1 loop order, which contribute to the parquet flow of g_1, g_2, g_3 and g_4 vertices.

The G^2 corrections to all four couplings are shown in Fig.19. Evaluating the integrals and following the recipe we obtain

$$\begin{aligned}\dot{g}_1 &= g_1^2 + g_3^2 \\ \dot{g}_2 &= 2g_2(g_1 - g_2) \\ \dot{g}_3 &= 2g_3(2g_1 - g_2 - g_4) \\ \dot{g}_4 &= -g_3^2 - g_4^2\end{aligned} \tag{90}$$

where we introduced $g_i = G_i^{full} N_0$ and $\dot{g}_i = dg_i/dL$

We note that the renormalizations of g_4 are still only in the Cooper channel and causes g_4 to reduce. But for g_3 we now have a counter-term from g_1, which pushes g_3 up. And the g_1 term is in turn pushed up by g_3. Thus already at this stage one can qualitatively expect g_3 to eventually get larger. Fig 20 shows the solution of (90)– the flow of the four couplings for this model. We see that, even if g_3 is initially smaller than g_4, it flows up with increasing L, while g_4 flows to smaller values. At some L_0, g_3 crosses g_4, and at larger L the pairing interaction $g_4 - g_3$ becomes negative (i.e., attractive). In other words, in the process of pRG flow, the system self-generates attractive pairing interaction. We remind that the attraction appears in the s^{+-} channel. The pairing interaction in s^{++} channel: $g_3 + g_4$ remains positive (repulsive) despite that g_4 eventually changes sign and becomes negative. It is essential that for $L \sim L_0$ the renormalized g_i are still of the same order as bare couplings, i.e., are still small, and the calculations are fully under control. In other words, the sign change of the pairing interaction is a solid result, and higher-loop corrections may only slightly shift the value of L_0 when it happens.

At some larger $L = L_c$, the couplings diverge, signaling the instability towards an ordered state (which one we discuss later). One-loop pRG is valid "almost" all the way to the instability, up to $L_c - L \sim O(1)$, when the renormalized g_i become of order one. At smaller distances from L_c higher-loop corrections become relevant. It is very unlikely, however, that these corrections will change the physics in any significant way.

The sign change of the pairing interaction can be detected also if the nesting is not perfect and $\Pi_{ph}(Q)$ does not behave exactly in the same way as $\Pi_{pp}(0)$. The full treatment of this case is quite involved. For illustrative purposes we follow the approach first proposed in Ref.[33] and measure the non-equivalence between $\Pi_{pp}(0)$ and $\Pi_{ph}(Q)$ by introducing a phenomenological parameter $d_1 = \Pi_{ph}(Q)/\Pi_{pp}(0)$ and treat d_1 as an $L-$ independent constant $0 < d_1 < 1$, independent on L. This is indeed an approximation, but it is at least partly justified by our earlier observation that the most relevant effect for the pairing is the sign change of $g_4 - g_3$ at some scale L_0, and around this scale d_1 is not expected to have strong dependence on L. The case $d_1 = 1$ corresponds to perfect nesting, and the case $d_1 = 0$ implies that particle-hole channel is irrelevant, in which case, we remind, $g_4 - g_3$ remains positive for all L.

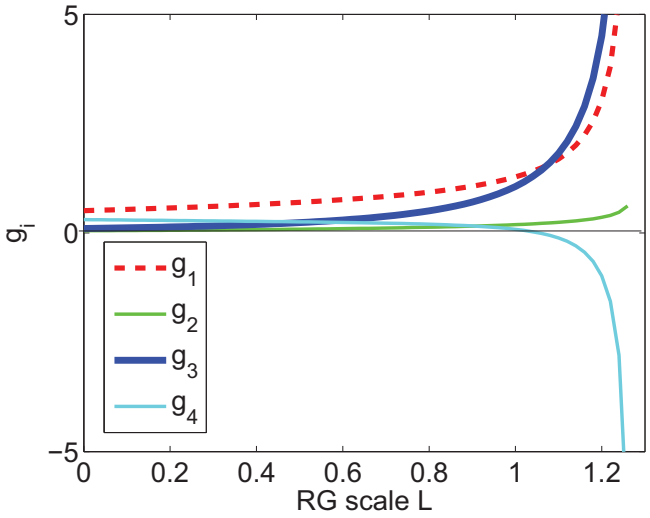

FIGURE 20. The flow of dimensionless couplings $g_{1,2,3,4}$. g_3 grows and eventually crosses g_4, which becomes negative at a large enough RG scale.

The pRG equations for arbitrary d_1 are straightforwardly obtained using the same strategy as in the derivation of (90), and the result is

$$\begin{aligned}\dot{g}_1 &= d_1(g_1^2+g_3^2)\\ \dot{g}_2 &= 2d_1 g_2(g_1-g_2)\\ \dot{g}_3 &= 2d_1 g_3(2g_1-g_2)-2g_3 g_4\\ \dot{g}_4 &= -g_3^2-g_4^2\end{aligned} \tag{91}$$

In Fig 21 we show the behavior of the couplings for representative $0<d_1<1$. Like before, we take bare value of g_4 to be larger than the bare g_3, i.e., at high energies the pairing interaction is repulsive. This figure and analytical consideration shows that for *any* non-zero d_1 the behavior is qualitatively the same as for perfect nesting, i.e., at some $L_0<L_c$ the running couplings g_3 and g_4 cross, and for larger L (smaller energies) pairing interaction in s^{+-} channel becomes attractive. The only effect of making d_1 smaller is the increase in the value of L_0. Still, for sufficiently small bare couplings, the range where the pairing interaction changes sign is fully under control in 1-loop pRG theory.

A way to see analytically that g_3-g_4 changes sign and becomes positive is to consider the system behavior near $L=L_c$ and make sure that in this region $g_3>g_4$. One can easily make sure that all couplings diverge at L_c, and their ratios tend to some constant values (see discussion around Eq. (103) below for more detail). Introducing $g_2=ag_1, g_3=bg_1$, and $g_4=cg_1$, and substituting into (91) we find an algebraic set of equations for a,b, and c. Solving the set, we find that

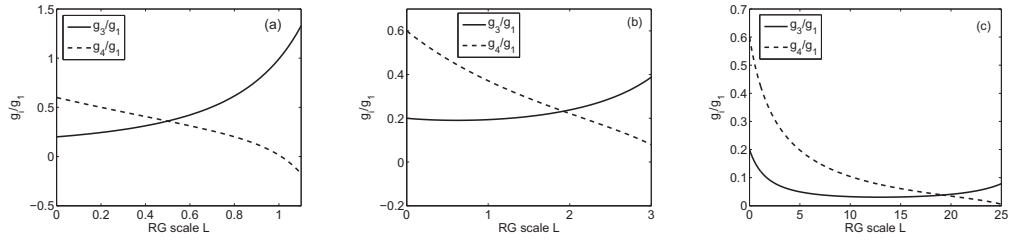

FIGURE 21. The flow of ratio of couplings g_3/g_1 and g_4/g_1 for different nesting parameters $d_1 = 1$(a), $d_1 = 0.3$(b),$d_1 = 0.05$(c). All cases are qualitatively similar in that g_3/g_1 eventually crosses g_4/g_1. The smaller is the nesting parameter, the 'later' is this crossing. If $d_1 = 0$, this crossing will never happen and $g_4 > g_3$ for all L.

$b = \frac{\sqrt{\sqrt{16d_1^4 - 4d_1^2 + 4} + 2 - d_1^2}}{d_1}$ and $c = \frac{d_1}{2}(3 - b^2)$. The negative sign of c and positive sign of b, combined with the fact that g_1 definitely increases under the flow and surely remains positive, imply that near L_c, g_4 is negative, while g_3 is positive (this is also evident from the Fig 21). Obviously then, g_3 and g_4 must cross at some $L_0 < L_c$.

pRG in patch models

We now show that similar behavior holds in patch models. Since the only difference between patch models for cuprates and for graphene is the number of patches (2 vs 3), we consider a generic model of n - patches with fermion-fermion interaction in the form

$$H_{\rm int} = \frac{1}{2}\sum_{\alpha=1}^{n} G_4 \psi_\alpha^\dagger \psi_\alpha^\dagger \psi_\alpha \psi_\alpha + \frac{1}{2}\sum_{\alpha\neq\beta}\Big[G_1 \psi_\alpha^\dagger \psi_\beta^\dagger \psi_\beta \psi_\alpha + G_2 \psi_\alpha^\dagger \psi_\beta^\dagger \psi_\alpha \psi_\beta + G_3 \psi_\alpha^\dagger \psi_\alpha^\dagger \psi_\beta \psi_\beta\Big] \tag{92}$$

Keeping again all diagrams which diverge logarithmically, we end up with the following set of pRG equations (using the same notations as before)

$$\begin{aligned} \dot{g}_1 &= d_1(g_1^2 + g_3^2) \\ \dot{g}_2 &= 2d_1 g_2(g_1 - g_2) \\ \dot{g}_3 &= -(n-2)g_3^2 - 2g_3 g_4 + 2d_1 g_3(2g_1 - g_2) \\ \dot{g}_4 &= -(n-1)g_3^2 - g_4^2 \end{aligned} \tag{93}$$

The equations look similar to the ones for the pocket model, up to the dependence on n, but there is one important difference: the derivative in the l.h.s. is with respect to $\log^2(\Lambda/E)$ rather than a first power of the logarithm. The extra logarithm

comes from the logarithmical enhancement of the density of states near Van-Hove density. The presence of extra logarithms makes the theory somewhat less controlled because already at second order there are terms of order $g^2\log^2$ and $g^2\log$. The set of equations (93) corresponds to keeping $g^2\log^2$ neglecting $g^2\log$ terms, and $\dot{g}_i$ in (93) is $\dot{g}_i = dg_i/d\log^2(\Lambda/E)$. Strictly speaking, this implies that RG scheme can be applied only at one-loop order, while extending Eq, 93 to two-loop and higher orders will require one to go beyond RG.

Like before, d_1, subject to $0 < d_1 < 1$, accounts for relative strength of $\Pi_{ph}(Q)$ compared to $\Pi_{pp}(0)$. In reality, $d_1 = \Pi_{ph}(Q)/\Pi_{pp}(0)$ depends on the running scale $L = \log^2(\Lambda/E)$, but we approximate it by a constants using the same reasoning as for the pocket model.

We show the solution of the set (93) in Fig. 22 for $n = 3$ ($n = 2$ result is identical to Fig. 20). Combining again the numerical analysis and the analytical reasoning similar to the one for the pocket model, we find that, for any n and any $d_1 > 0$, there exists a scale L_0 at which g_3 and g_4 cross, and at larger L (i.e., at smaller energies) the pairing interaction in the d-wave channel (for which the pairing vertex is proportional to $g_4 - g_3$) changes sign and becomes attractive.

The outcome of these studies is that in all three systems which we considered, the system self-generates attraction below some particular energy E_0, which is of order $\Lambda e^{-1/(N_0 G)}$ for the pocket model and of order $\Lambda e^{-1/(N_0 G)^{1/2}}$ for the patch models.

The reason for the sign change of the pairing interaction is clear from the structure of the pRG equation for g_3 the r.h.s. of which contains the term $4d_1 g_3 g_4$, which pushes g_3 up. We know from second-order KL calculation that the upward renormalization of g_3 comes from the magnetic channel and can be roughly viewed as the contribution from spin-mediated part of effective fermion-fermion interaction. Not surprisingly, we will see below that g_1 does, indeed, contribute to the SDW vertex. From this perspective, the physics of the attraction in pRG (or in fRG, which brings in the same conclusions as pRG) and in spin-fermion model is the same: magnetic fluctuations push inter-pocket/inter-patch interaction up, and below some energy scale the renormalized inter-pocket/inter-patch interaction becomes larger than repulsive intra-pocket/intra-patch interaction.

There is, however, one important difference between the RG description and the description in terms of spin-fermion model. In the spin-fermion model, magnetic fluctuations are strong, but the system is *assumed* to be at some distance away from an SDW instability. In this situation, SC instability definitely comes ahead of SDW magnetism. There may be other instabilities produced by strong spin fluctuations, like bond CDW[108, 109, 110], which compete with SC and, by construction, also occur before SDW order sets in In RG treatment (pRG or fRG), SDW magnetism and SC instability (and other potential instabilities) compete with each other, and which one develops first needs to be analyzed. So far, we only found that SC vertex changes sign and becomes attractive. But we do not know whether superconductivity is the leading instability, or some other instability comes first. This is what we will study next. The key issue, indeed, is whether superconductivity can come ahead of SDW magnetism, whose fluctuations helped convert repulsion

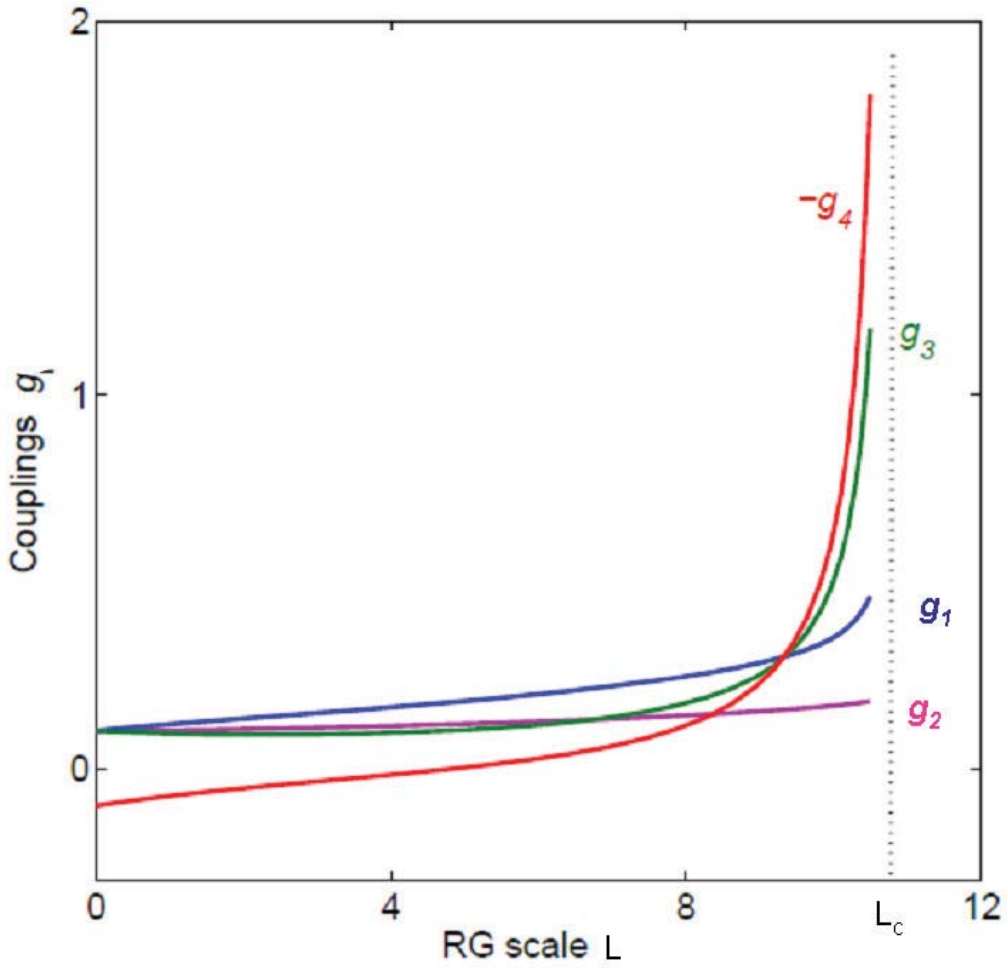

FIGURE 22. The flow of the couplings vs the pRG scale L in the 3-patch model. We assume that all couplings are repulsive. We see that g_3 increases under the flow, while g_4 decreases. Observe that the coupling g_4 eventually gets overscreened and changes sign. Taken from Ref. [34].

in the pairing channel into an attraction.

COMPETITION BETWEEN DENSITY WAVE ORDERS AND SUPERCONDUCTIVITY

Thus far, we identified an instability in a particular channel with the appearance of a pole in the upper frequency half-plane in the corresponding vertex – the vertex with zero total momentum in the case of SC instability, and the vertex with the total momentum Q in the case of SDW instability. Since our goal is to address

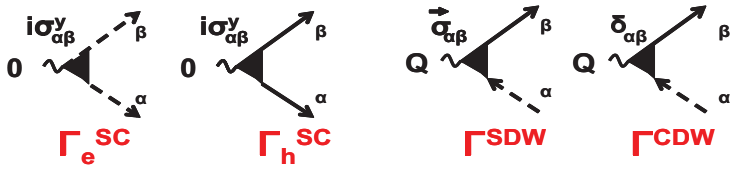

FIGURE 23. Superconducting and density-wave three legged vertices. Divergence of any of these vertices indicates that the system is likely to be unstable to the corresponding order. $\Gamma^{SC}_{h,e}$ are superconducting vertices, Γ^{SDW} is SDW vertex and Γ^{CDW} is CDW vertex.

the competition between these states, it is actually advantageous to use a slightly different approach: introduce all potentially relevant fluctuating fields, use them to decouple 4-fermion terms into a set of terms containing two fermions and a fluctuating field, compute the renormalization of these "three-legged" vertices and use these renormalized vertices to obtain the susceptibilities in various channels and check which one is the strongest. We will see that the renormalized vertices in different channels (most notably, SDW and SC) do diverge near L_c, but with different exponents. The leading instability will be in the channel for which the exponent is the largest. There is one caveat in this approach — for a divergence of the susceptibility the exponent for the vertex should be larger than 1/2 (Ref.[142]), but we will see below that this condition is satisfied for all three cases which we consider, at least for the leading instability.

Two pocket model

Let us see how it works for a two-pocket model. There are two particle-particle three legged vertices $\Gamma_{h,e}$ as shown in Fig 23. To obtain the flow of these vertices, i.e., $\Gamma^{SC}_{h,e}(L)$ we assume that external fermions and a fluctuating field have energies comparable to some E (i.e.,$L = \log \Lambda/E$) and collect contributions from all fermions with energies larger than E. To do this with logarithmical accuracy we write all possible diagrams, choose a particle-particle cross-section at the smallest internal energy $E' \geq E$ and sum up all contributions to the left and to the right of this cross-section, as shown in Fig 24. The sum of all contributions to the left of the cross-section gives the three legged vertex at energy E' (or $L' = \log \Lambda/E'$), and the sum of all contributions to the right of the cross-section gives the interaction g_i at energy L'. The integration over the remaining cross-section gives $\int^L dL'$ (with our normalization of g_i), and the equation for, e.g., $\Gamma_h(L)$ becomes

$$\Gamma^{SC}_h(L) = \int^L dL' \left(\Gamma^{SC}_h(L') g_4(L') + \Gamma^{SC}_e(L') g_3(L') \right) \tag{94}$$

Differentiating over the upper limit, we obtain differential equation for $d\Gamma^{SC}_h(L)/dL$ whose r.h.s. contains $\Gamma^{SC}_{h,e}(L)$ and $g_{3,4}(L)$ at the same scale L.

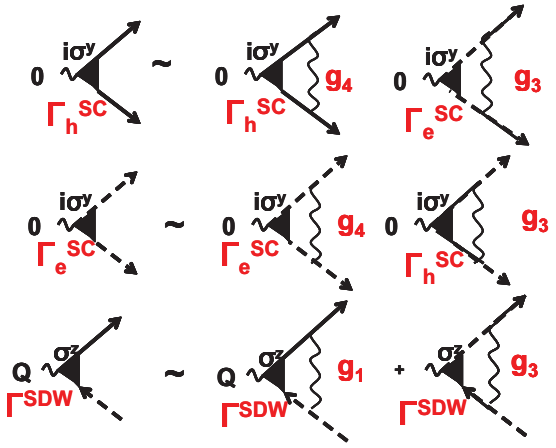

FIGURE 24. Diagrams to analyze the flow of the effective vertices: SC vertex (top two) and SDW vertex (bottom). The couplings g_i's here are running couplings in RG sense.

Collecting the contributions for $\Gamma_h^{SC}(L)$ an $\Gamma_e^{SC}(L)$ we obtain

$$\begin{aligned} \frac{d\Gamma_h^{SC}}{dL} &= \Gamma_h^{SC} g_4 + \Gamma_e^{SC} g_3 \\ \frac{d\Gamma_e^{SC}}{dL} &= \Gamma_e^{SC} g_4 + \Gamma_h^{SC} g_3 \end{aligned} \tag{95}$$

or

$$\begin{aligned} \frac{d\Gamma_{++}}{dL} &= (g_4 + g_3)\Gamma_{++} \\ \frac{d\Gamma_{+-}}{dL} &= (g_4 - g_3)\Gamma_{+-} \end{aligned} \tag{96}$$

where $\Gamma_{++} \equiv \Gamma_h^{SC} + \Gamma_e^{SC}$ and $\Gamma_{+-} \equiv \Gamma_h^{SC} - \Gamma_e^{SC}$. The first one is for s^{++} pairing, the second is for s^{+-} pairing. We have seen in the previous section that the running couplings $g_{3,4}$ diverge at some critical RG scale L_c. The flow equation near L_c is in the form $\dot{g} \sim g^2$, hence

$$g_i = \frac{\alpha_i}{L_c - L}. \tag{97}$$

Substituting this into Eq. 96 and solving the differential equation for Γ we find that the two SC three legged vertices behave as

$$\Gamma_{s^{++}} \propto \frac{1}{(L_c - L)^{-\alpha_3 - \alpha_4}}, \quad \Gamma_{s^{+-}} = \frac{1}{(L_c - L)^{\alpha_3 - \alpha_4}}, \tag{98}$$

The requirement for the divergence of $\Gamma_{s^{+-}}$ is $\alpha_3 > \alpha_4$, which is obviously the same as $g_3 > g_4$ (see (97)).

We follow the same procedure for an SDW vertex $\vec{\Gamma}^{SDW}$. We introduce a particle-hole vertex with momentum transfer Q and spin factor $\vec{\sigma}_{\alpha\beta}$, as shown in Fig 23, and obtain the equation for $d\vec{\Gamma}^{SDW}(L)/dL$ in the same way as we did for SC vertices. We obtain (see Fig. 24)

$$\frac{d\vec{\Gamma}^{SDW}}{dL} = d_1(g_1 + g_3)\vec{\Gamma}^{SDW} \tag{99}$$

Using Eq. 97 and following the same steps as above we obtain at $L \approx L_c$

$$\vec{\Gamma}^{SDW} \propto \frac{1}{(L_c - L)^{d_1(\alpha_1+\alpha_3)}} \tag{100}$$

For CDW vertex (the one with the overall factor $\delta_{\alpha\beta}$ instead $\sigma_{\alpha\beta}$), the flow equation is

$$\begin{aligned} \frac{d\Gamma^{CDW}}{dL} &= d_1(g_1 + g_3 - 2g_3 - 2g_2)\Gamma^{CDW} \\ &= d_1(g_1 - g_3 - 2g_2)\Gamma^{CDW} \end{aligned} \tag{101}$$

Using the same procedure as before we obtain

$$\Gamma^{CDW} = \frac{1}{(L_c - L)^{d_1(\alpha_1-\alpha_3-2\alpha_2)}} \tag{102}$$

The exponents α_i can be easily found by plugging in the asymptotic forms in Eq. 97 into the RG equations. This gives the following set of non linear algebraic equations in α_i

$$\begin{aligned} \alpha_1 &= d_1(\alpha_1^2 + \alpha_3^2) \\ \alpha_2 &= 2d_1\alpha_2(\alpha_1 - \alpha_2) \\ \alpha_3 &= 2d_1\alpha_3(2\alpha_1 - \alpha_2) - 2\alpha_3\alpha_4 \\ \alpha_4 &= -\alpha_3^2 - \alpha_4^2 \end{aligned} \tag{103}$$

Consider first the case of perfect nesting, $d_1 = 1$. The solution of the set of equations is $\alpha_1 = \frac{1}{6}$, $\alpha_2 = 0$, $\alpha_3 = \frac{\sqrt{5}}{6}$ and $\alpha_4 = -\frac{1}{6}$; Combining α's, we find that the exponents for superconducting and spin density wave instabilities and positive and equal:

$$\begin{aligned} \alpha_{s\pm} &\equiv \alpha_3 - \alpha_4 = \frac{1+\sqrt{5}}{6} \approx 0.539 \\ \alpha_{SDW} &\equiv \alpha_1 + \alpha_3 = \frac{1+\sqrt{5}}{6} \approx 0.539 \end{aligned} \tag{104}$$

while the exponent for CDW and $s++$ vertices are negative

$$\begin{aligned} \alpha_{CDW} &= \alpha_1 + \alpha_3 = \frac{1-\sqrt{5}}{6} \approx -0.206 \\ \alpha_{s++} &= -\alpha_3 - \alpha_4 = \frac{1-\sqrt{5}}{6} \approx -0.206 \end{aligned} \tag{105}$$

We see that the superconducting $(s+-)$ and SDW channels have equal susceptibilities in this approximation, while CDW channel is not a competitor.

The analysis can be extended to $d_1 < 1$. We define $\beta \equiv \alpha_4/\alpha_1$, $\gamma \equiv \alpha_3/\alpha_1$ and obtain

$$\begin{aligned} \gamma^2 &= \frac{\sqrt{16d_1^4 - 4d_1^2 + 4} + 2 - d_1^2}{d_1^2} \\ \beta &= \frac{d_1}{2}\left(3 - \gamma^2\right) \\ \alpha_1 &= \frac{1}{d_1}\frac{1}{1+\gamma^2} \end{aligned} \tag{106}$$

In Fig25 we plot $\alpha_{s\pm} = \alpha_3 - \alpha_4$, $\alpha_{SDW} = \alpha_1 + \alpha_3$, and $\alpha_{CDW} = \alpha_1 - \alpha_3$, We clearly see that (i) CDW channel is never a competitor, and (ii) as d_1 decreases (the nesting gets worse), the pairing vertex diverges with a higher exponent that SDW channel, hence s^{+-} superconductivity becomes the leading instability, overshooting the channel which helped SC vertex to change sign in the first place.

In real systems, pRG equations are only valid up to some distance from the instability at L_c. Very near L_c three-dimensional effects, corrections from higher-loop orders and other perturbations likely affect the flow of the couplings. Besides, in pocket models, the pRG equations are only valid for E between the bandwidth W and the Fermi energy E_F. At $E < E_F$, internal momenta in the diagrams which account for the flow of the couplings become smaller than external k_F, and the renormalization of g_i start depending on the interplay between all four external momenta in the vertices[85, 139]. The calculation of the flow in this case is technically more involved, but the result is physically transparent – SDW and s^{+-} SC channels stop talking to each other, and the vertex evolves according to Eqs. (98) and (99), with g_i taken at the scale E_F (or $L_F = \log \Lambda/E_F$). If $L_F > L_c$, the presence of the scale set by the Fermi energy is irrelevant, but if $L_F < L_c$ (which is the case for the Fe-pnictides because superconducting T_c and magnetic T_{SDW} are much smaller than E_F), then one should stop pRG flow at L_{E_F}. At perfect

nesting, the SDW combination g_1+g_3 is larger than s^{+-} combination g_3-g_4 at any $L<L_c$, hence SDW channel wins, and the leading instability upon cooling down the system is towards a SDW order. At non-zero doping, $\Pi_{ph}(Q)$ is cut by a deviation from nesting, what in our language implies that $d_1<1$. If bare g_3 and g_4 are not to far apart, there exists a critical d_1 at which g_3-g_4 crosses $d_1(g_1+g_3)$ at L_F, and at larger d_1 the crossing occurs before L_F. In this situation, s^{+-} SC becomes the leading instability upon cooling off the system.

The comparison between different channels can be further extended by considering current SDW and CDW vertices (imaginary Γ^{SDW} and Γ^{CDW}) and so on. We will not dwell into this issue because for all three cases we consider the real competition is between SDW and SC vertices.

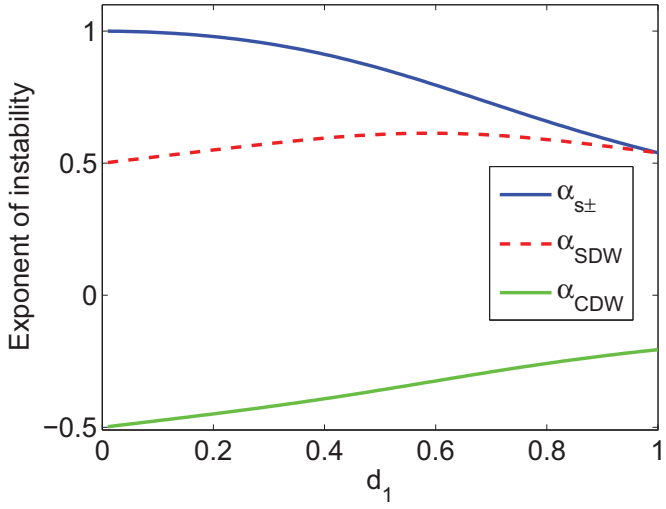

FIGURE 25. Exponents ($\alpha_{s\pm}$, α_{SDW} and α_{CDW}) for different values of the nesting parameter d_1 calculated near the critical RG scale, where the couplings diverge. The state with the largest exponent wins. SDW and SC are degenerate when $d_1=1$ (perfect nesting) and superconductivity wins for all other values of d_1. CDW is not a competitor.

Before moving on, we need to clarify one more point. So far we found that the vertices Γ^{SC} and Γ^{SDW} diverge and compared the exponents. However, to actually analyze the instability in a particular channel one has to compute fluctuation correction to susceptibility

$$\chi^i_{fl}(L)\sim\int^L dL'\left(\Gamma^i(L')\right)^2 \tag{107}$$

where Π_i is either $\Pi^{SDW}=\Pi_{ph}$ or $\Pi^{SC}=\Pi_{pp}$ (see Fig 26)
The fully renormalized susceptibility in a given channel is

$$\chi^{-1}(L)=r_0-\chi^i_{fl}(L) \tag{108}$$

where r_0 is some bare value of order one. The true instability occurs at L^* when $\chi^i_{fl}(L^*)=r_0$. At weak coupling, the critical L^* is close to L_c, and, indeed, the

FIGURE 26. (Left) The fluctuation correction to SC pairing susceptibility. (Right) The fluctuation correction to SDW susceptibility.

instability occurs first in the channel with the largest exponent for Γ^i. However, we need $\chi^i_{fl}(L)$ to diverge at L_c, otherwise there will no instability at weak coupling [142]. This requirement sets the condition that the exponent for the corresponding Γ must be larger than $1/2$. Fortunately, this condition is satisfied in the two-pocket model. For $d_1 = 1$, this is evident from (104). For $d_1 < 1$, the exponent for the SC channel only increases, while the one in SDW channel decreases but still remains larger than $1/2$ as it is evidenced from Fig25 where we plotted the exponents for SC and SDW vertices as a function of d_1. In the limit $d_1 \to 0$,

$$\alpha_{SDW} \approx \frac{1}{2} + \frac{d_1}{4} \tag{109}$$

.

The fact that both α_{SC} and α_{SDW} are larger than $1/2$ implies that in Landau-Ginzburg expansion in powers of SC and SDW order parameters (Δ and M, respectively), not only the prefactor for Δ^2 changes sign at T_c, but also the prefactor for M^2 term changes sign and becomes negative below some $T_m < T_c$. This brings in the possibility that at low T SC and SDW orders co-exist. The issue of the co-existence, however, requires a careful analysis of the interplay of prefactors for fourth order terms M^4, Δ^4, and $M^2\Delta^2$. We do not discuss this specific issue. For details see [144, 145]

Multi-pocket models

The interplay between SDW and SC vertices is more involved in more realistic multi-pocket models Fe-pnictides, with several electron and hole pockets. We recall that weakly doped Fe-pnictides have 2 electron pockets and 2-3 hole pockets. In multi-pocket models one needs to introduce a larger number of intra-and inter-pocket interactions and analyze the flow of all couplings to decide which instability is the leading one. This does not provide any new physics compared to what we have discussed, but in several cases the interplay between SC and SDW instabilities becomes such that superconductivity wins already at perfect nesting. In particular, in 3-pocket models (two electron pockets and one hole pockets) the exponent for the SC vertex gets larger than the exponent for the SDW vertex already at $d_1 = 1$. We show the flow of SC an SDW couplings for 3-pocket model in Fig.27. Once d_1 becomes smaller than one, SC channel wins even bigger compared to SDW channel.

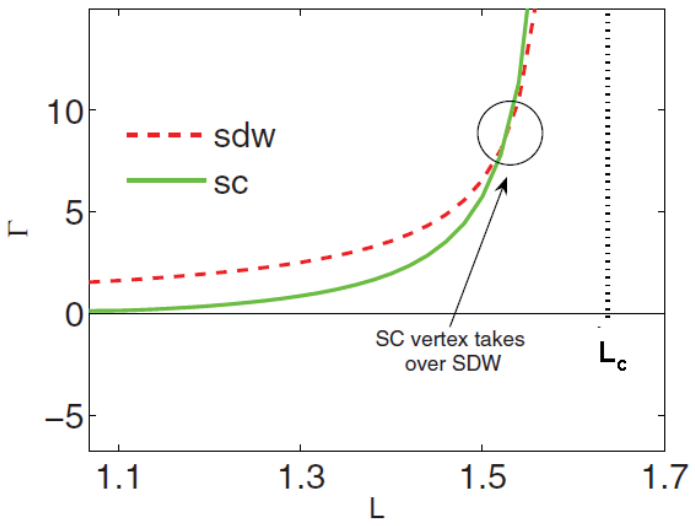

FIGURE 27. The flow of the SC and SDW vertices with the RG scale. Both diverge at a critical scale, L_c, but the SC vertex diverges stronger. Taken from Ref. [139].

Superconductivity right at zero doping has been detected in several Fe-pnictides, like LaOFeAs and LiFeAs, and it is quite possible that this is at least partly due to the specifics of pRG flow.

Patch models

The analysis of the patch model show a very similar behavior – SDW and d-wave SC vertices compete, and which one wins depends on the number of patches and (for $n = 2$) on the value of d_1.

For 2-patch model, the equations and the results are the same as in 2-pocket model: SDW wins at perfect nesting and SC winds at non-perfect nesting (see Fig 28).

For 3-patch model we have

$$\begin{aligned} \frac{d\Gamma^{SC}}{dL} &= 2(g_3 - g_4)\Gamma^{SC} \\ \frac{d\Gamma^{SDW}}{dL} &= 2d_1(g_1 + g_3)\Gamma^{SDW} \end{aligned} \tag{110}$$

and $g_i = \alpha_i/(L_c - L)$, so which channel wins depends on the interplay between $\alpha_{SC} = 2(\alpha_3 - \alpha_4)$ and $\alpha_{SDW} = 2d_1(\alpha_1 + \alpha_3)$

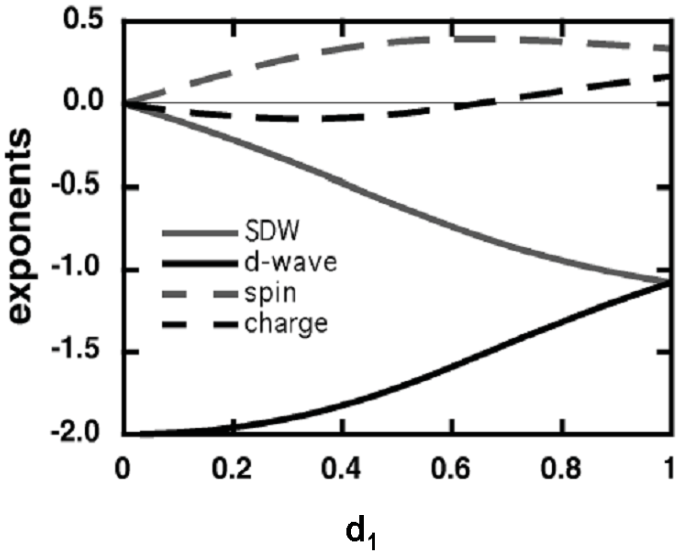

FIGURE 28. The exponents for various instabilities computed for different nesting parameters d_1. At perfect nesting ($d_1 = 1$) the SDW and SC channels have the same exponent, for $d_1 < 1$. The larger exponent is in the superconducting channel. Compare with Fig. 25. (Taken from Ref. [33].)

Substituting $g_i = \alpha_i/(L_c - L)$ into the set of pRG equations (93) we obtain

$$\begin{aligned} \alpha_1 &= d_1(\alpha_1^2 + \alpha_3^2) \\ \alpha_2 &= 2d_1\alpha_2(\alpha_1 - \alpha_2) \\ \alpha_3 &= -\alpha_3^2 - 2\alpha_3\alpha_4 + 2d_1\alpha_3(2\alpha_1 - \alpha_2) \\ \alpha_4 &= -\alpha_4^2 - 2\alpha_3^2 \end{aligned} \tag{111}$$

For $d_1 = 1$, the solution is

$$\alpha_1 \approx 0.14, \alpha_2 = 0, \alpha_3 = 0.35, \alpha_4 \approx -0.4. \tag{112}$$

Hence

$$\alpha_{SC} = 0.74; \quad \alpha_{SDW} \approx 0.48 \tag{113}$$

We see that already at perfect nesting SC vertex has a larger exponent, i,e superconductivity is the first instability of a system upon cooling. The same result has been obtained in fRG approach [122]. Observe that $\alpha_{SC} > 1/2$, i.e., the divergence of the SC three legged vertex does indeed lads to a SC instability (which, we recall, leads to a $d + id$ or $d - id$ state, each breaks time-reversal symmetry). However, $\alpha_{SDW} < 1/2$ what implies that in Ginzburg-Landau expansion the prefactor for the M_{SDW}^2 remains positive, at least around superconducting T_c. This generally makes the possibility that SC and SDW states co-exist below T_c less likely [143]

When $d_1 < 1$, α_{SC} gets larger and α_{SDW} gets smaller, i.e, SC instability becomes even more dominant. We show the behavior of α_{SC} and α_{SDW} at different d_1 in Fig29.

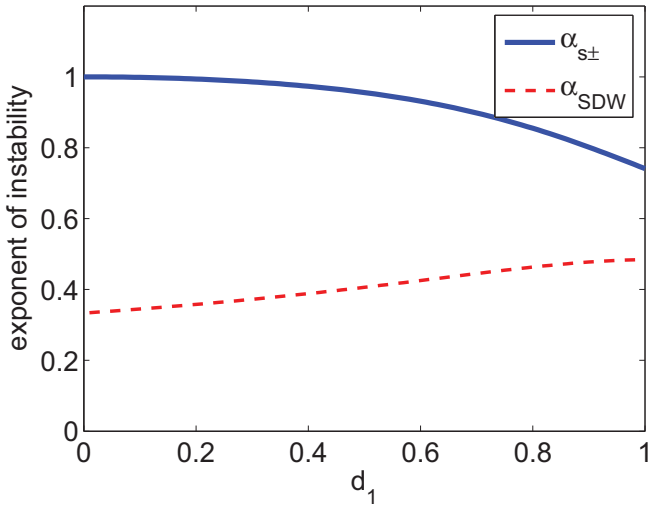

FIGURE 29. Plot of α_{SC} and α_{SDW} in 3-patch model vs d_1. Observe that α_{SC} is larger already at $d_1 = 1$. In this respect, the flow in 3-patch model is different from that in two-patch model (Fig 25), where α_{SDW} and α_{SC} were degenerate (to leading) order for $d_1 = 1$.

To summarize the results of pRG analysis:

- The SC vertex starts out as repulsive, but it eventually changes sign at some RG scale (L_0). This happens due to the "push" from SDW channel, which rives rise to upward renormalization of the inter-pocket/inter-patch interaction g_3.
- Both SDW and SC vertices diverge at RG scale L_c which is larger than L_0. The leading instability is in the channel whose vertex diverges with a larger exponent. At perfect nesting, SDW instability occurs first in 2-pocket and two-patch models, however in 3-patch model (and in some multi-pocket models) SC vertex has a larger exponent that the SDW vertex and SC becomes the leading instability.
- Deviations from perfect nesting (quantified by $d_1 < 1$) act against SDW order by reducing the corresponding exponent. At sufficiently small d_1 SC instability becomes the leading one in all models which we considered
- The necessary condition for the instability is the diverges of the fluctuating component of the susceptibility. This sets up a condition $\alpha > 1/2$, where α is the exponent for the corresponding vertex. For the leading instability, we found $\alpha > 1/2$ in all cases. For the subleading instability, α can be either larger or smaller than $1/2$. This affects potential co-existence of the leading and subleading orders at a lower T.

SUMMARY

The goal of these lecture notes was two-fold. First, to discuss Kohn-Luttinger mechanism of superconductivity in systems with nominally repulsive interaction, and, second, to provide a guideline how to perform calculations to analyze SC instability and its interplay with other potential instabilities, most notably SDW instability. These lecture notes is by no means a comprehensive review of this wonderful field and we apologize if we have missed some of the viewpoints and references. We have presented how a weak coupling perspective can be used (quite successfully) to describe not only superconductivity in many high T_c systems but interplay between competing orders.

We started by providing a very brief outline of the Fermi Liquid theory that is necessary to deal with interacting fermions. We used the Green's function formalism to define a 4-fermion scattering vertex $\Gamma_{\alpha\beta,\gamma\delta}(k_1, k_2; p_1, p_2)$. Quite generally, the appearance of a pole in this vertex function in the upper frequency half plane indicates that the Fermi Liquid is unstable against a particular order. We showed the presence of one such pole in the particle-particle (Cooper) channel at zero total momentum of the interacting particles, for arbitrary small attractive interaction.

In the bulk of these lecture notes we addressed the issue how one can get SC in systems with repulsive interaction. For isotropic systems, the first step is the observation that the pairing problem decouples between pairing channels with different angular momentum l, and to get SC one needs an attraction for just one value of l. The second step is the observation, made by Kohn and Luttinger, that Friedel oscillations of the screened repulsive fermion-fermion interaction give rise to the appearance of attractive components of the pairing interaction at large odd l, no matter how the screening affects the regular (non-oscillating) part of the interaction potential. Mathematically, the attraction is due to non-analyticity of the screened interaction at the maximum momentum transfer $2k_F$ between particles on the FS. We applied KL reasoning to weak coupling and showed that in 3D the attraction persists down to $l = 1$, and the partial component with $l = 1$ is the largest by magnitude. The outcome is that an isotropic 3D system with weak repulsive electron-electron interaction is unstable towards a $p-$wave pairing. The $p-$wave pairing is the leading pairing instability also in 2D case, but to get it one has to go to third order in the perturbation, while in 3D systems the attraction emerges already at second order.

Such a decomposition into decoupled angular momentum harmonics is, however, not possible in lattice systems due to reduced symmetry. One can only decouple between partial harmonics of the interaction belonging to different representations of a discrete lattice symmetry group. We showed that KL reasoning can be applied to lattice cases as well and considered as examples three 2D models: two-pocket model with small electron and hole pockets separated by $\mathbf{Q} = (\pi, \pi)$, two-patch model with one large FS on which there are two distinct regions with large density of states, and three-patch model, with three such regions. We argued that the first model is applicable to Fe-pnictides, the second one to optimally doped and overdoped cuprates, and the third one to graphene doped to a vicinity of a topological transition from multiple small FSs sheets to a single large FS.

For each model we found that superconductivity is possible if the interaction at large momentum transfer Q exceeds the interaction at a small momentum transfer ($g_3 > g_4$ in our notations). The emerging pairing state has s^{+-} symmetry for the Fe-pnictides, $d_{x^2-y^2}$ symmetry for the cuprates, and $d+id$ symmetry for doped graphene. In the latter case, superconductivity breaks time-reversal symmetry.

We found that KL renormalization, taken to order g^2, does produce an attractive component of the interaction. If bare g_3 and g_4 are identical (the case of the momentum-independent Hubbard-like interaction), KL mechanism is sufficient to explain the emergence of the attractive pairing interaction. However, in a more realistic case, g_4 (the interaction at small momentum transfer), is larger than g_3 (the interaction with large momentum transfer). In this situation, KL attraction has to overcome bare repulsion, and this is generally not possible, particularly at weak coupling. As a result, a lattice system can remain in the normal (non-SC) state down to $T = 0$.

We speculated how one can get SC by going beyond weak coupling and briefly discussed spin-fermion model in this context. We argued that the KL renormalization can be viewed as the first term in the series which gives rise to effective interaction mediated by collective spin fluctuations. We then explored a peculiar situation when the renormalization in particle-hole channel is almost as strong as the renormalization in the particle-particle (Cooper) channel. This is the case when the FS is nested, and we argued that nesting is present in all three cases which we considered. We argued that the nesting case can be studied beyond second-order by applying a parquet renormalization group technique. This is a fully controlled weak coupling theory which neglects higher terms in the dimensional couplings g_i but keeps corrections in $g_i\Pi_{pp}(0)$ and $g_i\Pi_{ph}(Q)$ to all orders.

We found that in all three examples which we considered, RG flow of the couplings is such that the system self-generates an attraction below some energy scale. Specifically, we demonstrated that at some RG scale the initially repulsive pairing interaction changes sign and beyond this scale (at smaller energies) becomes attractive. We argued that this conversion of repulsion into an attraction is a universal phenomenon which does not depend on the details of the underlying model, as long as particle-hole bubble is comparable to particle-particle bubble and RG analysis is applicable.

Finally, we analyzed the interplay between superconductivity and other orders. The competition with SDW order is a particularly relevant issue because SDW fluctuations are responsible for the appearance of an attraction in the SC channel. We argued that in some cases of near-perfect nesting SDW order occurs first, but at deviations from nesting SC instability eventually occurs prior to a magnetic instability. In other cases, SC instability comes first even at perfect nesting, overshooting the interaction which made attraction in the pairing channel possible.

We hope to have fairly addressed the phenomenon of superconductivity in systems with repulsive interactions, but we fully understand that we left a near-infinite amount of interesting physics that comes along with it. Our main hope is that the readers, particularly graduate students, will find this subject interesting and worth studying in more detail and depth.

ACKNOWLEDGMENTS

We are thankful to Profs. A. Avella and F. Manchini for organizing the school in which one of us (A.C.) was a lecturer. It was time-consuming but quite interesting task to write these notes in the combination "professor-graduate student", and we have had numerous discussions between the two of us about various aspects of the electronic pairing mechanism. One of us (A.C.) worked on KL mechanism about 25 years ago with M. Kagan, and it was quite interesting to return to this issue after so many years and look at high T_c superconductivity though the prism of KL physics. The work by Raghu et. al. (Ref. [46]) was very stimulating in this regard.

The two of us discussed various aspects of electronic pairing with a large number of our colleagues, and we want to thank all of them for fruitful discussions and various comments. This work has been supported by the DOE grant DE-FG02-ER46900. SM acknowledges support from ICAM-DMR-084415.

REFERENCES

1. H. Kamerlingh Onnes, Commun. Phys. Lab. Univ. Leiden 120b (April 1911), reprinted in Proc. K. Ned. Akad. Wet. **13** , 1274 (1911).
2. F. W. London, "Macroscopic Theory of Superconductivity". Dover (1960).
3. E.M. Lifshitz and L.P. Pitaevskii, Statistical Physics (Part 2), Pergamon Press, Reprinted in 2002.
4. P.W. Anderson, Phys. Rev. **130**, 439 (1963).
5. P.W. Higgs, Phys. Rev. **145**, 1156 (1966).
6. F. Wilczek, Nuclear Physics A **663**, 257 (2000).
7. J. Bardeen, L. Cooper, J. R. Schrieffer, Phys. Rev. **108**, 1175-1204 (1957).
8. J. Bardeen and D. Pines, Phys. Rev. **99**, 1140-1150 (1955).
9. W. L. McMillan, Phys. Rev. **167**, 331 (1968).
10. N.N. Bogolubov, V.V. Tolmachev, and D.V. Shirkov, Consultants Bureau, (1959).
11. L. Cooper, Phys. Rev. **104**, 1189 (1956).
12. S. L. Bud'ko, G. Lapertot, C. Petrovic, C. E. Cunningham, N. Anderson, and P. C. Canfield, Phys. Rev. Lett. **86**, 1877 (2001).
13. W. L. McMillan and J. M. Rowell, In: *Superconductivity*, Vol. 1, p. 561, Edited by R. D. Parks, Marull, Dekker Inc. N.Y. (1969).
14. D. J. Scalapino, In: *Superconductivity*, Vol. 1, p. 449, Edited by R. D. Parks, Dekker Inc. N.Y. (1969).
15. E. Maxwell, Phys. Rev. **78**, 477 (1950).
16. A. Reynolds, B. Serin, W. H. Wright, and L. B. Nesbit, Phys. Rev. **78**, 487 (1950).
17. A.A.Abrikosov, L.P. Gorkov, I.E. Dzyloshinksi, 'Methods of Quantum Field Theory in Statistical Physics'.
18. G. M. Eliashberg, Sov. Phys. JETP **11**, 696 (1960).
19. F. Marsiglio and J.P. Carbotte, "Electron - Phonon Superconductivity" in 'The Physics of Conventional and Unconventional Superconductors' edited by K.H. Bennemann and J.B. Ketterson (Springer-Verlag).
20. A.J. Leggett, Rev. Mod. Phys. **47**, 331(1975), R. Balian, R. and N. R. Werthamer, Phys. Rev. **131**, 1553 (1963). P.W. Anderson, and W.F.Brinkman, Phys. Rev. Lett. **30** , 1108 (1973).
21. D. Vollhardt and P. Woelfle, Superfluid phases of Helium 3, Taylor and Francis, London, 1990.
22. J. G. Bednorz, K. A. Mueller, Zeitschrift für Physik B **64**(2),189 (1986).
23. See for example: In: *Proceedings of Materials and Mechanisms of Superconductivity: High Temperature Superconductors VI* in Physica C (Amsterdam), **341-348** (2000).

24. Y. Kamihara, T. Watanabe, M. Hirano, H. Hosono, Iron-based layered superconductor La $O_{1-x}F_xFeAs$ ($x \sim 0.05-0.12$) with $T_c = 26K$ J. Am. Chem. Soc. **130**, 3296(2008).
25. J. Friedel, Phil. Mag. **43**, 153 (1952).
26. W. Kohn, J.M. Luttinger, Phys. Rev. Lett. **15**, 524 (1965).
27. J.M. Luttinger, Phys. Rev.**150**, 202 (1966).
28. D. Fay and A. Layzer, Phys. Rev. Lett. **20**, 187 (1968).
29. M. Y. Kagan and A. V. Chubukov, JETP Lett. **47**, 614 (1988); M. Baranov, A. V. Chubukov, and M. Y. Kagan, Int. J. Mod. Phys. **6**, 2471 (1992); M.Y. Kagan and V. V. Val'kov, JETP **140**, 179 (2011).
30. D.D. Osheroff, R.C. Richardson, and D.M. Lee, D. M., Phys. Rev. Lett., **28**, 885 (1972).
31. A. V. Chubukov, Phys. Rev. B **48**, 1097 (1993).
32. A. V. Chubukov, D. Efremov, and I. Eremin, Phys. Rev. B **78**, 134512 (2008); V. Cvetkovic and Z. Tesanovic, Phys. Rev. B **80**, 024512(2009).
33. N. Furukawa, T. M. Rice, and M. Salmhofer, Phys. Rev. Lett. **81**, 3195 (1998); M. Salmhofer *et al*, Prog. Theor. Phys. **112**, 943 (2004).
34. R. Nandkishore, L. Levitov, A. Chubukov, Nature Physics **8**, 158-163 (2012).
35. A. Abanov, A. V. Chubukov and J. Schmalian, Adv. Phys. **52**, 119 (2003).
36. A. Sedeki, D. Bergeron, C. Bourbonnais, Phys. Rev. B. **85**, 165129 (2012).
37. F. Wang, H. Zhai, Y. Ran, A. Vishwanath, and D.-H. Lee, Phys. Rev. Lett. **102**, 047005 (2009); H. Zhai, F. Wang, and D.-H. Lee, Phys. Rev. B **80**, 064517 (2009).
38. R. Thomale, C. Platt, J. Hu, C. Honerkamp, and B. Andrei Bernevig Phys. Rev. B **80**, 180505(R) (2009).
39. D.J. Scalapino, Phys. Rep., **250**, 329 (1995); D. J. Scalapino, Rev. Mod. Phys. 84, 1383 (2012).
40. E.M. Lifshitz and L.P. Pitaevskii, Statistical Physics (Part 1), Pergamon Press, Reprinted in 2002.
41. L.P. Gorkov and T.K. Melik-Barkhudarov, Sov. Phys. JETP, **13**, 1018 (1961).
42. see e.g., M. Randeria and E. Taylor, Annual Reviews of Condensed Matter Physics. Vol. 5 (2014) and arXiv:1306.5785, and references therein.
43. A.V. Chubukov and D.L. Maslov, Phys. Rev. B **86**, 155136 (2012).
44. D.V. Efremov, M.S. Mar'enko, M.A. Baranov, M. Y. Kagan. JETP **90**, 861 (2000).
45. J. Mráz and R. Hlubina, Phys. Rev. B **67**, 174518 (2003).
46. S. Raghu, S. A. Kivelson, and D. J. Scalapino, Phys. Rev. B. **81**, 224505 (2010).
47. S. Raghu and S.A. Kivelson, Phys. Rev. B **83**, 094518 (2011); A. V. Chubukov and M. Yu. Kagan, J. Phys. Condens. Mat. **1**, 3135 (1989).
48. A. S. Alexandrov and V. V. Kabanov, Phys. Rev. Lett. **106**, 136403 (2011); S. Raghu, E. Berg, A. V. Chubukov, and S. A. Kivelson, Phys. Rev. B **85**, 024516 (2012).
49. A. V. Chubukov, A. M. FinkelŠstein, R. Haslinger, and D. K. Morr, Phys. Rev. Lett. **90**, 077002 (2003).
50. G. J. Conduit, C. J. Pedder, and A. G. Green , Phys. Rev. B **87**, 121112(R) (2013).
51. Li Liu, H. Yao, E. Berg, S. R. White, and S. A. Kivelson, Phys. Rev. Lett. **108**, 126406 (2012).
52. H. Yao, W.-F. Tsai, and S. A. Kivelson, Phys. Rev. B **76**, 161104 (2007).
53. P. A. Lee, N. Nagaosa, and X.-G. Wen, Rev. Mod. Phys. **78**, 17 (2006).
54. S. Onari, H. Kontani, M. Sato, Phys. Rev. B. **81**, 060504(R) (2010), H. Kontani, S. Onari, Phys. Rev. Lett. **104**, 157001 (2010), T. Saito, S. Onari, H. Kontani, Phys. Rev. B **82**, 144510 (2010).
55. S. Johnston, F. Vernay, B. Moritz, Z.-X. Shen, N. Nagaosa, J. Zaanen, T. P. Devereaux Phys. Rev. B **82**, 064513 (2010).
56. W.S. Lee, S. Johnston, T.P. Devereaux, Z.-X. Shen Phys. Rev. B **75**, 195116 (2007).
57. M. Einenkel, K. B. Efetov, Phys. Rev. B **84**, 214508 (2011).
58. Yu.E. Lozovik, A.A. Sokolik, Phys. Lett. A **374**, 2785 (2010).
59. F.-C. Hsu et al. , Proc. Natl. Acad. Sci. U.S.A. **105** , 14262 (2008).
60. K.-W. Yeh, T.-W. Huang, Y.-L. Huang, T.-K. Chen, F.-C. Hsu, P. M. Wu, Y.-C. Lee, Y.-Y. Chu, C.-L. Chen, J.-Y. Luo, D. C. Yan, and M. K. Wu, Europhys. Lett. **84** , 37002 (2008) .
61. S. Margadonna, Y. Takabayashi, M. T. McDonald, K. Kasperk- iewicz, Y. Mizuguchi, Y. Takano, A. N. Fitch, E. Suard, and K. Prassides, Chem. Commun. Cambridge 5607 (2008).

62. M. H. Fang, H. M. Pham, B. Qian, T. J. Liu, E. K. Vehstedt, Y. Liu, L. Spinu, and Z. Q. Mao, Phys. Rev. B **78** , 224503 (2008).
63. X. H. Chen, T. Wu, G. Wu, R. H. Liu, H. Chen, D. F. Fang, Nature **453**, 761(2008).
64. G. F. Chen, Z. Li, D. Wu, G. Li, W. Z. Hu, J. Dong, P. Zheng, J. L. Luo, and N. L. Wang, Phys. Rev. Lett. **100**, 247002 (2008).
65. Z.-A. Ren, *et. al.*, Europhys. Lett. **83**, 17002 (2008).
66. M. Rotter, M. Tegel, D. Johrendt, Phys. Rev. Lett. **101**, 107006 (2008).
67. K. Sasmal, B. Lv, B. Lorenz, A. M. Guloy, F. Chen, Y.-Y. Xue, and C.-W. Chu, Phys. Rev. Lett. **101**, 107007 (2008).
68. N. Ni, A. Thaler, J. Q. Yan, A. Kracher, E. Colombier, S. L. Bud'ko, P. C. Canfield, Phys. Rev. B **82**, 024519 (2010).
69. T. Sato, K. Nakayama, Y. Sekiba, P. Richard, Y.-M. Xu *et al* Phys. Rev. Lett. **103**, 047002 (2009); T. Terashima *et al.*, J. Phys. Soc. Japan **79**, 053702 (2010).
70. J. K. Dong, S. Y. Zhou, T. Y. Guan, H. Zhang, Y. F. Dai *et al* Phys. Rev. Lett. **104**, 087005 (2010); K. Hashimoto, A. Serafin, S. Tonegawa, R. Katsumata, R. Okazaki *et al.*, Phys. Rev. B 82, 014526 (2010).
71. J.-G. Guo *et al.*,
Phys. Rev. B **82**, 180520(R) (2010).
72. T. Qian *et al.*, arXiv:1012.6017 (unpublished).
73. X. C. Wang, *et. al.*, arXiv:0806.4688v3;
S.V, Borisenko, V. B. Zabolotnyy, D. V. Evtushinsky, T. K. Kim, I. V. Morozov, A. N. Yaresko, A. A. Kordyuk, G. Behr, A. Vasiliev, R. Follath, and B. Buechner Phys. Rev. Lett. **105**, 067002 (2010).
74. M. H. Fang et al., Phys. Rev. B **78**, 224503 (2008)
75. C. de la Cruz, Q. Huang, J. W. Lynn, J. Li, W. Ratcliff II, J. L. Zarestky, H. A. Mook, G. F. Chen, J. L. Luo, N. L. Wang and P. Dai, Nature **453**, 899-902 (2008).
76. Y. Nakai, T. Iye, S. Kitagawa, K. Ishida, H. Ikeda, S. Kasahara, H. Shishido, T. Shibauchi, Y. Matsuda, T. Terashima, Phys. Rev. Lett. **105**, 107003 (2010).
77. Y. Kamihara, T. Watanabe, M. Hirano, and H. Hosono, J. Am. Chem. Soc. **128**, 10012 (2006).
78. D.C. Johnston, Adv. Phys., **59**, 803 (2010).
79. J-P Paglione and R.L. Greene, Nature Phys. **6**, 645 (2010).
80. I.I. Mazin, Nature **464**, 183 (2010).
81. H.H. Wen and S. Li, Annu. Rev. Condens. Matter Phys., **2**, 121 (2011).
82. S. Graser, T. A. Maier, P. J. Hirschfeld, and D. J. Scalapino. New J. Phys., **11**, 025016 (34pp) (2009).
83. A. F. Kemper, T. A. Maier, S. Graser, H.-P. Cheng, P. J. Hirschfeld, and D. J. Scalapino, New J. Phys. **12**, 073030 (2010).
84. K. Kuroki, H. Usui, S. Onari, R. Arita, and H. Aoki, Phys. Rev. B **79**, 224511 (2009).
85. A. V. Chubukov Physica C **469**, 640(2009).
86. I.I. Mazin and J. Schmalian, Physica C, **469**, 614 (2009).
87. P.J. Hirschfeld, M.M. Korshunov, and I.I. Mazin, Rep. Prog. Phys. **74**, 124508 (2011).
88. D.N. Basov and A.V. Chubukov, Nature Physics 7, 272 (2011).
89. M. Norman. Physics, **1**, 21 (2008).
90. C. Xu and S. Sachdev, Nature Physics, **4**, 898(2008).
91. A.V. Chubukov, Annual Reviews in Condensed-Matter Physics, **3**, 57 (2012).
92. A.V. Chubukov, M.G. Vavilov, A.B. Vorontsov Phys. Rev. B **80**, 140515(R) (2009).
93. V. Cvetkovic, O. Vafek arXiv:1304.3723 (2013).
94. see e.g R. Thomale, C. Platt, J. Hu, C. Honerkamp, and B. Andrei Bernevig Phys. Rev. B **80**, 180505(R) (2009), S. Maiti, M. M. Korshunov, T. A. Maier, P. J. Hirschfeld, and A. V. Chubukov, Phys. Rev. Lett. **107**, 147002 (2011).
95. K. Suzuki, H. Usui, and K. Kuroki, Phys. Rev. B **84**, 144514 (2011). S. Maiti, M. M. Korshunov, T. A. Maier, P. J. Hirschfeld, and A. V. Chubukov, Phys. Rev. B. **84**, 224505 (2011), R. Thomale, C. Platt, W. Hanke, J-P Hu, and B. Andrei Bernevig, Phys. Rev. Lett. **107**, 117001 (2011). T. A. Maier, S. Graser, P. J. Hirschfeld, and D. J. Scalapino, Phys. Rev. B **83**, 100515(R) (2011).
96. D. J. Scalapino, E. Loh, and J.E. Hirsch, Phys. Rev. B **34**, 8190 (1986).

97. A. Damascelli, Z. Hussain, and Z-X. Shen, Rev. Mod. Phys. **75**, 473 (2003).
98. S.Sachdev, Rev. Mod. Phys. **75** 913 (2003).
99. N. P. Armitage, P. Fournier, and R. L. Greene, Rev. Mod. Phys. **82**, 2421 (2010).
100. A.J. Millis, S. Sachdev, and C.M. Varma, Phys. Rev. B **37**, 4975 (1988).
101. M. R. Norman, D. Pines, C. Kallin Adv. Phys. **54**, 715 (2005).
102. S. Huefner, M.A. Hossain, A. Damascelli, G.A. Sawatzky, Rep. Prog. Phys. **71**, 062501 (2008).
103. K. LeHur and T.M. Rice, Annals of Physics, **324** 1452-1515 (2009).
104. P. Monthoux, A. V. Balatsky, and D. Pines, Phys. Rev. Lett. **67**, 3448 (1991); P. Monthoux and D. Pines Phys. Rev. B 47, 6069 (1993); P. Monthoux and D. J. Scalapino Phys. Rev. Lett. **72**, 1874 (1994).
105. P. Monthoux and G. Lonzarich, Phys. Rev. B **63**, 054529 (2001); P. Monthoux, D. Pines, and G. G. Lonzarich, Nature **450**, 1177 (2007).
106. A.-M.S. Tremblay, Theoretical methods for Strongly Correlated Systems, in Springer series, edited by F. Mancini and A. Avella, 2011 (arXiv:1107.1534).
107. S. R. Hassan, B. Davoudi, B. Kyung, and A.-M. S. Tremblay, Phys. Rev. B **77**, 094501 (2008); Bumsoo Kyung, Jean-Sébastien Landry, and A.-M. S. Tremblay, Phys. Rev. B **68**, 174502 (2003).
108. M.A. Metlitski and S. Sachdev, Phys. Rev. B. **82**, 075128 (2010).
109. K. B. Efetov, H. Meier, C. Pépin, arXiv:1210.3276 (2012).
110. A.V. Chubukov, Physics **3**, 54 (2010).
111. M. Platé, J. D. F. Mottershead, I. S. Elfimov, D. C. Peets, Ruixing Liang, D. A. Bonn, W. N. Hardy, S. Chiuzbaian, M. Falub, M. Shi, L. Patthey, and A. Damascelli, Phys. Rev. Lett. **95**, 077001 (2005).
112. L. Van Hove, Phys. Rev. **89**, 1189 (1953).
113. F. Guinea, R. S. Markiewicz, and M. A. H. Vozmediano, Phys. Rev. B **69**, 054509 (2004).
114. A.H. Castro Neto, F. Guinea, N.M.R. Peres, K.S. Novoselov, and A.K. Geim, *Rev. Mod. Phys.* **81**, 109 (2009).
115. J. L. McChesney, A. Bostwick, T. Ohta, T. Seyller, K. Horn, J. Gonzalez, and E. Rotenberg, Phys. Rev. Lett. **104**, 136803 (2010).
116. J. Gonzalez, *Phys. Rev. B* **78**, 205431 (2008).
117. B. Valenzuela B. and M. AH. Vozmediano, *New. J. Phys.* **10** 113009 (2008).
118. I Martin,C.D. and Batista, *Phys. Rev. Lett.* **101**, 156402 (2008).
119. T. Li, http://arxiv.org/abs/1103.2420 (2011) (unpublished).
120. D. Makogon, R. van Gelderen, R. Roldan,and C. Morais Smith, *Phys. Rev. B* **84**, 125404 (2011).
121. R. Nandkishore, A.V. Chubukov, Phys. Rev. B **86**, 115426 (2012)
122. M. Kiesel, C. Platt, W. Hanke, D. A. Abanin, R.Thomale, Phys. Rev. B **86**, 020507 (2012).
123. T. E. Weller, M. Ellerby, S. S. Saxena, R. P. Smith and N.T. Skipper, Nature Phys. **1**, 39 (2005).
124. G. Csanyi, P. B. Littlewood, A. H. Nevidomskyy, C. J. Pickard, and B. D. Simons, Nature Phys. **1**, 42 (2005).
125. R. Hlubina, S. Sorella, and F. Guinea, Phys. Rev. Lett. **78**,1344 (1997).
126. J. Ruvalds, C. T. Rieck, S. Tewari, J. Thoma and A. Virosztek, Phys. Rev. B, **51**, 3804 (1995).
127. H. Meier, C. Pépin, K. B. Efetov, Phys. Rev. B **84**, 205131 (2011).
128. D. F. Mross, J. McGreevy, H. Liu, T. Senthil Phys. Rev. B **82**, 045121 (2010).
129. G.E. Volovik, Phys. Lett. A **128**, 277 (1988).
130. M. Sigrist, and K. Ueda, Rev. Mod. Phys. **63**, 239 (1991).
131. M. Vojta, Y. Zhang, S. Sachdev, Phys. Rev. Lett. **85**, 4940(2000).
132. G. Moore, and N. Read, Nucl. Phys. B **360**, 362 (1991).
133. D.A. Ivanov, Phys. Rev. Lett. **86**, 268 (2001).
134. L. Fu, and C.L. Kane,Phys. Rev. Lett. **100**, 096407 (2008).
135. X.L. Qi , T. Hughes, S. Raghu, S.-C. Zhang, Phys. Rev. Lett. **102**, 187001 (2009).
136. M. Cheng, M. Sun, V. K. Galitski, and Das Sarma, S. Phys. Rev. B **81**, 024504 (2010).
137. D.L. Maslov and A.V. Chubukov, Phys Rev. B. **81**, 045110 (2010).

138. M. Dzero and L. P. GorŠkov Phys. Rev. B **69**, 092501 (2004).
139. S. Maiti and A.V. Chubukov, Phys. Rev. B **82**, 214515(2010).
140. R. Shankar, Rev. Mod. Phys. **66**, 129 (1994).
141. V.S. de Carvalho, Hermann Freire, Europhys. Lett. **96**, 17006 (2011).
142. The authors are thankful to Oskar Vafek for clarifying this point to them.
143. For more detailed discussion on possible co-existence of SC and SDW orders in 3-patch model see Ref. [121].
144. A.B. Vorontsov, M.G. Vavilov, A.V. Chubukov, Phys. Rev. B **81**, 174538 (2010). M. G. Vavilov, A. V. Chubukov, A. B. Vorontsov, Supercond. Sci. Technol. **23**, 054011 (2010).
145. R. M. Fernandes, J. Schmalian, Phys. Rev. B **82**, 014521 (2010).